Integrated analysis of seismic attributes and well-logs in reservoir characterization: seismic-facies classification and reservoir facies mapping

by

Luke Rijfkogel

B.S., Fort Hays State University, 2017

A THESIS

Submitted in partial fulfillment of the requirements for the degree

MASTER OF SCIENCE

Department of Geology
College of Arts and Sciences

KANSAS STATE UNIVERSITY
Manhattan, Kansas

2020

Approved by:

Major Professor
Dr. Abdelmoneam Raef

Copyright

Abstract

Carbonate reservoir characterization introduce challenges that constantly require updates based on new seismic and production data. Understanding the connection between seismic response and litho-petrophysical properties is a crucial component to producing tangible results in hydrocarbon reservoir characterization, particularly in carbonate reservoirs. Applying models in seismic interpretation is essential to integrating data from a variety of disciplines including geology, geophysics, petrophysics and reservoir engineering.

In this study, three post-stack seismic attributes (instantaneous bandwidth and peakedness along with volume attributes such as Root Mean Square - RMS energy) are used to distinguish and identify seismic classes pertaining to variations in litho/petrophysical facies from the Mississippian saline aquifer hosted in a carbonate reservoir from the Wellington Field, Sumner County, Kansas.

Neutron porosity, bulk density, and sonic well logs provided a correlation with seismic amplitude, which in turn reflects reservoir properties associated to acoustic impedance. Neutron porosity logs were characterized into three classes. Class one representing a porosity less than eight percent, Class two representing a porosity class of greater than eight and less than twelve percent and Class three representing a porosity greater than twelve percent.

The impedance differences across a seismic reflector are the controlling parameter of reflectivity. By having seismic and well log data sets provide the connection to characterize the reservoir to be modeled for porosity prediction based on amplitude and seismic facies classification for the effects of enhanced oil recovery (EOR) or geological sequestration of CO_2.

Using an unsupervised neural network and selecting three facies classes to correlate with three petrophysical classes. Three well-log classes are defined to describe the reservoir in terms

of porosity using neutron porosity well logs. Seismic facies three has the highest porosity (greater than 12 percent), landed in structurally low areas and likely resemble dolomite prone area. The second-facies has porosity between 7 and 13 percent resemble a transitional zone from structurally low to high showing reworked brecciated limestone facies from CT scans. Seismic facies one has porosity less than 11 percent and resemble a structurally high erosional area.

The seismic facies prediction map was constructed by correlating reservoir porosity using neutron porosity logs and seismic amplitude attributes in a carbonate reservoir. Due to the nature of elastic properties and mineralogy of carbonates that render the reservoir porosity the most significant factor controlling amplitude variation.

Seismic amplitude attributes (bandwidth, peakedness, and RMS energy) reveal some unexpected features interpreted as small-scale faults associated with the Nemaha Uplift. Using the same three attributes as an input for an unsupervised neural network and selecting three seismic facies produces results that correlate with one out of the three porosities, providing a correlation between well-logs and seismic amplitude that can be used to predict reservoir facies in terms of porosity especially for higher porous zones.

A CT scan of the top of Wellington KGS #1-32 core indicates slit-shaped (fracture) porosity and vuggy porosity dominate at the top of the reservoir. The bottom of the reservoir is dominated by fractured porosity ranging from 1.1 mm to 0.1 mm in size. The slit-shaped porosity is orientated vertically while the vuggy porosity was located within the diagenetic dolomite which was contained within the chert. Wellington KGS #2-32 core is dominated by slit-shaped porosity ranging in size from 0.4mm to 0.07mm. Slit shaped porosity shown from the middle CT scan in the Wellington KGS #2-32 shows faulting is associated after diagenesis of the dolomite.

The vuggy porosity are the result from diagenetic processes and the slit-shaped porosity is associated to faulting from the Nemaha Uplift.

This study illustrates the ability to use a data driven approach to an unsupervised neural network to identify seismic facies that relate to porosity classes by integrating well-logs, seismic attributes, and CT scans to characterize a carbonate petroleum reservoir system.

Table of Contents

List of Figures

Acknowledgements

I would like to acknowledge to following individuals and organizations during my academic and professional career:

My advisor Dr. Abdelmoneam Raef, for his insights during Seismic Interpretations and his dedication towards his students. Throughout my numerous office visits and conversations with my advisor the experience at K-State was enriched through the connection of geophysics and geology.

Dr. Goldberg and Dr. Totten for their patience and guidance through my MS thesis research.

Kansas State University, Department of Geology for providing me the opportunity to teach a course that has enriched my education and provided a chance to inspire students about geology.

Paul and Deana Strunk scholarship and Gary and Kathie Sandlin scholarship that has contributed to completing my degree.

AAPG Bill Barrett Family Named Grant to support my thesis research.

Fort Hays State University professors, for developing me and instilling a passion to pursue geology as a career.

I would like to thank Dr. Lynn Watney for his devotion, leadership, and talents for the geosciences.

AAPG & SEG for student membership access to publications that enriched my research.

The following software companies: OpendTect, Kingdom IHS, and Petrel for allowing students utilize their software and help facilitate students as they learn.

SEG for accepting me in the Student Leadership Symposium sponsored by Chevron and Student Education Program sponsored by ExxonMobil.

University of Texas at Austin for their guidance and support to add additional insights by having CT scans.

Dedication

To my parents for instilling one of the most important values in life; hard work and for their continued encouragement and instilling values that influence my day-to-day interactions with each individual.

To my previous employer and friend Burt for providing me a job that ignited my pursuit to understand geosciences.

To my beloved friend Barbara, who encouraged me to earn an education in my younger years of life but was unable to see me graduate.

Chapter 1 - Introduction

The phrase ‘state-of-the-art’ compared to ‘state-of-the-science’ has a meaning that scientists should consider in terms of understanding the connection between creative solutions to solving geological problems vs. taking a purely formula-driven approach. I mention the use of “art” as a progression of the sciences because it continues to evolve and progress in the field of applied geophysics. In other words, technology creates innovative solutions to improve human life, whereas science goals are to pursue knowledge for its own sake (Difference.com, 2019).

In contrast, if taking a purely formula-driven approach by applying physical constraints to geophysical methods, then results would be as easy as punching numbers on a calculator to get the correct answer, which is not reality when it comes to geosciences. The Earth is heterogeneous, evolving, and complex (Werthington et al., 2018), which draws scientists to this field to derive creative solutions to complex situations. To this extent, a vivid imagination, comprehensive understanding of physical laws and theories (Laszlo, 2007), and strong work ethic are critical to develop the field of geophysics.

Discovering and utilizing resources is a fundamental part to advancing society (Krehel, 2017). Carbonate reservoirs contain about 60% of the world’s oil reserves; describing and characterizing these reservoirs remains puzzling, because of their heterogeneity and complex microstructure (Sayers, 2008). The inherent complexity associated with diagenesis can create secondary porosity in carbonates, creating greater porosity and density variations in carbonates than siliciclastic (Xu and Payne, 2009).

After discovering an economical hydrocarbon field, development and primary production takes course and depletion becomes inevitable, but oil reservoirs can have a considerable amount of oil left in place, with some reservoirs as much as 80%-90% still in place (Melzer, 2012). At this point several options are possible; plug the well if no economic resources are recoverable, investigate for other hydrocarbon-producing zones, or convert the field to secondary recovery by injecting produced water. In some cases, after secondary production 50% to 70% of residual oil can be left in the reservoir. One of the last procedures for a depleted hydrocarbon reservoir is to commence tertiary enhanced oil recovery (EOR) methods (Melzer, 2012). Over the entire life cycle of a field, constantly improved reservoir characterization (e.g. Raef et al., 2017) is essential especially for CO_2-EOR methods.

The Department of Energy (DOE) and National Energy and Technology Laboratory (NETL) emphasize the most critical factor for selecting candidates for CO_2-EOR is the growing consensus among experts that more detailed geophysical mapping of the remaining oil in a reservoir is needed, particularly in geological heterogeneous formations (NETL, 2010). This thesis presents a case study to utilize available data sets such as 3D seismic survey, well-logs, and cores to characterize the producing formation for CO_2-EOR recovery of hydrocarbons left in place.

Amid energy awareness that hydrocarbons are a finite resource, efficiency of energy usage, technology to advance and development of an oil field, and enhanced oil recovery projects play vital roles in supplying affordable energy while reducing greenhouse gases (NETL, 2010). In addition to the need to preserve the environment, efforts such as cleaner alternatives are being investigated but newer forms of renewable energy have still to meet the demands (Krehel, 2017). In order to meet this two-fold situation, the capture and sequestration of CO_2 into a producing hydrocarbon reservoir can reduce atmospheric CO_2 and enhance production of a producing hydrocarbon field (Melzer, 2012). The Department of Energy, National Energy Technology Lab, Berexco, and several education institutions such as Kansas State University, University of

Kansas, and the Kansas Geological Survey collaborated to test the containment, monitoring, and injecting CO_2 into the Mississippian age limestone (Ohl and Raef, 2014) in Wellington and Anson-Bates Field, Sumner County, Kansas, shown in Figure 1.1. Wells used to calculate average porosities for the Mississippian reservoir are shown below, indicated by a red stars and black dots showing core locations.

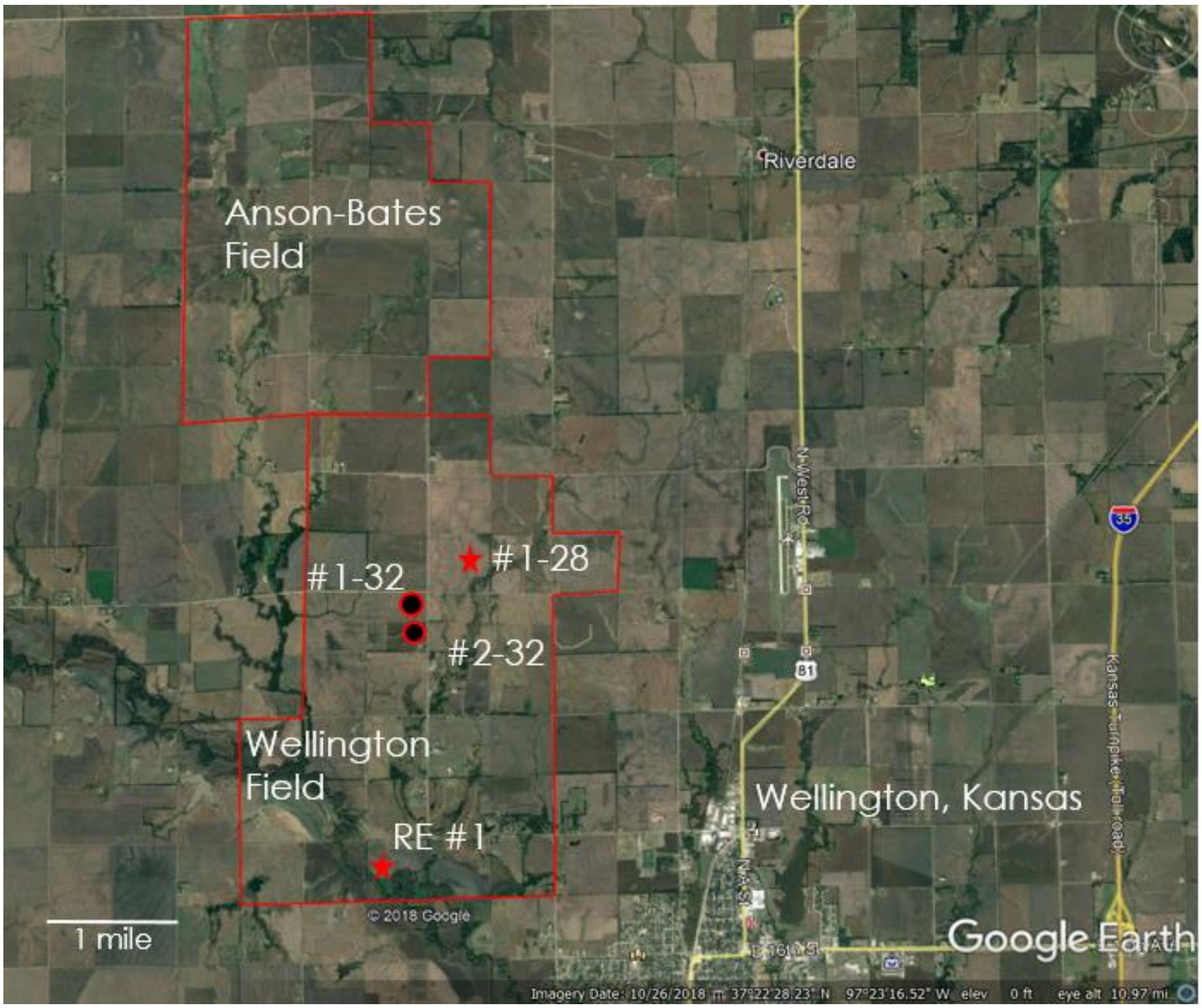

Figure 1.1 Outline (in red) of two 3D seismic data sets merged together, which indicate the whole study area. Bottom polygon outlines the Wellington Field. Top polygon outlines the Anson-Bates Field, acquired by Noble Energy.

To our knowledge, no litho-petrophysical map of the subsurface has been produced from seismic data. The goals of this study are to use geophysical well logs to identify petrophysical classes (based on reservoir properties) and integrate seismic attributes (e.g. instantaneous and acoustic impedance) to interpret seismic facies and estimate reservoir porosity quality and facies distribution.

Complex seismic trace attributes including measurements of amplitude, phase and frequency have been used in the past to map seismic lithology (Marfurt et al., 1998). Seismic waveform classification can define reservoir properties with greater detail than traditional time and amplitude mapping when mapping facies (Anderson and Boyd, 2004).

The detail of investigation depends strictly on the scale, which is controlled by the resolution of the seismic data (Lee et al., 2009). However, specific attributes provide details that enhance the seismic signal, such as composite amplitude attributes. These provide volumetric details, whereas peakedness and bandwidth that provide instantaneous details about the seismic horizon (Chen & Sidney, 1997). With the advancements in CO_2-EOR, all aspects of the data must be integrated to monitor and ensure containment of the CO_2 (Watney et al., 2015).

Geophysical well-logs provide details over a given depth to classify litho-petrophysical facies (Asquith and Gibson, 1982), while CT scans provide a magnified view of the reservoir pore structure and display the electron density variations within the object scanned in a two dimensional X-ray image (Sprunt et al., 1987) and seismic amplitude attributes provide an encompassing view of the reservoir (Anees, 2013).

In this study we, focused on predicting seismic facies using seismic attributes by training an unsupervised neural networks to differentiate seismic facies by integrating petrophysical data, such as well logs for porosity classes and CT scans from cores for further analysis of pore size, structure, and mineral density. It is worth noting that the resolution of seismic data (tens of meters) is less than that of well logs (in centimeters to meter) (Tittman, 1991) and CT scans (micrometers). In order to address scaling issues, we averaged well log properties and used selected slices from a CT scan of three inch thick cores from the top, middle, and bottom of the Wellington KGS #1-32 and Wellington KGS #2-32 segment of reservoir, to provide smaller scale properties that contribute to the seismic signal (Simms & Bacon, 2014).

Chapter 2 - Background

Enhanced Oil Recovery via CO_2

Carbon dioxide is one of many gases within the Earth's atmosphere. Today the main source of CO_2 in the atmosphere is generated by natural sources, such as oceans degassing, although a significant percentage comes from anthropogenic sources, such as industries and especially power plants that use fossil fuels to generate electricity (Liu, 2012)). Given the finite amount of hydrocarbon resources, and the concern for green-house gases, enhanced oil recovery can have a significant role in meeting energy needs while reducing CO_2 into the atmosphere. Carbon dioxide has beneficial results for meeting the energy needs, if captured and sequestrated where possible. In order to reduce CO_2 amounts via carbon sequestration requires detailed evaluation of the potential reservoir.

Major contributors to anthropogenic CO_2 production are coal power plants, corn ethanol factories and other industrial plants, but these industries are also great sources for capturing CO_2. Unfortunately, most currently lack the infrastructure for CO_2 capture, making these methods challenging to transport CO_2 to the oil fields (Mezler, 2012). Figure 2.1 shows the locations of these various industries in Kansas relative to the locations of oil fields (grey areas).

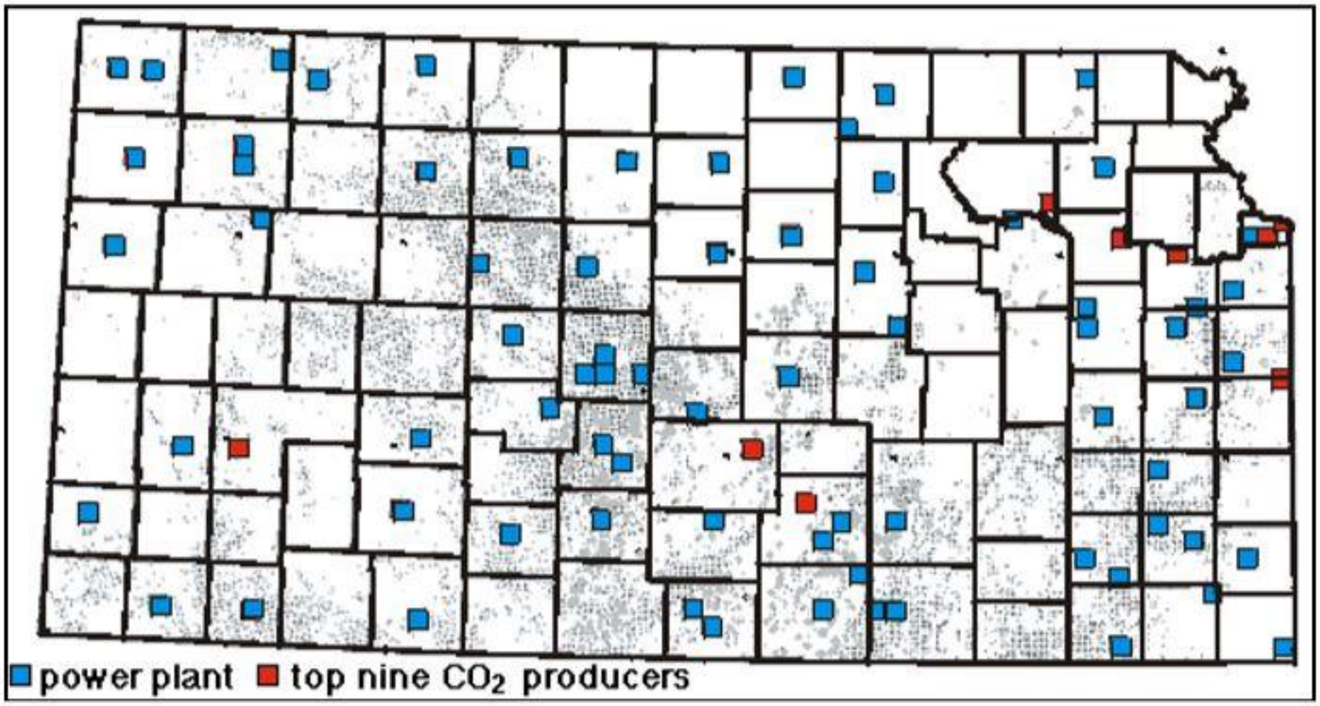

Figure 2.1 Indicating CO_2 producers. Blue are minor producers (ethanol plants) and red are major producers (coal power plants). Gray areas are oil fields and potential sites for carbon geosequestration. (http://www.kgs.ku.edu/CO2/resource/lansing.html)

The process of CO_2-EOR is typically proceeded by secondary recovery methods of water flooding a field. Water flooding provides insights into CO_2-EOR feasibility, as hydrocarbon reservoirs successful with water flooding are typically prime candidates for CO_2-EOR flooding (DOE/NETL, 2010). When CO_2 is injected into a reservoir, it becomes miscible with crude oil, given that it is at critical pressure and temperature conditions (Verma, 2015). Well placement and design of the injection process must be organized and understood for fluid migration (Watney, 2015). Well placements and spacing using available wells drilled at specific zones must be known. Injection considerations include timing of injection fluids within the well, well placement patterns associated to fluid migration, alternation of water and gas (CO_2) fluids injected from the well and amounts of fluids (NETL, 2010).

In Figure 2.2, CO_2 can be injected continuously or alternated with slugs of water, known as water-alternating-gas (WAG) injections. Water Air Gas reduces the effect of CO_2 residing in the formation, and facilitates in sweeping the formation of CO_2 using water as the pushing mechanism (Krehel, 2017).

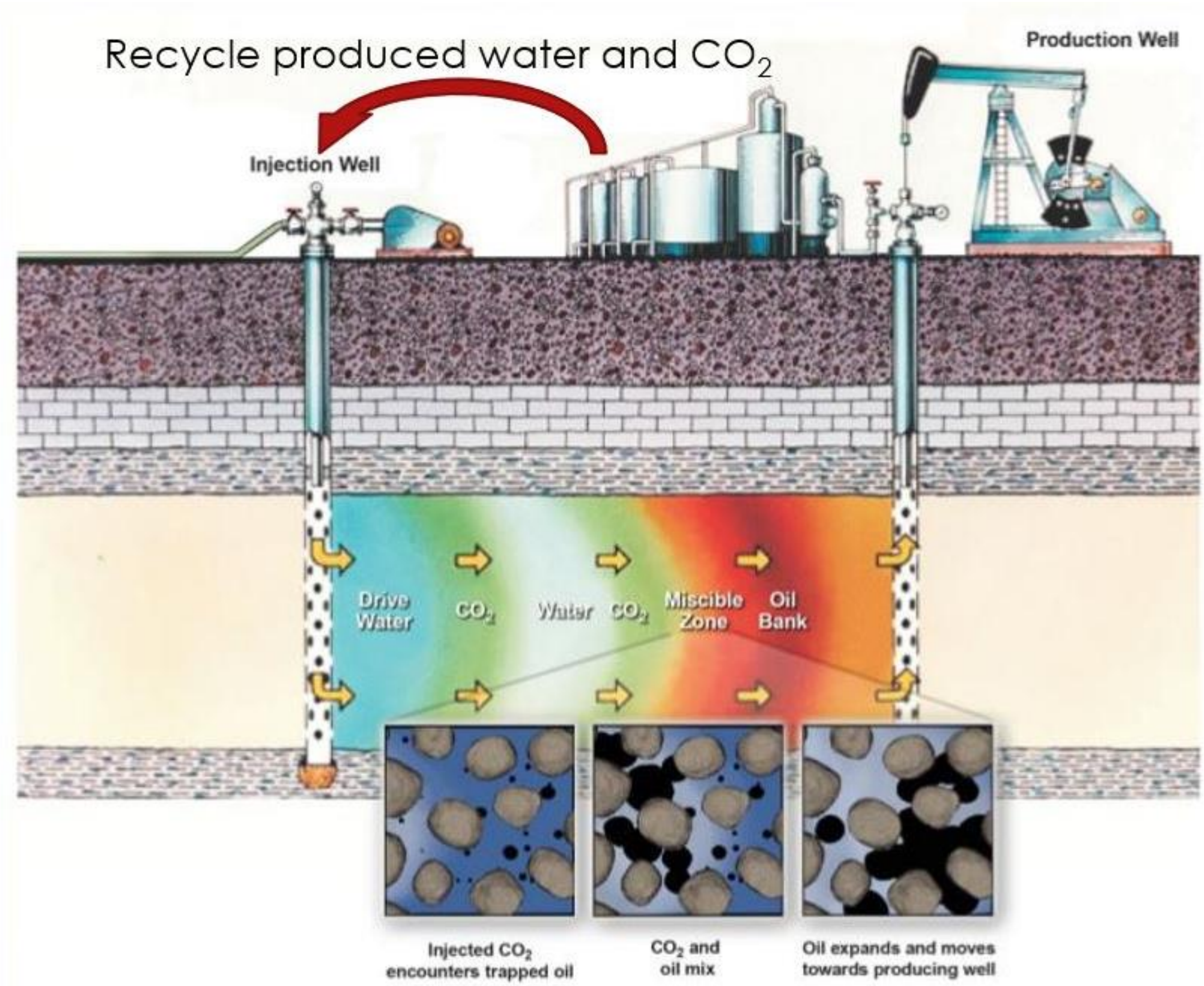

Figure 2.2 Cross section illustrating how WAG can be used to flush out oil from a reservoir by recycling CO_2 and produced water. (NETL, N..2010 "Carbon Dioxide Enhanced Oil Recovery- Untapped domestic energy supply and long term carbon storage solution." The Energy Lab.)

CO_2 must be pressurized to a super critical stage before injecting into the reservoir, given that the reservoir provides a pressure and temperature to keep the CO_2 within the super critical stage (Verma, 2015). The reaction between CO_2 and oil is a miscible reaction that reduces viscosity of oil to enhance recovery of residual oil in the field (DOE and NETL, 2011). During the enhanced oil recovery process CO_2 will be extracted from the well bore. For most operations it would be in their best interests to separate and recycle the CO_2 with new CO_2. Although recycling the CO_2 helps reduce greenhouse gas a majority of CO_2 stays in the reservoir stuck in dead-end pores or trapped to the reservoir wall (Melzer, 2012).

Field History & Technological Advancements

The Mississippian age limestone in Kansas and Oklahoma contains a unique reservoir system that has produced oil since the early 1900's (Kansas Geological Survey (KGS) Energy Resources Website, https://maps.kgs.ku.edu/oilgas/index.html) (Figure 2.3). Located 2.5 kilometers (1.5 miles) N-NW of Wellington, Kansas, the field has produced 20,889,452 cumulative bbls of oil as of 2019 (Kansas Geological Survey https://maps.kgs.ku.edu/oilgas/index.html, 2019). The Anson Southeast field was discovered in the late 1950's by Beardmore drilling (Ohl & Raef, 2012) and has produced a cumulative production of 4,329,071 bbls of oil in 2019 (Kansas Geological Survey Energy Resources Website, https://maps.kgs.ku.edu/oilgas/index.html). In the 1980's the field was converted to a water-flood due to the average drop in production of the field (Watney, 2015).

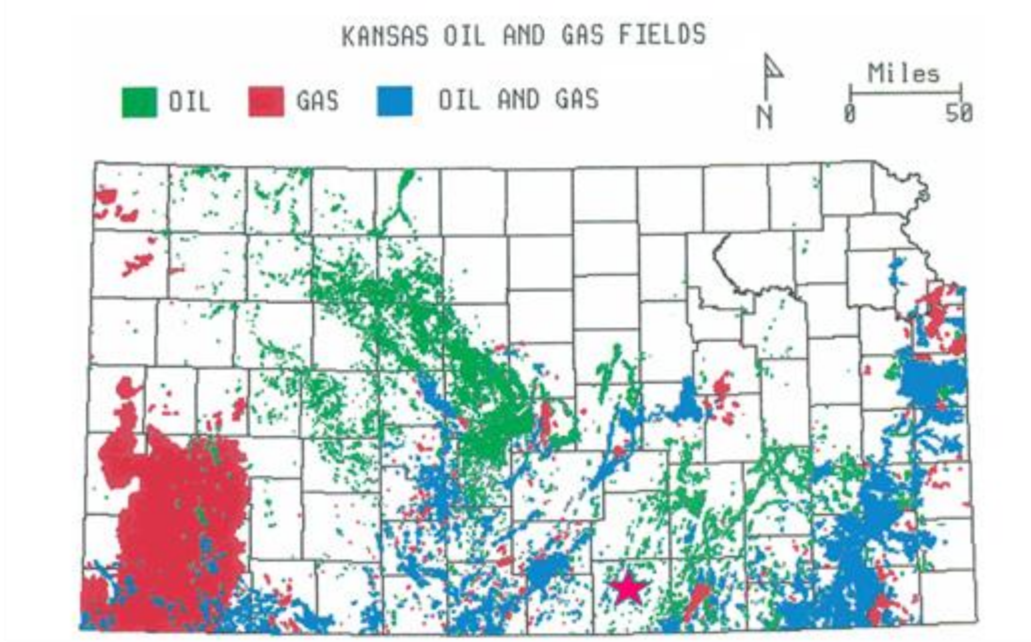

Figure 2.3 Oil and gas fields in Kansas; star indicates study area (Newell et al., 1987).

Newly acquired data from wells drilled and seismic data sets acquired over time for hydrocarbon exploration allow opportunities for professionals by consistently updating reservoir models and development plans to achieve better well-placement results and improve the economics of hydrocarbon field's developments (Martin et al., 2017). Designing future development of the field requires seismic attribute technology to extract and integrate information from the seismic that is hidden within the data to enhance the area of study (Chen and Sidney, 1997).

Amplitude attributes provide insights into reservoir conditions, and recent advancements in horizontal drilling allow for optimal recovery from the reservoir (Chen and Sidney, 1997). Numerous research projects have stemmed from the DOE, NETL funded projects, which have led to a greater understanding on characterizing the reservoir. Watney (2015), Raef (2012), Ohl (2012), Suriamin and Pranter (2018), Mazzullo (2009), and many others have published on various aspects about the Mississippian carbonate reservoir that have contributed to this research. Changes in velocity are due to several factors, but one of the most important is due to porosity, especially in carbonate, where mineralogy is not variable and pore-fluid composition has minimal effect (Simm and Bacon, 2014).

Ohl and Raef (2014) presented a case study for the Mississippian carbonate, characterizing this reservoir through integration of post-stack seismic coherency and amplitude attributes, well log porosities and seismic petrophysical facies classification. They evaluated changes in petrophysical lithofacies and revealed structural facies-controls in the study area. Cross-plots of class-type wells in the selected attributes were used to train the neural network; petrophysical classes/cluster labels correspond to petrophysical classes. Class III corresponds to porosity values above 12%, Class II corresponds to porosities between 8-12%, while Class I refers to petrophysical facies with porosities <8% for the Mississippian formation. They validated the network by training three different wells and three volume seismic attributes, extracted from a time window including the wavelet of the reservoir-top reflection. For proper understanding of these features a special emphasis should be placed on studying these smaller features, which may have implications for the movement of the CO_2 plume (Ohl and Raef 2014).

The input layer for the ANN comprised of three seismic attributes: energy, bandwidth, and peakedness from the Mississippian horizon using OpendTect. Chopra and Marfurt (2008), concluded that post-stack 3D seismic attributes are useful for mapping stratigraphic features in a consistent way and the application of neural networks for multiple-attributes analysis contributes effectively to stratigraphic interpretation. Mapping reservoir properties can be enhanced using geostatistical techniques (Barnes and Laughlin, 2002). While linear regression techniques are straightforward to implement, the interpreter needs to be aware that there may be potential for bias in the use of well-log averages or simply as a result of inadequacies in well sampling (Simm and Bacon, 2014).

In addition, Ohl and Raef (2014) put special emphasis on using seismic attributes (Figure 2.4) (coherency and amplitude using Opendtect) for detection, analysis and seismic interpretation of structural features related to the Nemaha Uplift. After the successful training of the ANN, application of the trained network resulted in a waveform classification into three petrophysical/lithofacies classes from the 3D seismic event of the Mississippian horizon.

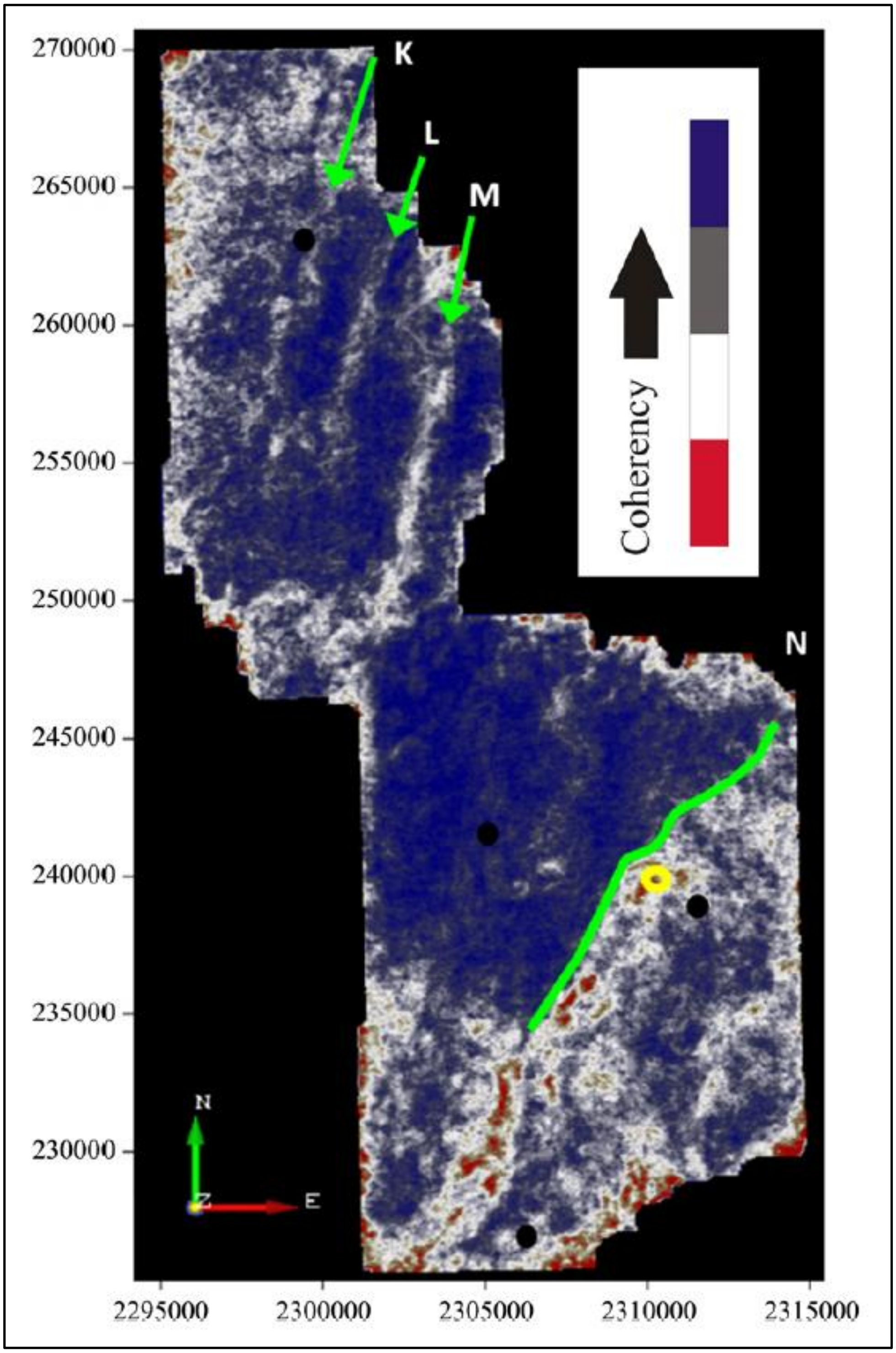

Figure 2.4. Coherency attribute of the Mississippian horizon from the Anson-Bates (north portion) and Wellington Field (south portion), Kansas, showing linear trends indicating structural features caused by the Nemaha Uplift. The green arrow denotes the fault/fracture orientation within the study. Yellow circle indicates recommended injection site for carbon dioxide (Ohl and Raef, 2012).

Numerous theses, presentations, and papers have been published within our field area due to the funding from Department of Energy and partnership with Berexco LLC and the Kansas Geological Survey. Projects that stand out focus on formation characterization for carbon dioxide geosequestration using seismic amplitude and coherency attributes. Seismic petrophysical facies classification contributed a fundamental understanding for integrating multiple disciplines. (Watney, (2015); Ohl, (2012); Raef, (2012); Mazzullo, (2009) have laid the groundwork to be able to integrate multi-scale data sets, such as geophysical well logs, 3D seismic reflection data, regional basement tectonic faults and depositional and stratigraphic frameworks to pursue rock characterization.

Project Background

The typical Mississippian-age reservoirs in Kansas that have undergone secondary recovery methods (water flooding) are suitable candidates for CO_2 based EOR (NETL, 2010) Due to normal decline in production from water flooding will keep fluid and reservoir pressures close to original operating pressures (Melzer, 2012). It has been previously estimated that recoverable potential for Mississippian reservoirs in Kansas using CO_2 EOR is 250-350 million barrels of oil (Holubnyak et al., 2017). At the Wellington Field, after initial recovery dropped in the late 1950's secondary recovery methods (water flooding) were put into action in the 1980's as shown in Figure 2.5. Since then, secondary recovery methods are experiencing a steady decline in production. The steady decline curve of Mississippian-age reservoirs such as the one in the Wellington Field points to a prime candidate for tertiary EOR CO_2-injection.

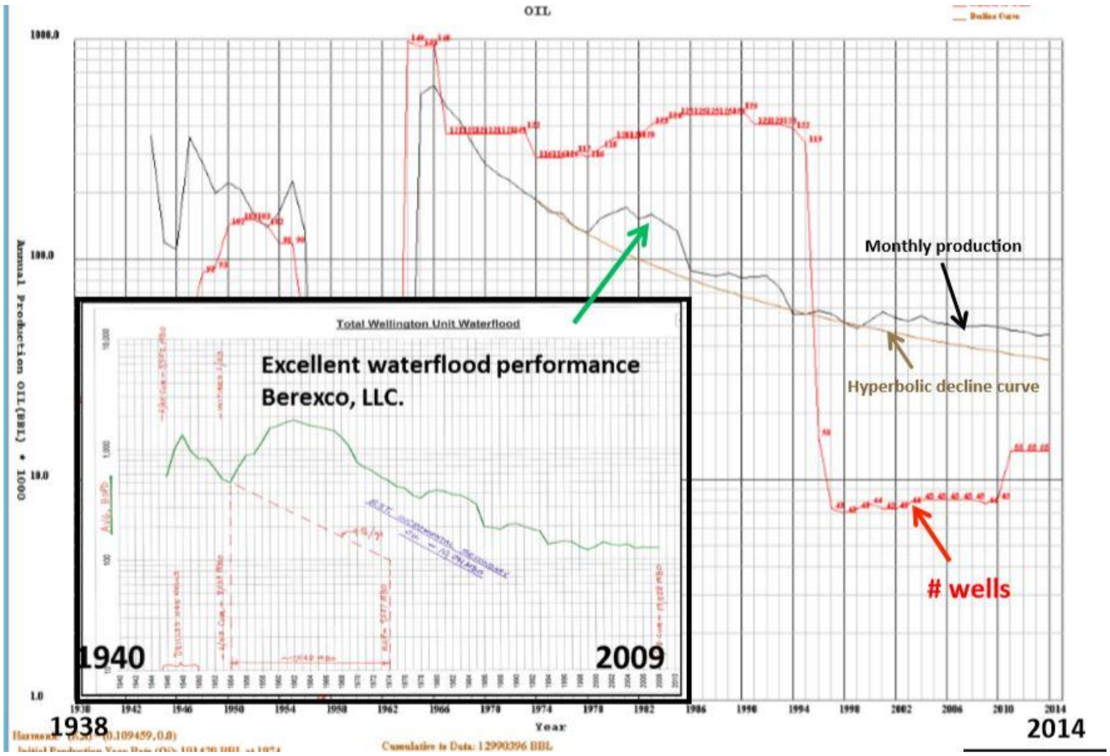

Figure 2.5 Oil Production Curve from the Wellington Field showing an increase in production in the 1980's as a result of an excellent waterflooding (Watney, 2015).

The Mississippian reservoir has been analyzed using a multitude of data, including core, suite of well logs, multi-component 3-D seismic data, and remote sensing surveys by Watney et al., (2011).

Geological Background

Kansas sediments are located on a basement complex of the North American Craton which has undergone several orogenic events that have shaped basins. Uplifted anticlines were some of the first oil discoveries in Kansas that have been exploited by hundreds of oil and gas operators (Merriam, 1963). Fault complex showing wrench-fault patterns during Precambrian age in Kansas are plotted (Figure 2.6) for regional framework of this study. The Nemaha Anticline, probably one of the most well-known structures in Kansas, is a major pre-

Desmoinesian post-Mississippian element that crosses all of Kansas (Merriam, 1963). Since 1914, when oil was discovered along its trend in Butler County, the Nemaha has been subjected to intense exploration (Merriam, 1963).

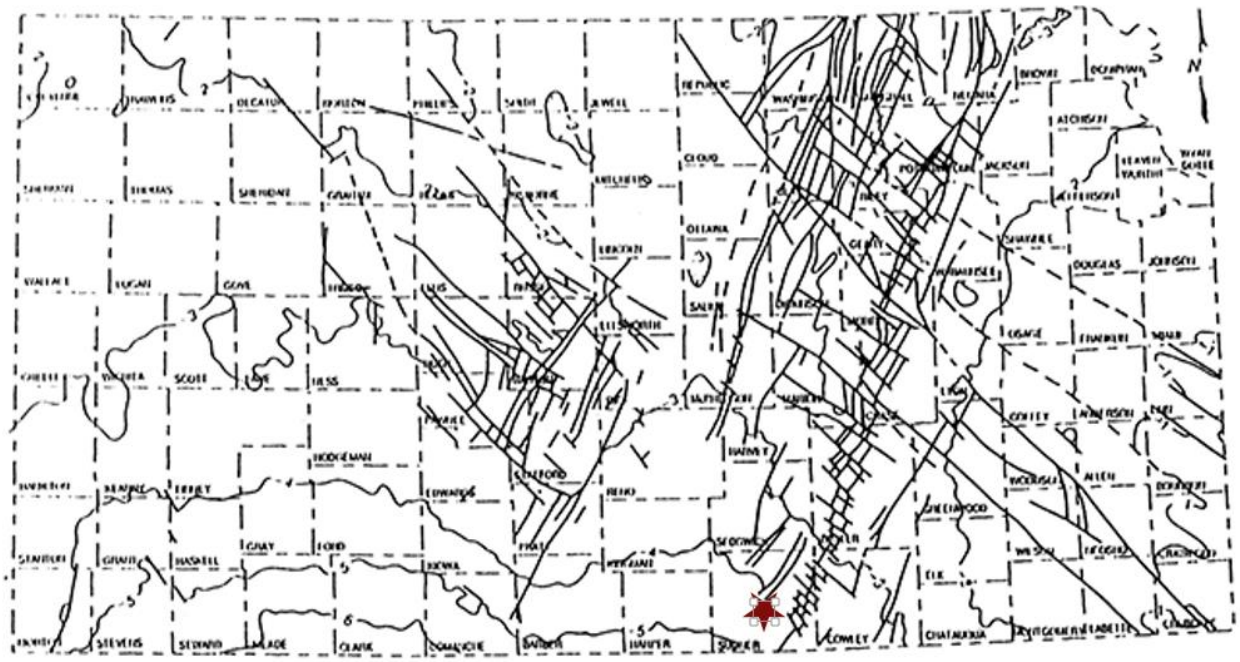

Figure 2.6. Map of Kansas showing generalized fault patterns in Precambrian basement; red star indicates study area. (http://www.kgs.ku.edu/Publications/Bulletins/162/index.html)

The Wellington Field is in the central part of Sumner County, southern Kansas, which borders the east edge of the Sedgwick Basin and the west edge of the Nemaha Uplift as shown in Figure 2.7. The geometry of the Sedgwick Basin is a south-west dipping shelf and is connected to the deeper Anadarko Basin. On the west side of the Nemaha Ridge, the Mississippian increases in thickness towards the south; on the east side of the Nemaha Ridge the Mississippian decreases in thickness towards the south (Mazzulo, 2009). This thinning of the Mississippian limestone is due to tectonic activity during the Ouachita orogeny (Mazzullo, 2011), thus having a critical understanding of unconformities is essential for hydrocarbon exploration (Mazzullo, 2011).

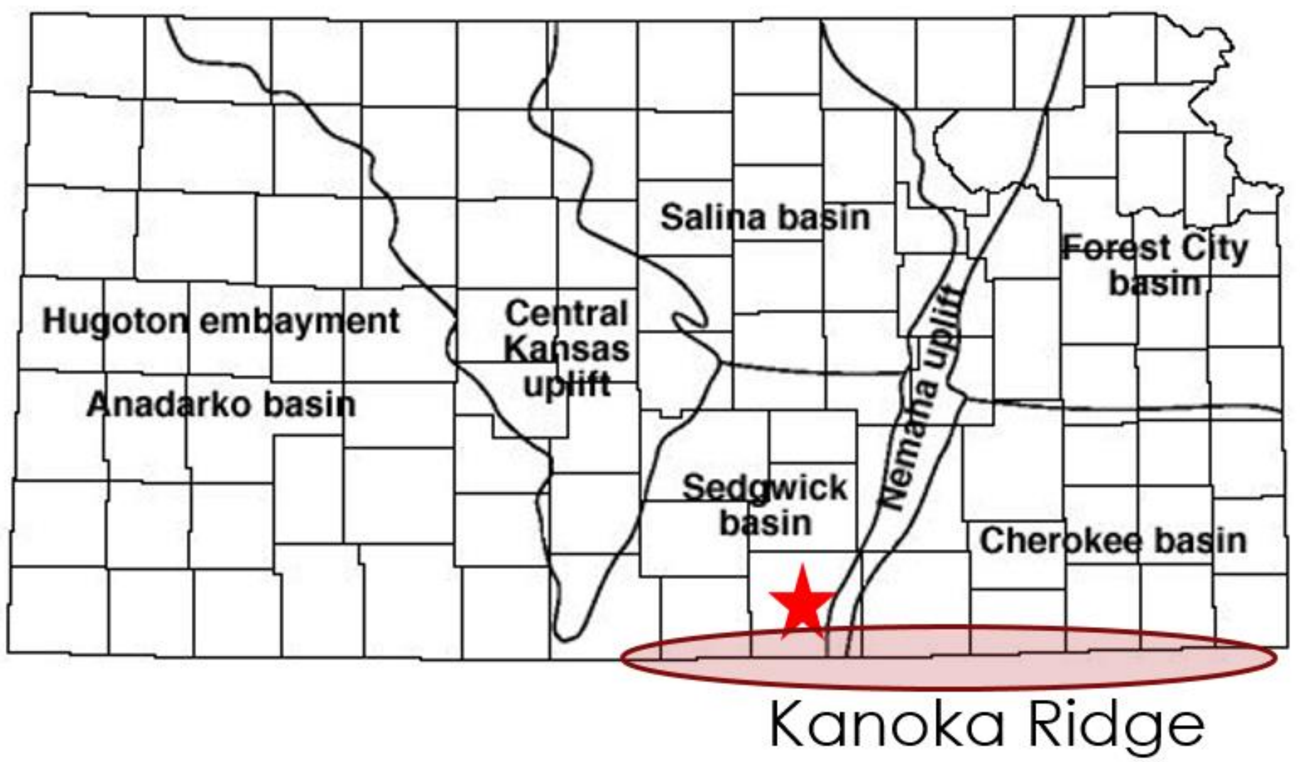

Figure 2.7. Map of Kansas basins and structural areas. Red star indicates study area in Sumner County, Kansas and highlighted oval represents the Kanoka Ridge. (http://www.kgs.ku.edu/Publications/Oil/primer09.html)

In Grant County, Oklahoma (south of Sumner County, Kansas), much, if not all of the Osagean is eroded away from the Kanoka Ridge, which runs along the border of Kansas and Oklahoma (Mazzullo, 2009). The Ouachita Orogeny began early in the Mississippian, changing the basin geometry and causing facies/lithologic changes that coincide with the syndepositional tectonics (Mazzullo, 2011). During the Mississippian transgressing and regressing seas spread over a large part of North America (Figure 2.8) (Suriamin and Pranter, 2018). This period represented a transitional time from greenhouse to icehouse conditions, with associated deposits that reflect an overall regression during this time span (Buggisch et al. 2008). The Mississippian Limestone of the Mid-Continent was deposited as a series of high frequency transgressive-regressive, shallowing-upward cycles (Watney et al., 2001; Mazzullo et al., 2009).

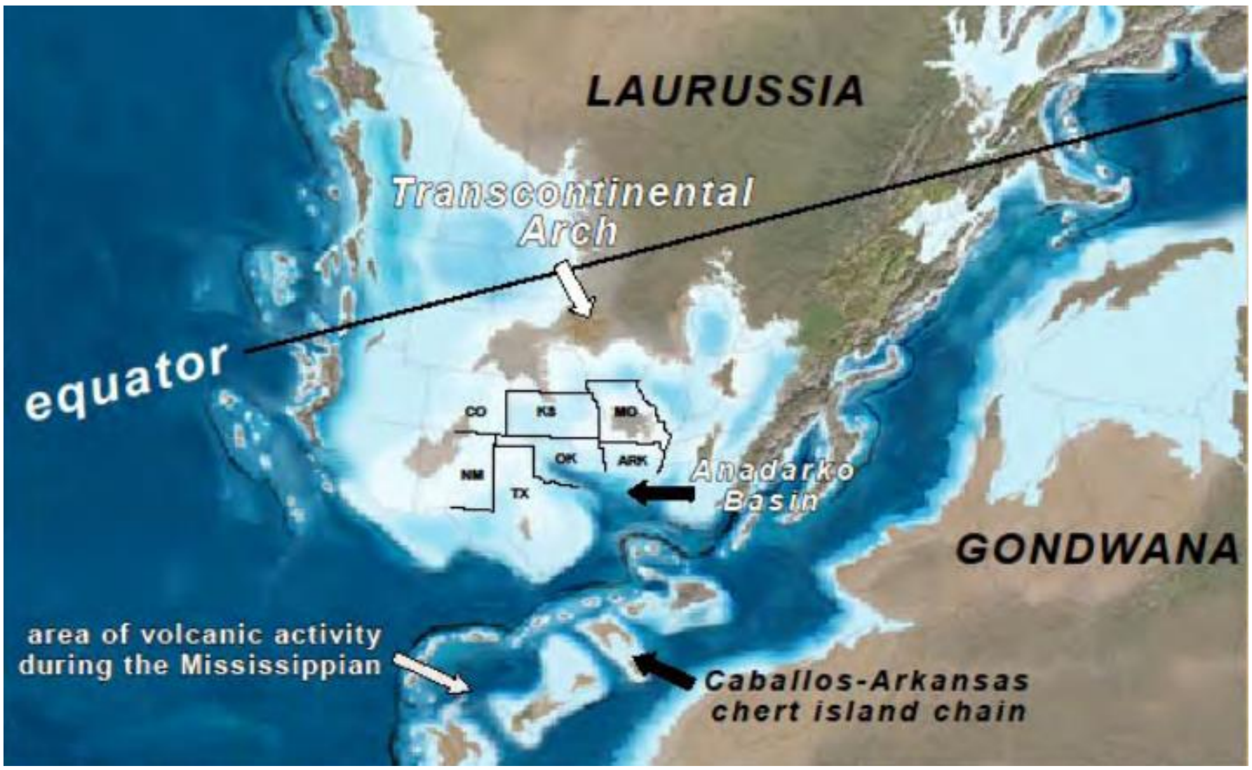

Figure 2.8. Map of Kansas during Mississippian period with an orientation of states (early) (Blakey, 2010) (https://www2.nau.edu/rcb7/).

Stratigraphy

The limestone and chert reservoirs have been informally referred to as the Mississippi Lime or Mississippi Chat. The chert-rich intervals were coined “chat” by drillers because of the chattering noise and bit-bounce during drilling (Rogers, 2011). As described herein, the Mississippian limestone refers to the Mississippian-age limestone and chert deposits that overlie the Woodford Shale (Suriamin and Pranter, 2018).

The Mississippian formation, commonly referred to as the Mississippian Lime Play, was deposited on a ramp dipping towards the Anadarko Basin. The relative change in sea level and tectonic activity influenced the deposition of different types of sedimentary rocks, which include shales, carbonates, and cherts (Watney, 2015). Precambrian basement rock is the only non-sedimentary formation. Watney describes deposits on the ramp as resembling lithofacies and geometries that resemble cool-water shelf margins from both ancient and modern analogs, including in-situ demosponge and bryozoan colonization of the seafloor.

Watney et al. (2015), indicated the formation of interest is Mississippian age, deposited during the Chesterian and Meramecian stages, which are 19.8 meters (65 feet) below the top of the Mississippian, based on gamma ray signature and nuclear magnetic resonance logs, seen in Figure 2.9.

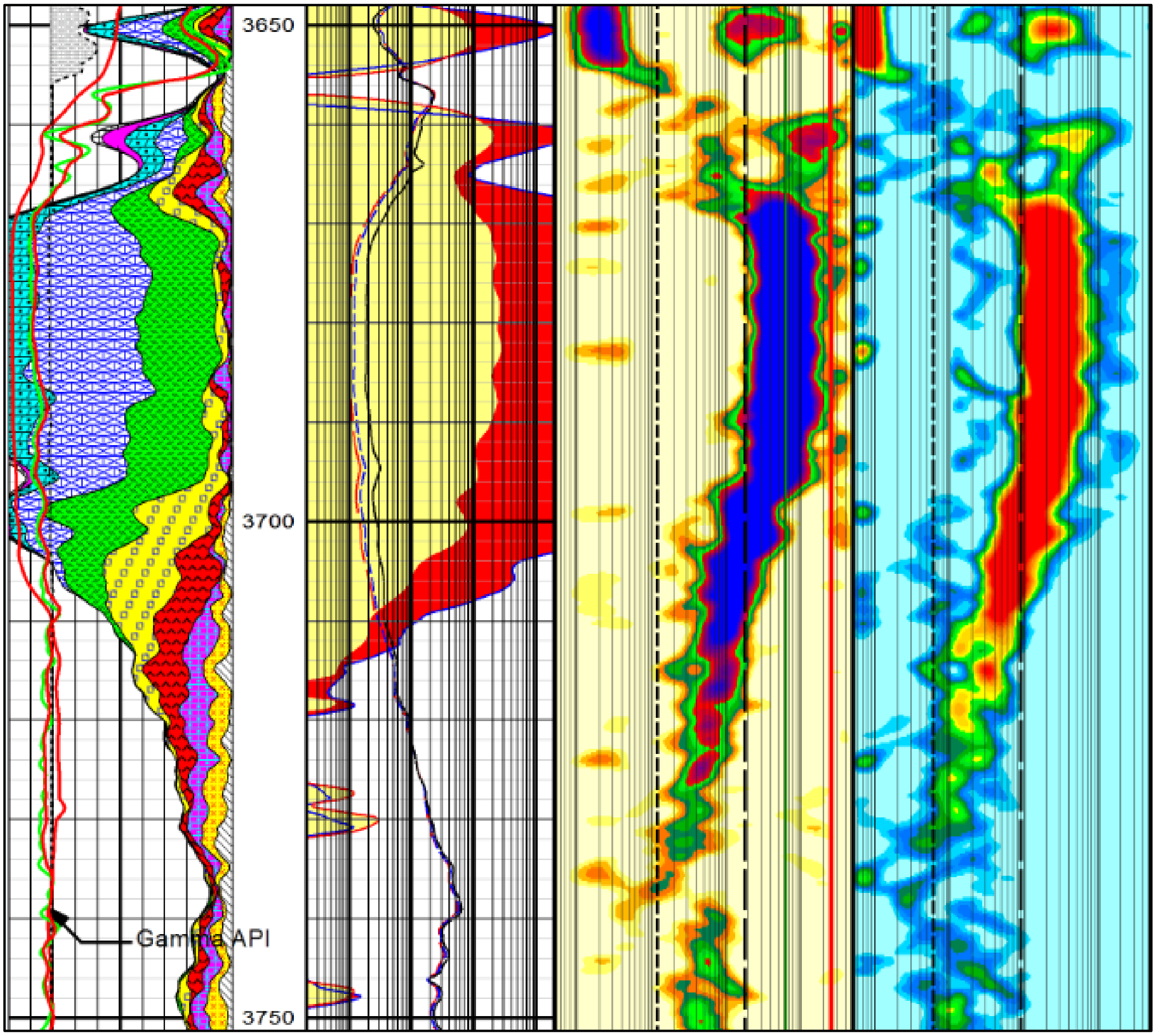

Figure 2.9 Geophysical well-logs of the Mississippian age reservoir of interests. From left to right, GR-gamma ray, CAL-caliper, NMR-nuclear magnetic resonance T1 distribution, and T2 distribution (Wellington KGS #1-32 NMR log from KGS, https://maps.kgs.ku.edu/oilgas/index.html)

The Mississippian strata at the base of the Pennsylvanian becomes younger in a southwestward and westward direction away from the Central Kansas and Nemaha uplifts, respectively (Nissen et al., 2004; Franseen, 2006). Figure 2.10 illustrates the inner ramp deposits as bedded spiculite with subaerial exposure surfaces, the medial ramp as lenticular, nodular, flaser-bedded dolomitized spiculite, and the outer ramp deposits as dolomitic spiculite to argillaceous organic dolomitic siltstones towards the basin (Mazzullo et al. 2009). This indicates that the reservoir of interest should be structurally low while structurally highs areas which would indicate that little or no reservoir present.

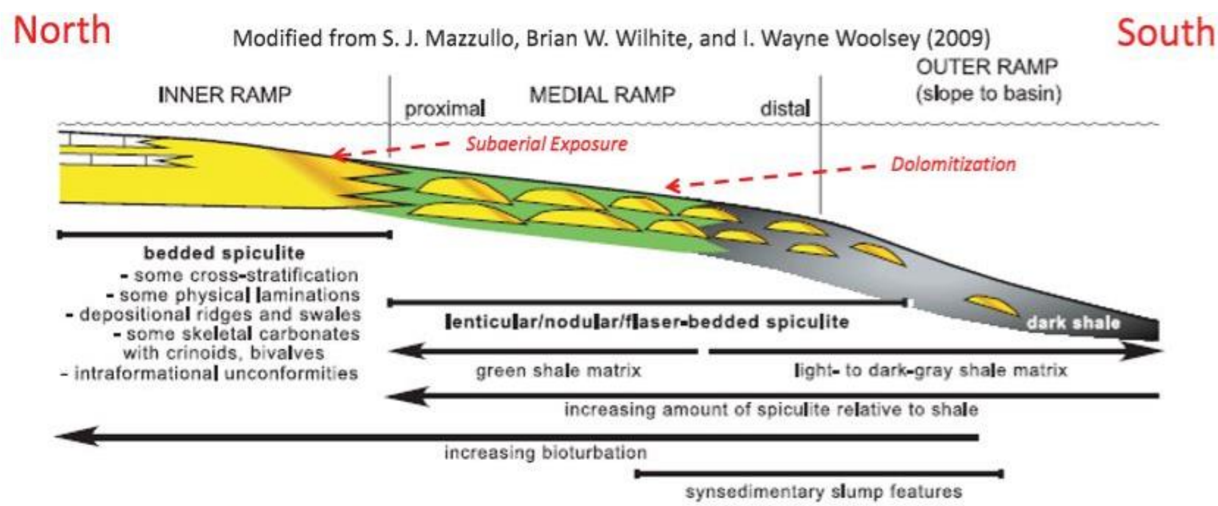

Figure 2.10. Expected lithofacies of the Mississippian carbonate ramp. Modified by Mazzullo et al., (2009)

The Mississippian age group rocks can be broken into 4 periods, Kinderhookian, Osagean, Meramecian and Chesterian in Kansas, as seen in Figure 2.11. The producing formation is the Osagean/Meramecian periods from the Cowley formation are of interests for containing the CO_2.

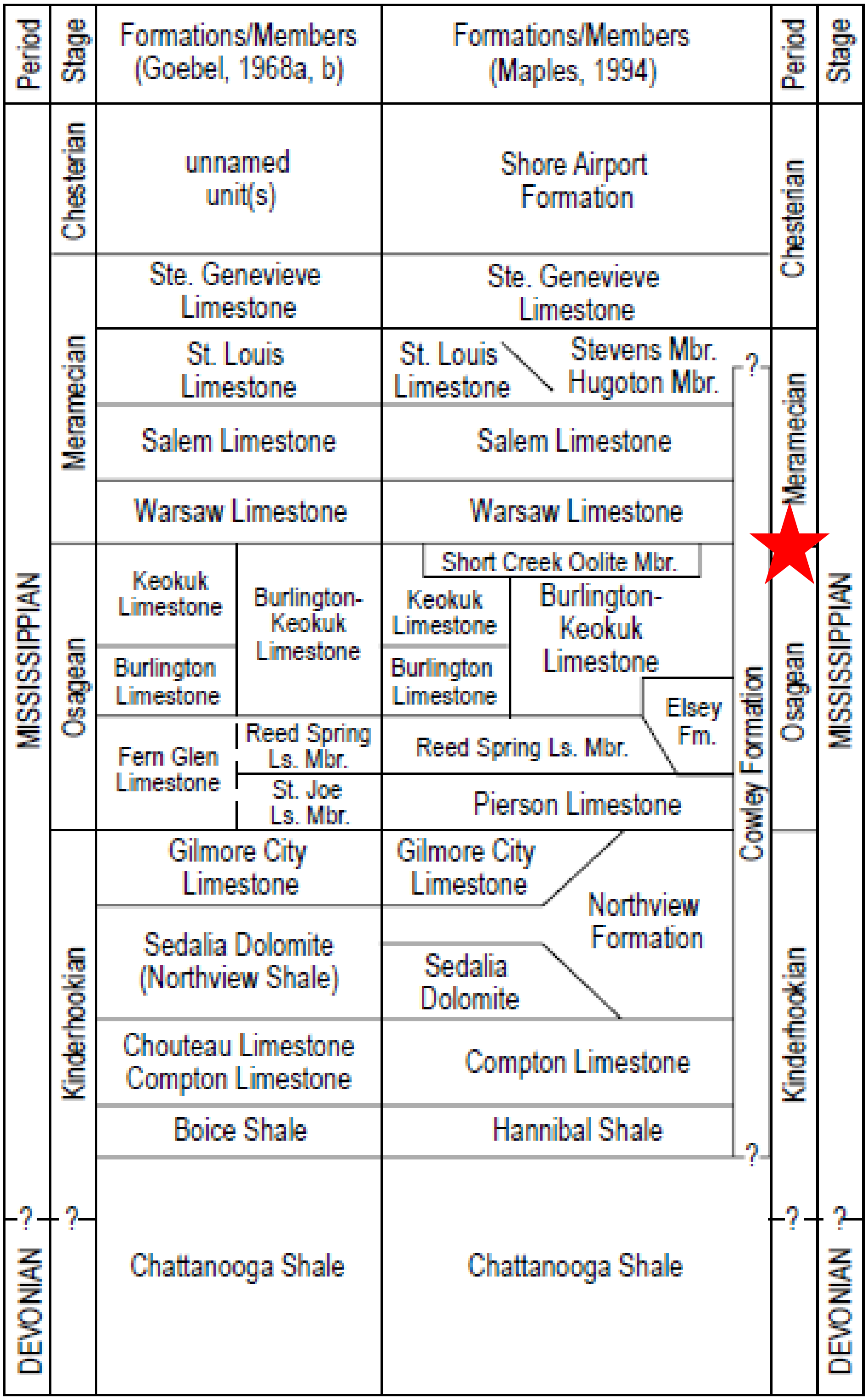

Figure 2.11 Kansas Mississippian stratigraphic column from Watney (2015), with the target interval marked by red star.

Diagenesis have altered the carbonates, exposed to sub aerial alteration via tectonism. Petrologic analysis of the Mississippian strata reveals a range of important early and late diagenetic events that have collectively influenced porosity and permeability distribution (Suriamin and Pranter, 2018). Early and later subaerial exposure and burial diagenesis, including hydrothermal fluid migration, led to several episodes of silicification and dolomization, evaporite precipitation, porosity development including moldic, micro vuggy and fracture pores in brecciated and nodular cherty, early sucrosic (intra-crystalline porosity) dolomite, and less porous dolosiltite (Watney, 2015).

The top of the Mississippian Formation at the Wellington KGS #1-32 consists of twelve feet of brecciated chert that overlie cherty sucrosic dolomite with intermittent vuggy porosity the latter of which consists of reservoir quality porosity hosted in limestone and dolomite. The seal above the reservoir receiving the CO_2 is provided by several different formations including the Cherokee and Pennsylvanian shales, Sumner Anhydrite, and the Hutchinson Salt (Ohl, 2012).

Numerous theses, presentations, and papers have been published within our field area due to the funding from Department of Energy and partnership with Berexco LLC and the Kansas Geological Survey. Projects that stand out focus on formation characterization for carbon dioxide geosequestration using seismic amplitude and coherency attributes. Seismic petrophysical facies classification contributed a fundamental understanding for integrating multiple disciplines. (Watney, (2015); Ohl, (2012); Ohl and Raef, (2014); Mazzullo, (2009) have laid the groundwork to be able to integrate multi-scale data sets, such as geophysical well logs, 3D seismic reflection data, regional basement tectonic faults and depositional and stratigraphic frameworks to pursue rock characterization.

Core Description

A core analysis from Weatherford Laboratories and described by Lynn Watney, 2011, with a spacing of 0.3 meter (~1 foot), has already been conducted on the Wellington KGS #1-32, providing results for permeability, density, porosity, saturation of water and saturation of oil. The core provides data 9.1 meters (30 feet) above the top of the reservoir and extends to the Precambrian basement (472.4 meters or 1,550 feet deep). However, no data has been collected via Computed Tomography (CT) throughout the Mississippian reservoir, which could provide detailed images of pores size, pore size distribution, structure, and / or fractures located within higher porosity intervals the Mississippian Reservoir.

The following descriptions are in from Thin Section from the Mississippian Pay Zone (3669'-3700'), (2011) analyzed by Robin Barker and Saugata Datta and Weatherford Laboratories and described by Lynn Watney, (2011). The top portion of the Mississippian reservoir from the Wellington KGS #1-32 was interpreted at a measured depth (MD) of 1,116.2 meters (3,662 feet) the rocks are described as a "pale yellowish brown siliceous autoclastic breccia with tripolite nodules and lenses of porcelain gray-green chert in a matrix of tripolitic chert. Oil stains within nearly vertical fractures are common" (Weatherford Laboratories, 2011).

Below the brecciated tripolite chert at MD of 1,116.8 meters (3,664 feet), lies a "pale yellowish chert with multi-centimeter chert clasts with gray to yellow green color."

At MD 1117.4 meters (3,666' feet) a layer of "centimeter-size, pale yellowish-brown chert clasts and fine breccia clasts have been diagenetically altered. Scattered cavities with subhorizontal lenses of grayish yellow shales and few fractures. Clasts of oil stained tripolite giving a brown mottled appearance" see Figure 2.12.

Figure 2.12. Thin section from Mississippian reservoir at 3670.6’. Image provided from Robin Barker and Saugata Datta, 2011. Mississippian Pay Zone Mineralogy Unpublished manuscript.

From MD between 1117.7 and 1125.0 meters (3,667 and 3,691 feet) the core consist of “pale yellowish brown brecciated chert in a microporous tripolite chert with brecciated clasts and non-porous porcelain chert clasts filled with tripolite” see Figure 2.13. Pore space and vugs in chert bands with porous and permeable fractures that make up the Mississippian reservoir pore structure. (Description provided by Weatherford Laboratories, 2011).

Miss. Pay Zone Mineralogy

3681.95’

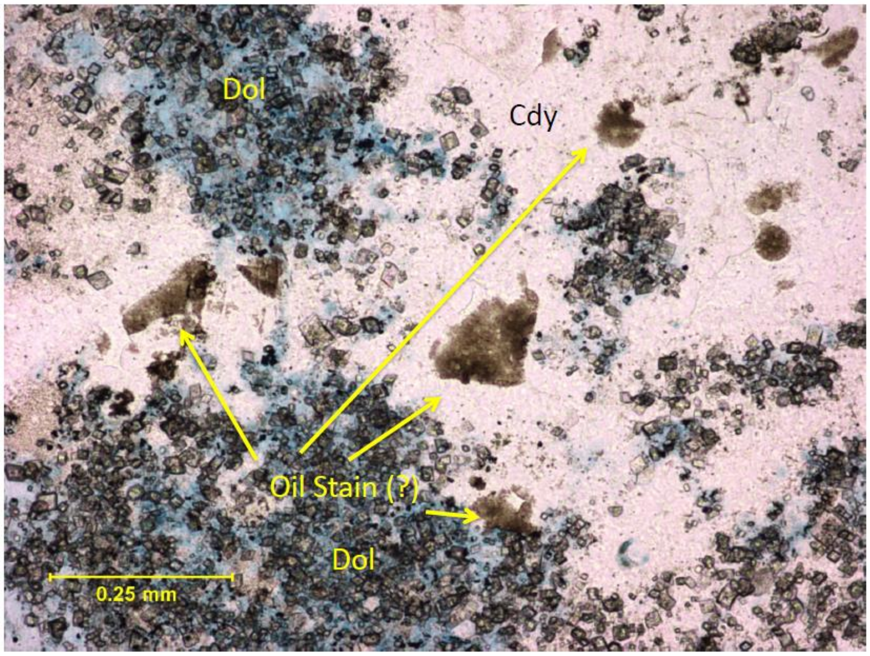

- Plain light (10x zoom)
- Close up of possible oil stain on chert
- Fine grained dolomite in porous zone

Cdy = Chalcedony;
Dol = Dolomite

Figure 2.13. Thin section from the Mississippian reservoir at 3681.95’. Image provided from Robin Barker and Saugatta Datta, 2011. Miss Pay Zone Mineralogy. Unpublished manuscript.

Chapter 3 - Data and Methods

The methods used for this study include, well-log analysis, seismic interpretation software (Kingdom IHS, 2019), seismic attribute analysis and neural networking analysis tool (Opendtect), Computer Tomography (CT) scans (conducted at University of Texas at Austin CT laboratory) .

Geophysical Well-logs

Geophysical well logs from Wellington KGS #1-28, Wellington KGS #1-32, Wellington KGS #2-32, and the Renn-Erickson #1 located in the Wellington Field (Figure 3.1) are one of a few methods to investigate the subsurface. The geophysical well-log utilizes three general principles: electrical, nuclear, and acoustic or sonic properties (Asquith and Krygowski, 2004). The neutron logs are calibrated for a limestone matrix with a density of 2.71 gm/cc. Acoustic logs can be correlated with seismic logs through acoustic impedance, which is a function of porosity. A combination of neutron and density logs is commonly used to determine porosity that is largely free of lithology effects (Doveton, 1999). The neutron-density porosity logs that show a cross-over are good indications of a porous zone. The neutron and density logs are a response to all sizes of pores. However, field observations over many years have shown that the sonic log can be a measure of interparticle (intergranular and intercrystalline) porosity, but it is largely insensitive to either fractures or vugs (Doveton, 1999).

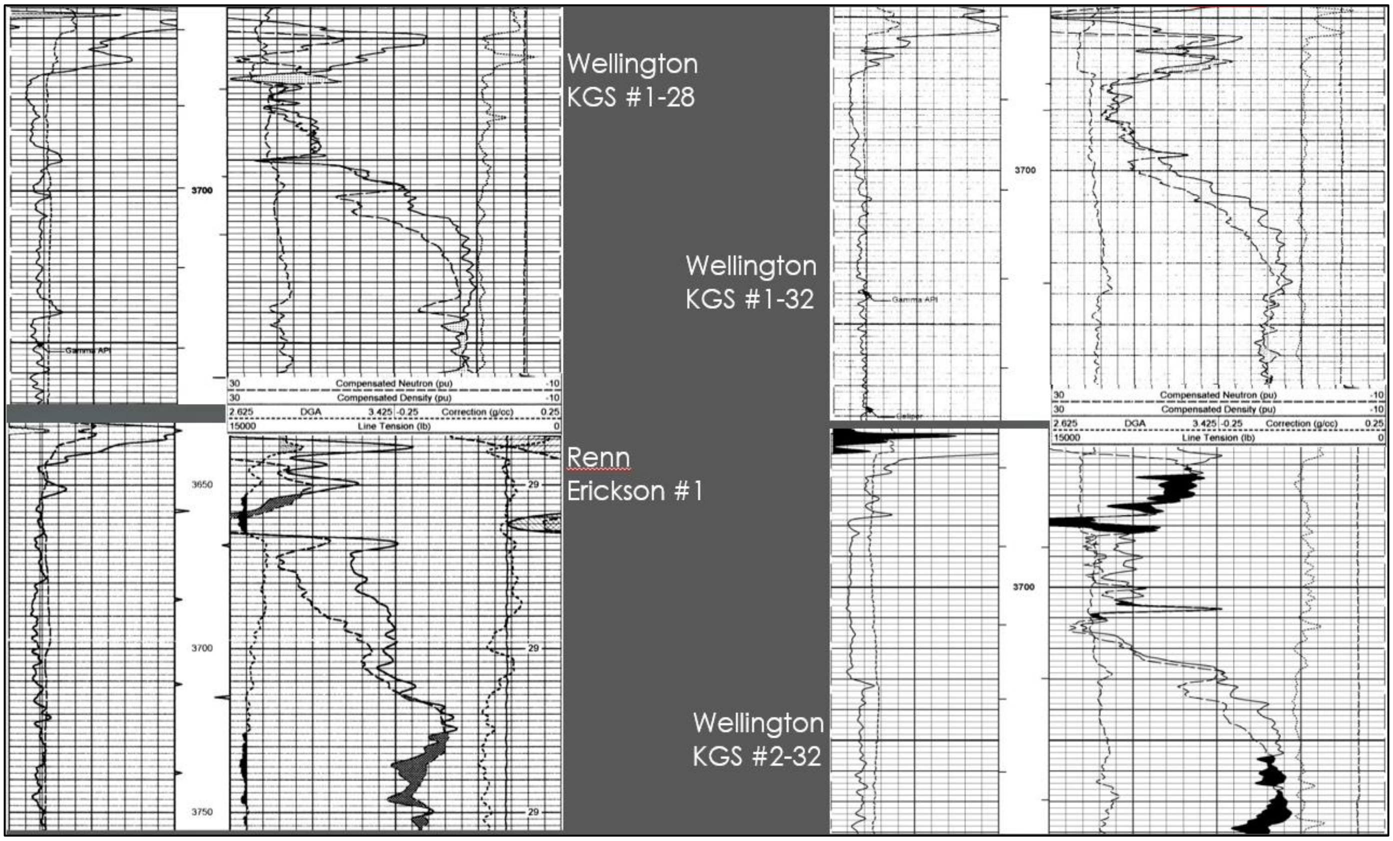

Figure 3.1. Gamma ray, neutron and compensated density logs from Wellington KGS #1-28 (top left), Wellington KGS #1-32 (top right), Renn-Erickson #1 (bottom left), and Wellington KGS #2-32 (bottom right). Intervals marked in black are cross-overs between neutron and density logs, interpreted as porous zones (https://maps.kgs.ku.edu/oilgas/index.html

Resistivity logging tools are another method used to provide insights into the lithologic/petrophysical properties of a formation. Although we don't use them in quantifying seismic facies, they can provide qualitative information on the Mississippian reservoir in terms of mud penetration (Doveton, 1999), as seen in the Wellington KGS #2-32 (lower right of Figure 3.2). The similarity of the deep, medium, and shallow resistivity logs is a good indication that the fluids/saline aquifer have pushed the drilling mud from the bore wall. The wells in Figure 3.2 were all drilled with water based mud.

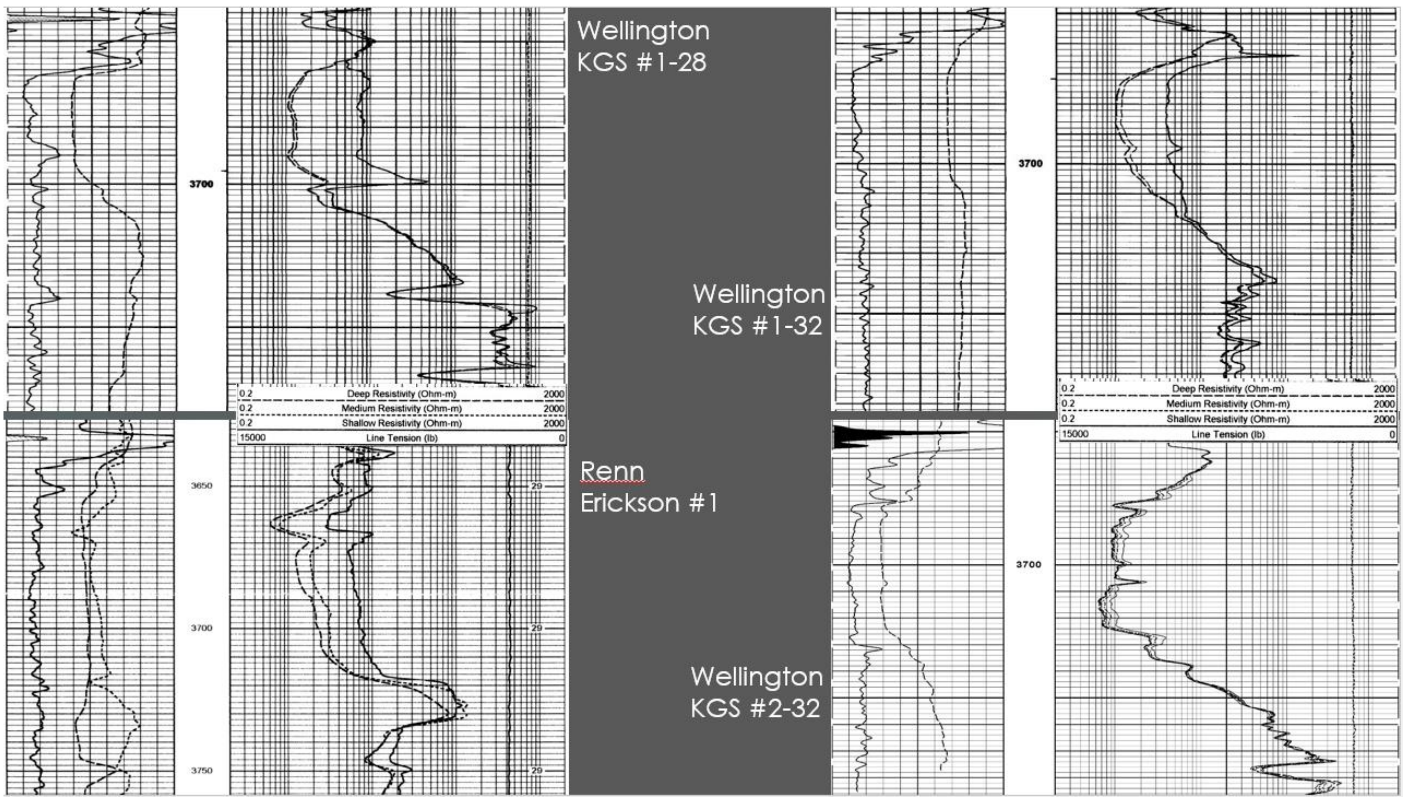

Figure 3.2. Gamma ray and resistivity logs from Wellington KGS #1-28 (top left), Wellington KGS #1-32 (top right), Renn-Erickson #1 (bottom left), and Wellington KGS #2-32 (bottom right). Separation of resistivity well logs indicate mud penetration into the well bore suggesting permeability. (https://maps.kgs.ku.edu/oilgas/index.html)

Seismic Method

The seismic reflection method relies on the existence of interfaces between rock types where acoustic properties change, thus producing reflections. The change in acoustic impedances of rock layers is the product of density and velocity (Brown, 2010). The encompassing thought behind interpreting seismic data are building and updating models to aid the meaning of seismic amplitude anomalies for the specific geologic conditions (Simm and Bacon, 2014). The seismic trace can be considered a function of the wavelet generated at the surface, convoluted by the Earth's reflected surfaces plus noise caused by anthropogenic sources such as traffic and natural sources such as wind and wildlife see Equation 1, (Brown, 2010). The parameters in Equation 1 are the wavelet $w(t)$ convolved with the reflection coefficient series $e(t)$ in addition to noise.

$$x(t) = w(t) * e(t) + noise$$

Equation 1. Seismic waveform as a function of the source wavelet convoluted with the reflection coefficient series plus noise.

The Earth's shallow subsurface (lithosphere) reflectivity can be expressed as a function of density and velocity of the two media. Reflection is generated by the contrast in acoustic impedance of two rock types that are in contact. In fact, impedance and lithology normally correlate with one another, so that impedance boundaries and lithological boundaries normally concur (Brown, 2010). The reflectivity equation can be expressed as the product of velocity and density of the layer below minus the product of velocity and density of the layer above divided by the product of velocity and density of the layer below plus the product of the velocity and density of the layer above as shown below (Equation 2).

$$e(t) = \frac{V2\rho2 - V1\rho1}{V2\rho2 + V1\rho1}$$

Equation 2. Reflection coefficient as a function of velocity (*V*) and density (ρ). The change in velocity and density from the layer above and below gives impedance boundaries. *V*2 and ρ2 from layer below and *V*1 and ρ1 is from layer above.

3D P-wave seismic reflection data

Description and Loading of 3D Seismic Data

A 3D seismic survey was acquired in the Wellington Field on March/April of 2010 by Paragon Geophysical Services, from Wichita, Kansas (Figure 3.3). Equipment used to conduct the survey were as follows: two 62,000 pound vibroseis trucks, Scorpion recording system, and three component digital geophone. The source and receiver interval was 165 feet, receiver line was 495 feet and source line interval was 660 feet. The vibroseis sweep included a range in energy of 16 to 130 Hz at four sweeps lasting twelve seconds and a recording time of 5 seconds (Ohl, 2012).

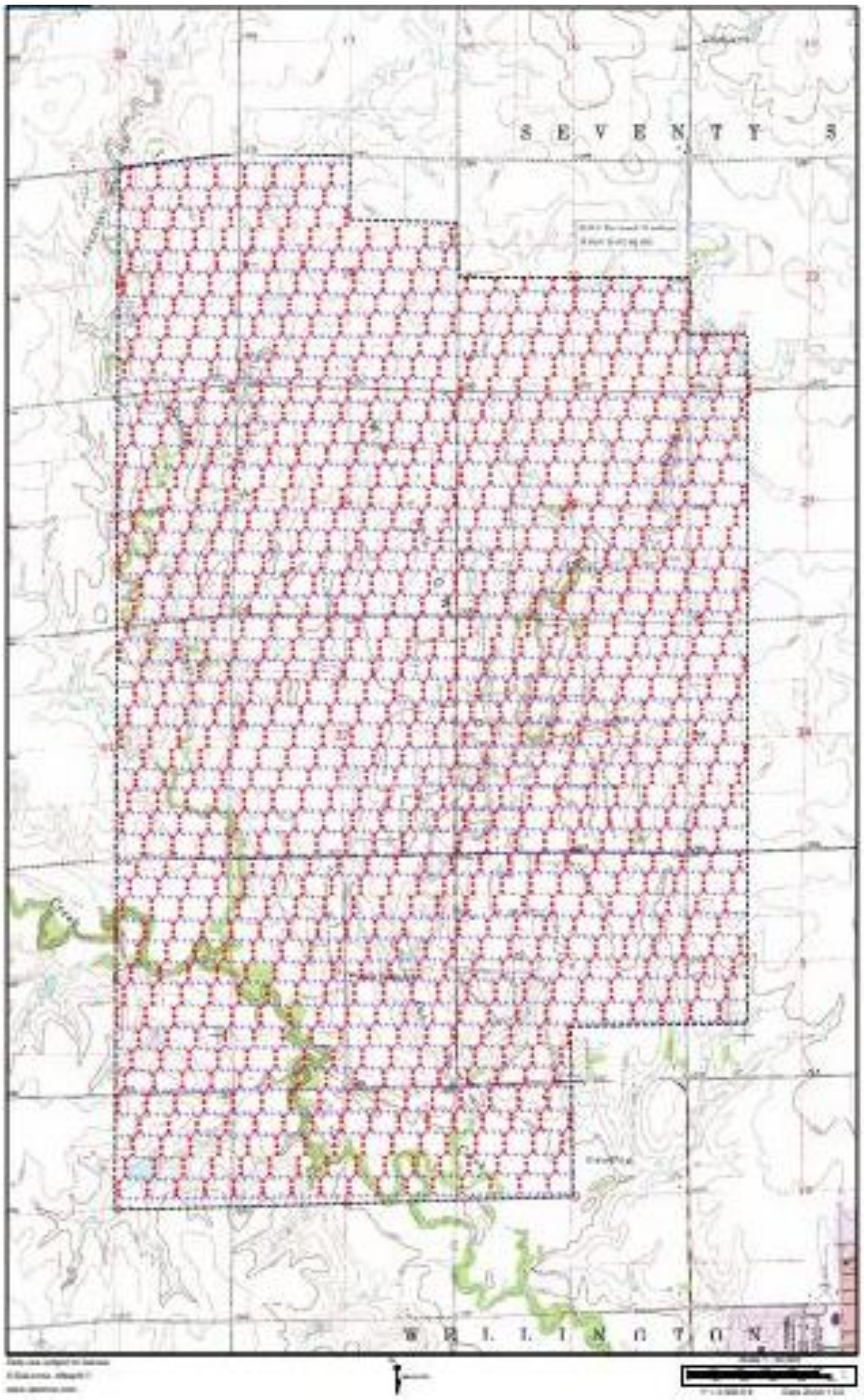

Figure 3.3. Wellington KGS 3D seismic acquisition geometry plan on topographic map using Delorme 5.2 version. Survey boundary over extends the Anson-Bates and Wellington Field by 0.5 mile. (Image from Paragon Geophysical Services Inc. Report, 2010, Unpublished manuscript)

Seismic Interpretation

As mentioned by Sheriff (1980), seismic interpreters are trying ‘to reveal the meaning of wiggles’ from seismic data (Figure 3.4). In order to accurately interpret seismic data, which is a function of time, a correlation must be established with well log information, which is a function of depth. There are other wave phenomena present in the data, such as multiples, energy conversions from longitudinal shear waves and anelastic effects caused by attenuation and dispersion of the source (Steeghs and Drijkoningen, 2001). The sonic well-log is an acoustic logging tool used to measure speed of an acoustic signal. By calculating the inverse of slowness one can calculate the velocity. Density well-logs measure the density. The objective of seismic to well tie is to match seismic horizons with corresponding stratigraphic tops. Interpretation was conducted using Kingdom IHS software 2019.

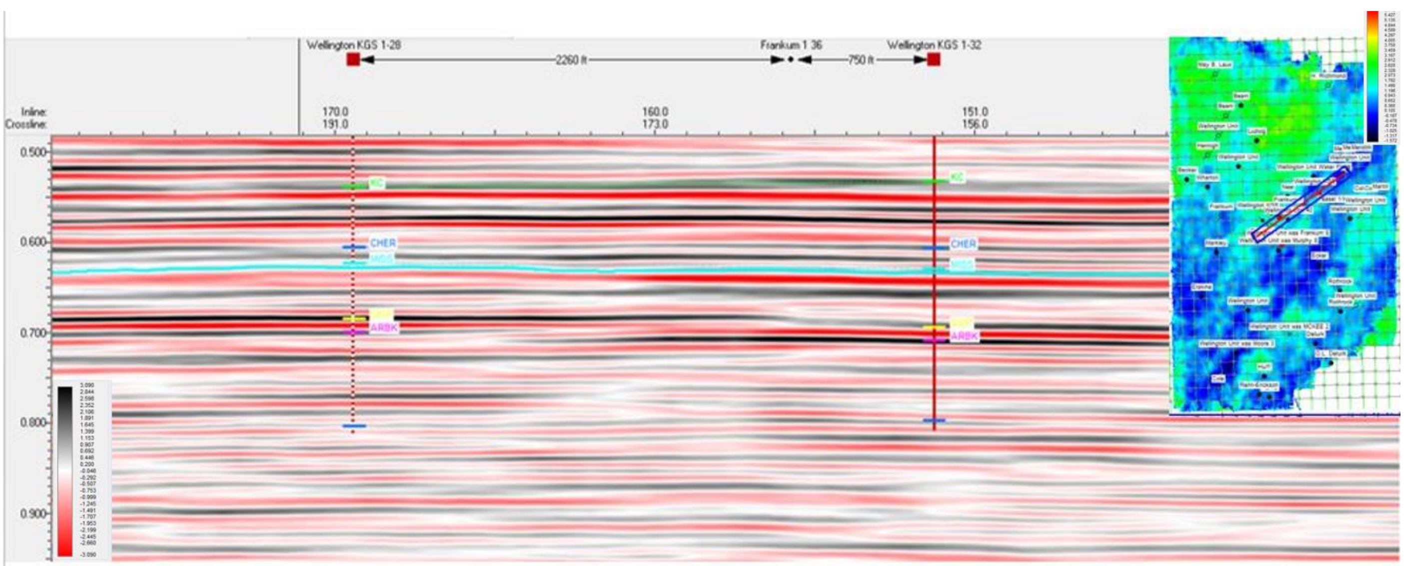

Figure 3.4. Arbitrary seismic amplitude line going through the Wellington KGS #1-28 and Wellington KGS #1-32 well. Mississippian Horizon in blue. Top right: Amplitude map showing arbitrary line.

Vertical Resolution

An important aspect when interpreting seismic data is the ability to resolve bed thickness. Resolution is limited by the bandwidth and wavelet shape (Simm and Bacon, 2014). In practical applications, tuning thickness can be considered vertical resolution. Vertical seismic resolution is defined by the ability to distinguish adjacent stratigraphic units exhibiting a contrast in acoustic propagation from variances in rock and fluid properties (Yilmaz, 2009). We can define tuning thickness by the following equations. Tuning thickness = $\lambda/4$ (Widess, 1973) Lambda (λ) is the dominant wavelet of the represented seismic data; λ is a product of velocity in meters per second) divided by the dominant frequency (in Hertz), i.e. $\lambda = V_p$ (m/s) / F_d (Hz). The dominant frequency is 1 divided by the period 'T' measured in seconds from trough to trough or peak to peak, or $F_d = 1/T$.

Well–to-Seismic Tie

Connecting geophysical well-logs and seismic data provides numerous advantages for seismic data interpretation compared to the situation where no seismic to well tie exists. A well-to-seismic tie is conducted by taking the sonic and density well-logs and calculating a series of reflections with depth, where the seismic series is shown by horizons (impedance contrasts). The well tie can then be bulk shifted and stretched or squeezed to match the seismic data. Advantages range from better identification of stratigraphic units, correlating physical properties and allowing the interpreter a chance to conduct an experiment to test the connection between the geology and the seismic data (Simm and Bacon, 2014). A synthetic tie from the Wellington KGS #1-32 that has not been bulk shifted, stretched, or squeezed can be seen in Figure 3.5 using

Kingdom IHS software 2019 version. A bulk shift with stretched and squeezed synthetic well logs will be shown later in Chapter 4.

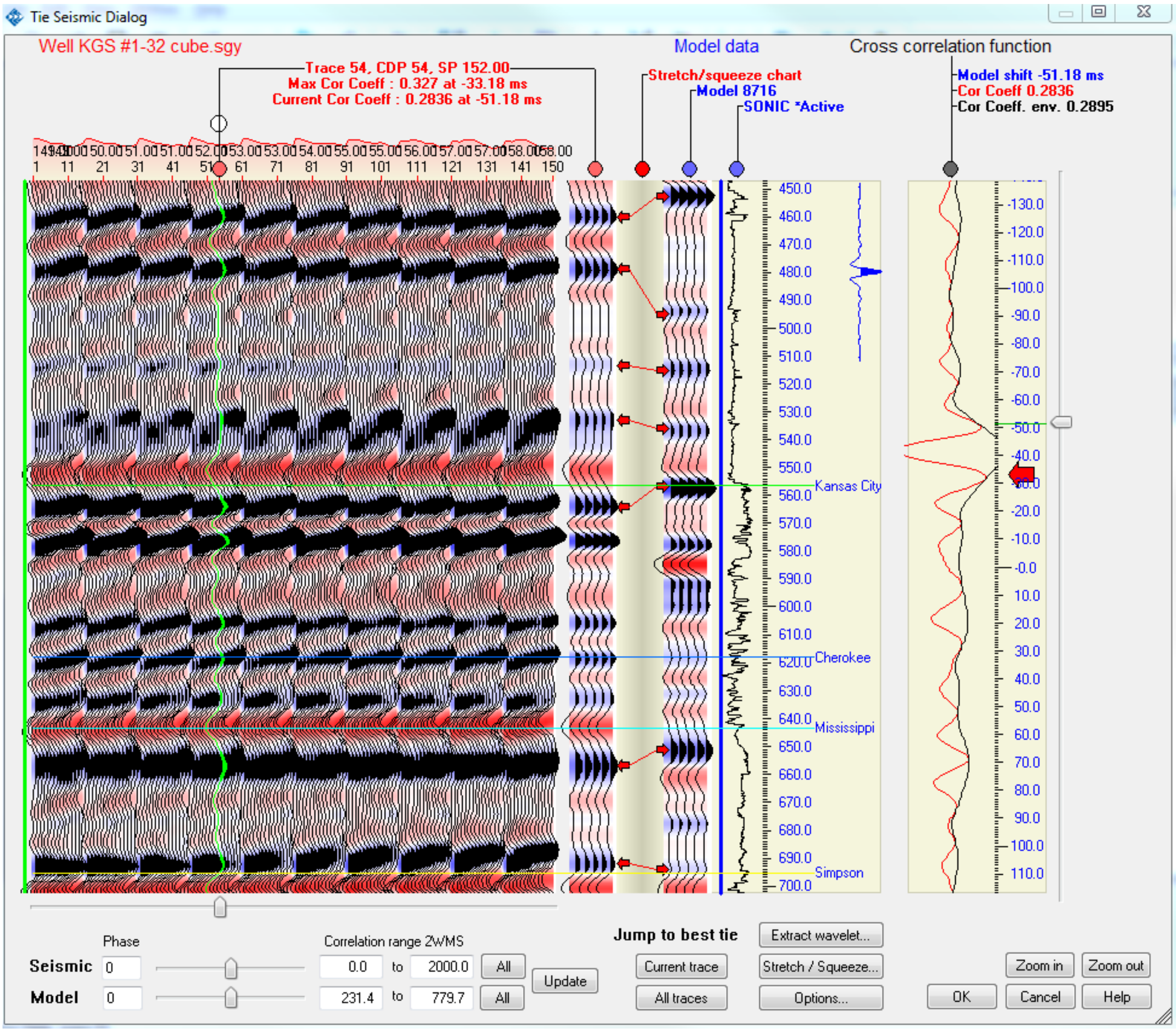

Figure 3.5. Seismic to well tie of the Wellington KGS #1-32 that has not been bulk shifted, stretched, or squeezed.

Horizon Tracking

Tracking horizons was conducted manually due to the crust being an anisotropic medium with varying velocities and faulting throughout the Mississippian formation. For instance, in a vertically fractured limestone reservoir, velocity in the fractured direction is lower than velocity in the direction perpendicular to the plane of fracturing (azimuthal anisotropy) (Yilmaz, 2009). A potential cause for vertical fractures are from uplifts and faulting which break the ridged limestone. Tracking was done manually around faults to limit the chance of picking the incorrect horizon due to faults in the study area. The horizons were traced along surfaces of amplitude diminishing and near tuning. Figure 3.6 is an example of this as amplitude changes due to changing lithology and petrophysical conditions.

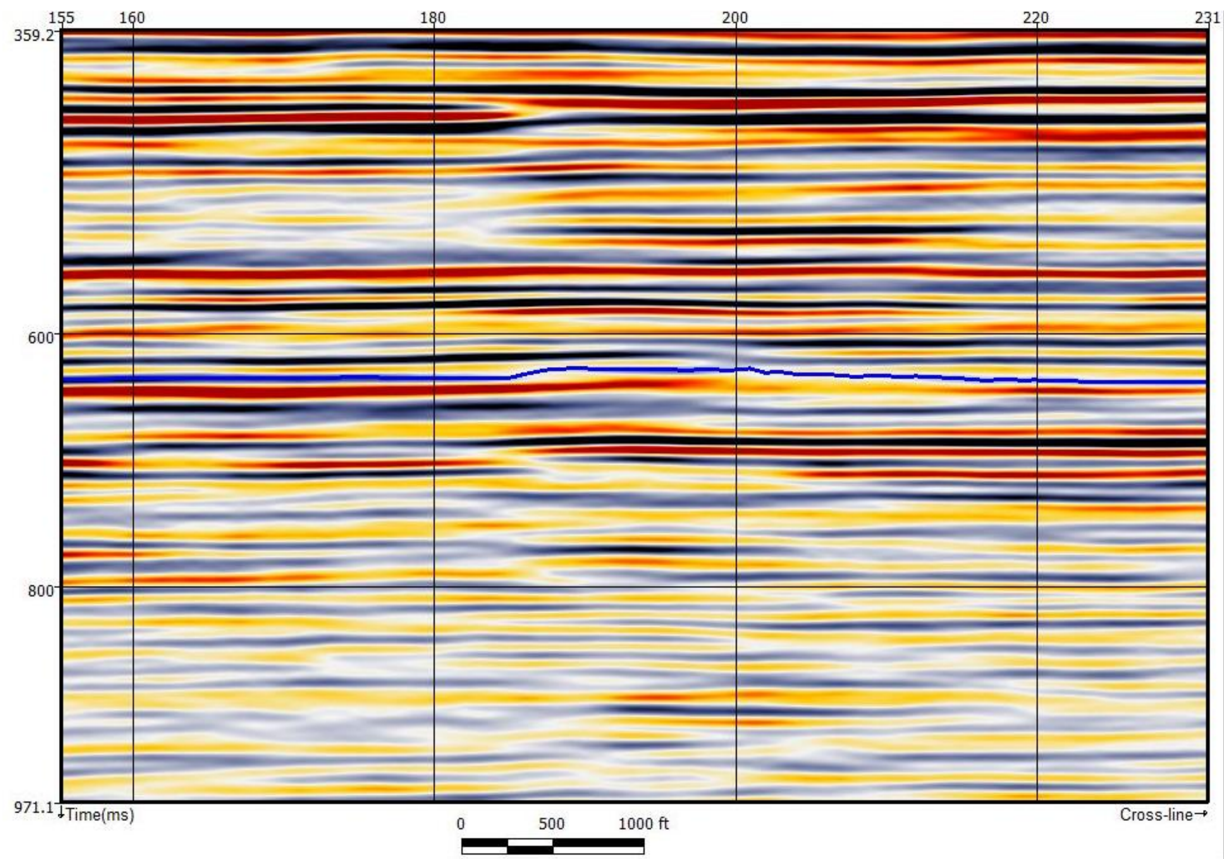

Figure 3.6 Horizon tracking using the change in amplitude along the Mississippian (blue horizon).

Seismic Attributes

A simple approach to mapping reservoir properties from seismic data is to apply a transform to the seismic attribute map based on cross-section plotting of seismic and well data (Simm and Bacon, 2014). For example, Stanulonis and Tran (1992) describe how porosity can be linearly related to seismic amplitude on the North Slope of Alaska. Post-stack amplitude inversion is used to estimate the acoustic impedance model of the crust that is connected to petrophysical properties within the reservoir.

The specific goal(s) for this study is/are reservoir characterization based on structural and stratigraphic inversion of seismic data and calibration of petrophysical properties derived from well data (Yilmaz, 2009) by using a data-driven unsupervised neural network. Seismic attributes are a suite of tools that can be used for enhancing the amplitude of the seismic signal and provide interpreters numerous ways to view the data. Inline, crossline, time slice, and horizons or seismic volumes known as an isochron are all options for interpreting seismic data. Having the ability to view the data allows seismic attributes to provide detailed aspects that represents changes in acoustic impedances.

Seismic data volumes are large data volumes and consist of highly repetitive data. It is now established that their analysis can be optimized by applying efficient data reduction algorithms that preserve essential features of the seismic character (Coléou et al., 2003). In order to utilize seismic data, a time slice (Figure 3.7) was calculated to show structure of the interpreted Mississippian horizon. Seismic attributes were calculated using Kingdom IHS and Opendect.

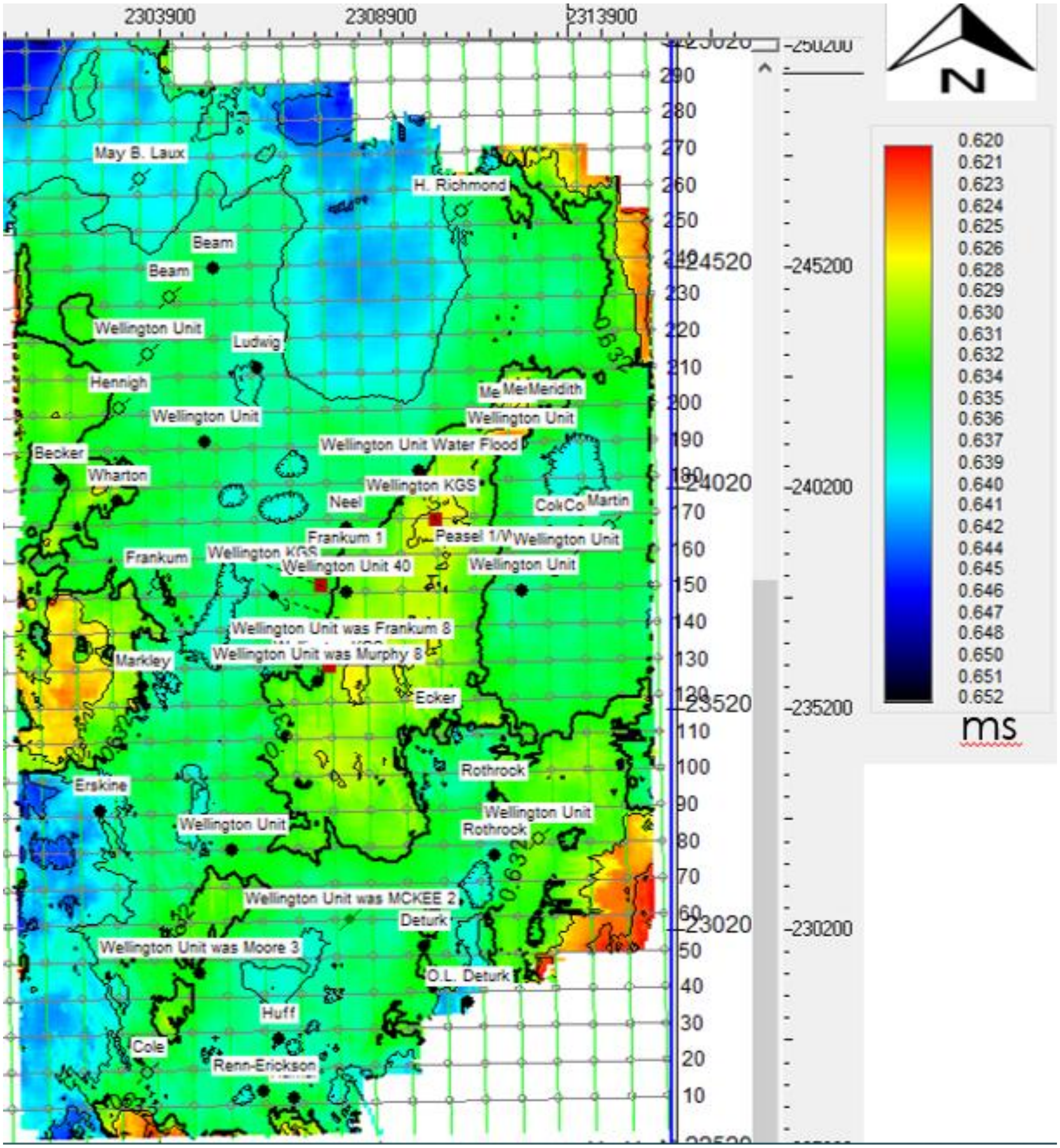

Figure 3.7 Time structure map of the Wellington field.

The specific seismic attribute used as inputs for the unsupervised neural network consisted of instantaneous seismic attribute (bandwidth and peakedness) and a time interval (volume) attribute (Root mean square energy) which are all related to seismic amplitude.

The volume attribute used for the unsupervised neural network are Root Mean Square (RMS) Energy, which is the sum of amplitude squared in a time-gate. The Root Mean Square Energy attribute highlights packages with different reflection strength and can be interpreted as variations in lithology and porosity. Root Mean Square Energy is a volume attribute that measures the reflectivity amplitude in a time gate. The higher the energy, the higher the amplitude (dGB Earth Sciences). For example, a porous reservoir containing fluids or gas will create a higher amplitude seismic signal than one without fluids or gas due to the change in density and velocity.

Instantaneous Bandwidth was introduced by Barnes (1993) as a complex-trace attribute that can be estimated from the local spectrum. Bandwidth measures the absolute value of the rate of change of the trace envelope amplitude, which equates to the absolute value of the envelope time derivative. Steeghs and Drijkoningen (2001) defined local bandwidth as the variance around the mean frequency.

The Instantaneous Peakedness attribute is related to amplitude that is used as an input for the unsupervised neural network. It is the action between the extreme values and the distance between next and previous zero crossing.

Travel-times, however, are only one of the two components of recorded seismic wavefields: amplitudes are the other component. After seismic attributes are calculated, petrophysical properties within the depositional unit can be conducted by inversion of reflection amplitudes (Yilmaz 2009). The specific petrophysical property of interest is porosity.

The similarity from each attribute anomaly calculated of each can provide details on continuity of the Mississippian horizon and details within the reservoir. This continuity of each attribute may reflect a geologic cause that has shaped the reservoir rather than artifacts related to processing or acquisition. The Nemaha Uplift system illustrated in **Error! Reference source not found.**, illustrates the en-echelon character that can affect reservoir conditions shown in seismic attributes in the following chapter.

Unsupervised Artificial Neural Networks

An artificial neural network use an algorithmic process that recognizes vector quantization and self-organizing maps from seismic attributes. Unlike the supervised approach that uses seismic attributes as the input layer and uses porosity well logs as a layer to guide the neural network (Ohl and Raef, 2014) an unsupervised neural network does not. Unsupervised artificial neural networks are used by all other artificial neural networks but differ by not biasing the outputs (Coléou T et al., 2003).

This study emphasizes the data-driven approach using unsupervised neural networks. The objective of the facies classification process is to describe enough variability of the seismic data to reveal details of the underlying geologic features (Coléou et al., 2003).

Unsupervised neural networks encompass all neural classification methods but differ on not biasing the outputs (Coléou et al., 2003). Unsupervised neural networks are based on recognizing self-organizing patterns to describe seismic facies maps (Zhao et al., 2015). Using the unsupervised mode, attributes at specific locations in a specified pick set are clustered (segmented) into the specified *number of classes*. At each iteration, when a vector of values has been assigned to a cluster, the cluster center is moved to minimize the (Euclidean) distance with the different vectors of attributes values. In the application phase the input attributes are compared to each cluster center. The input is assigned to the winning segment, which is a number from 1 to N, where N is the number of clusters. The number N was selected to represent 3 classes that could be used to correlate to the different petrophysical classes using well-logs. In addition, the network calculates how close the input is to the cluster center of the winning cluster. This measure of confidence is called a *match*, which can range between 1 (perfect match, i.e. input and cluster center are the same) and 0 (input and cluster center are completely different)" (dGB Earth Sciences, 2019).

Computer Tomography Scans

X-ray micro-computed tomography (CT scans) is an emerging technique used for digital rock physics (Madonna et al., 2012). It allows analysis of representative volume with a resolution to the nanometric scale (Holzer and Catoni, 2011). Computed Tomography Scanning (CT scan) is a non-invasive method initially used by the medical field; however, under difference operating conditions, it can be used to image the inside of a core. A CT scan uses an x-ray source to pass the x-rays through the core being scanned to a detector on the other side. The results produce a 1D projections, but when rotating the source and receiver one can reconstruct the 1D projections into a 2D (slice) cross section using algorithms (Perm Lab (https://perminc.com/). Like cutting a slice of bread, a CT slice has a thickness which can be equated to a volumetric slice called voxels.

The x-ray attenuation is reflected as gray levels in a CT slice, which reflect the proportion of x-rays scattered or absorbed as they pass through the core. A voxel is the representation of a 3D volume in a 2D image. The attenuation of x-rays is a function of x-ray energy, void space, density, and atomic number of materials being imaged (UTCT (https://www.ctlab.geo.utexas.edu/)).

Figure 3.8 displays pictures taken at the Kansas Geological Survey core lab of the Wellington KGS #1-32 core at selected depths that represent the top three inches, middle three inches, and bottom three inches of the Mississippian reservoir. Visible porosity is contained within the chert nodules (white).

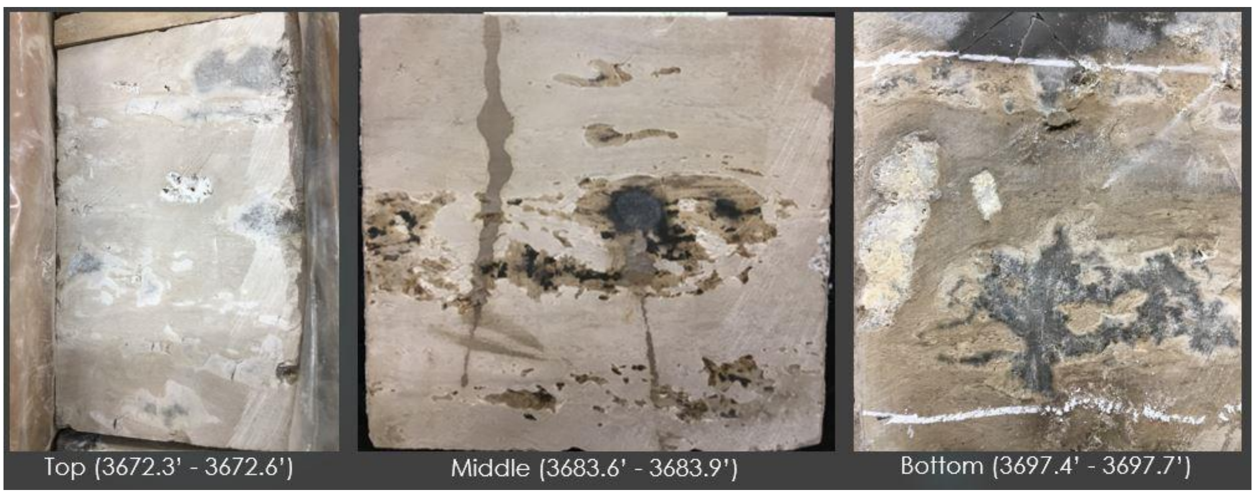

Figure 3.8. Pictures of the Wellington KGS #1-32 core slabs showing the top, middle, and bottom of the Mississippian reservoir.

In Figure 3.9 the Wellington KGS #2-32 core displays pictures taken at the Kansas Geological Survey core lab. The core was not slabbed, so transversal pictures of the core tops were taken of the top three inches, middle three inches, and bottom three inches of the Mississippian reservoir (Figure 3.8 & 3.9 are selected segments of the core and pictures taken by author). These are the sections that will be CT scanned at UTCT facilities by a ACTIS scanner.

Figure 3.9. Picture of the Wellington KGS #2-32 showing top, middle, and bottom of the Mississippian reservoir.

Chapter 4 - Results

1D seismic modeling synthetics

The Wellington KGS #1-28 was used to establish a seismic-to-well tie for the Wellington Field using SEG positive polarity. A wavelet was extracted using ten in-lines above and below and ten cross-lines left and right, with forty millisecond time window above and below the Mississippian. A replacement velocity of 10,000 ft/sec was used for the difference between the seismic datum (1,300ft) and the start depth of each sonic well-log for the four wells in the Wellington Field.

Out of the four wells initially used the Wellington KGS #1-28 had a high correlation coefficient. When making the Wellington KGS #1-28 synthetic (Figure 4.1), special attention was used to avoid excessive stretching and squeezing after the initial bulk shift. The highest correlation coefficient was over 0.52. The majority of the wells having lower correlation coefficients were caused by phase mismatch of real seismic data wavelet, which is a mixed phase (Ziolkowski et al., 1998), and zero phase/constant phase wavelet used in the convolution of the reflectivity series that was calculated by well-logs (Henry, 2000).

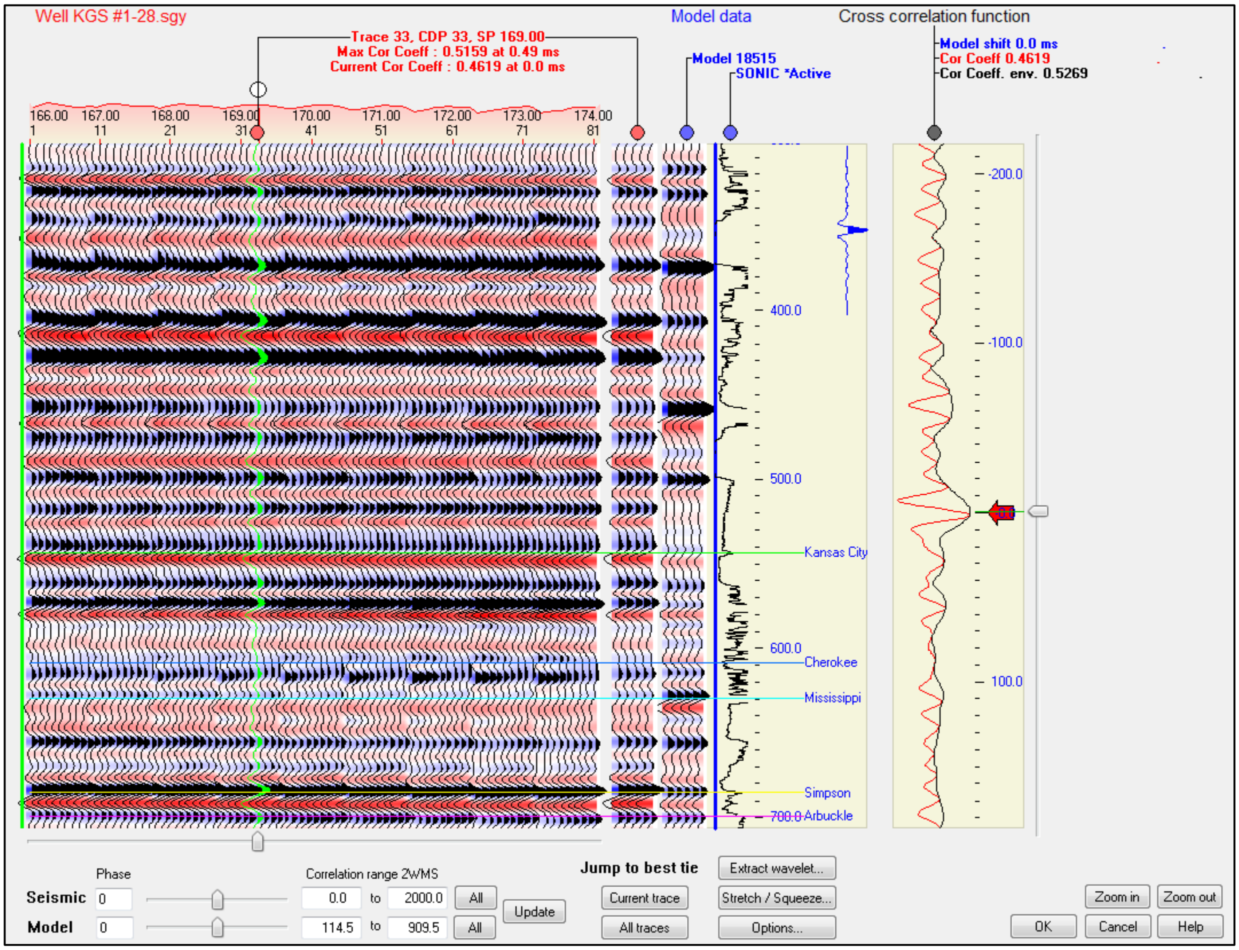

Figure 4.1. 1D synthetic log from the Wellington KGS #1-28 well after applying a bulk shift and applying minor stretching and squeezing.

Impedance porosity trends

Figure 4.2, Figure 4.3, and Figure 4.4 are plots of porosity vs impedance for the three Wellington wells: Wellington KGS #1-28, Wellington KGS #1-32 and Wellington KGS #2-32.

The impedance is calculated from well-logs using the sonic log and density log data; porosity values plotted are neutron porosity (Images produced using Microsoft, Excel, 2016). Starting from the top of the Mississippian reservoir and going 19.8 to 21.3 meters (65 to 70 feet) down using gamma ray logs, these figures illustrate this negative correlation in terms of porosity and impedance.

The Wellington KGS #1-28 is located on a structural high (see Figure 3.7) and formed in a shallow marine environment (Suriamin and Pranter, 2018). This can have an adverse effect on the porosity-impedance cross-plot, because eroded or non-deposited material isn't taken into account. Such an effect can be seen in in the lower R^2 value for the correlation for Wellington KGS #1-28 (Figure 4.1). Higher porosity (16 - 26) is concentrated around the lower impedance (27,000 to 34,000) represented by the top 20 feet (yellow and gray dots) of the reservoir. The range in both impedance and porosity gives rise to concern that the porosity prediction map will have a too wide range.

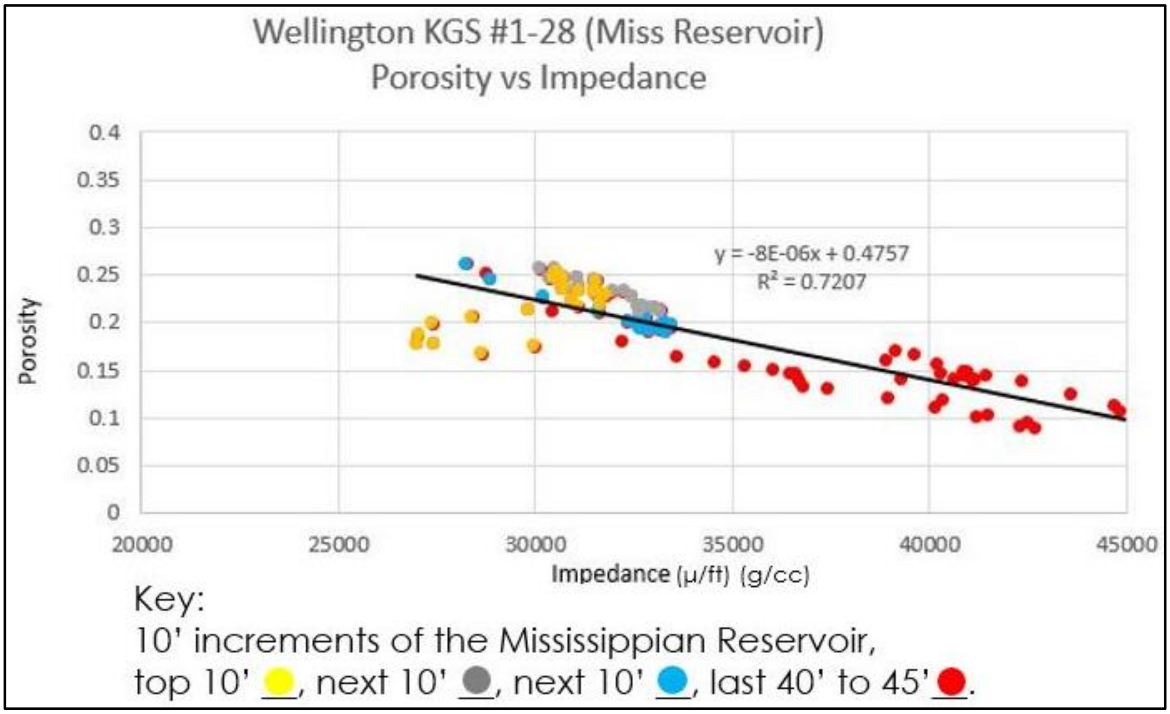

Figure 4.2. Calculated impedance using sonic and density logs against neutron porosity logs for the Wellington KGS #1-28.

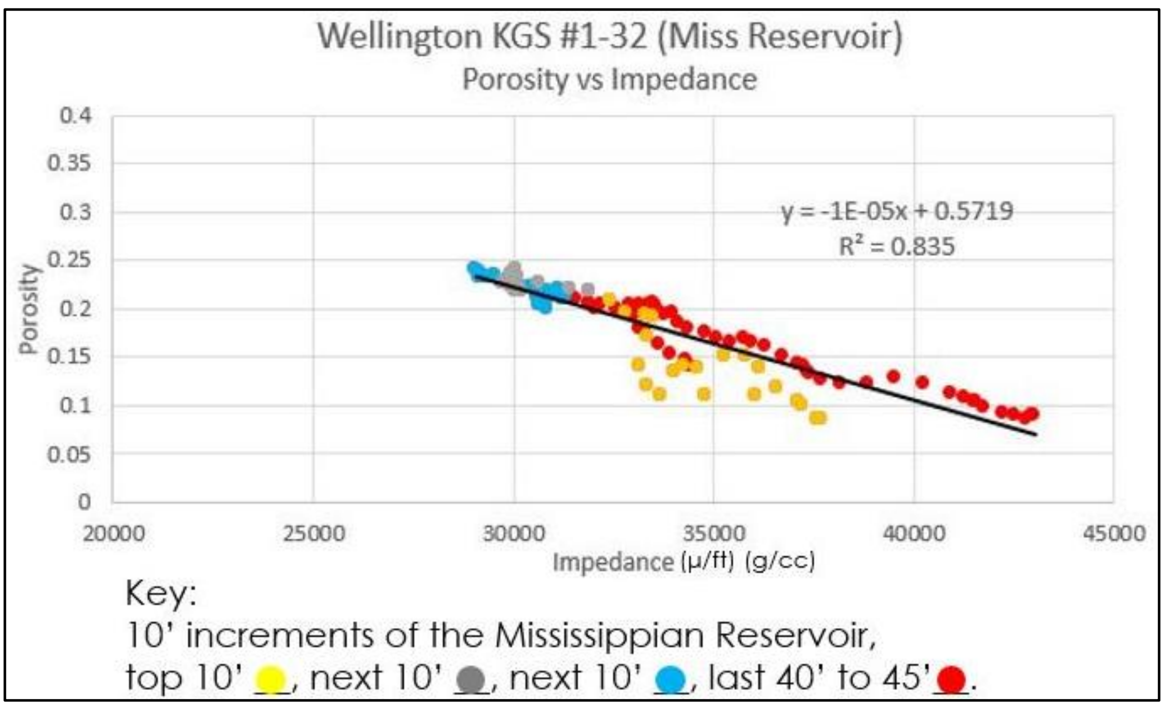

Figure 4.3. Calculated impedance using sonic and density logs against neutron porosity logs for the Wellington KGS #1-32.

The Wellington KGS #1-32 (Figure 4.3) has the highest R^2 value among the three wells, which is attributed to the distance further from the sub-parallel faulted horst block to the east. The top 10 feet of the reservoir represented by yellow dots range have an impedance of 33,000 to 37,000 and a porosity ranging from 9 to 15. Twenty feet from the top of the reservoir have an impedance of 30,000 to 32,000 and a concentrated porosity of 24. These differences are attributed to vuggy porosity and precipitation of chert (see Figure 5.3).

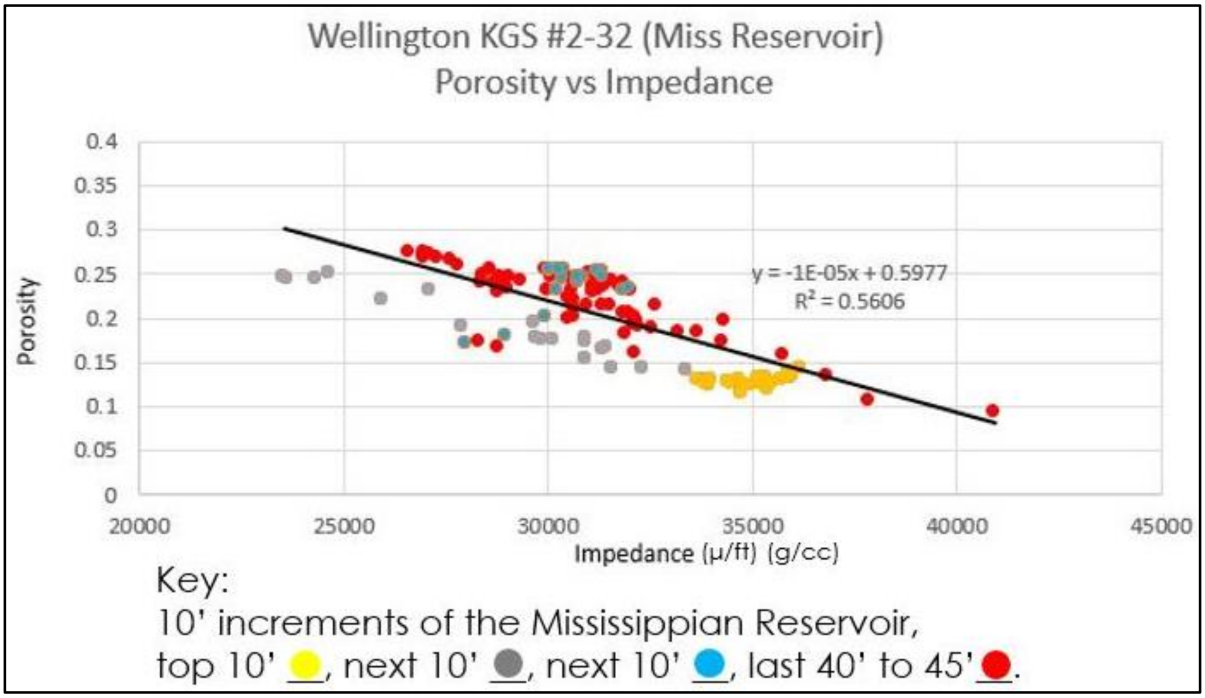

Figure 4.4. Calculated impedance using sonic and density logs against neutron porosity logs for the Wellington KGS #2-32.

The Wellington KGS #2-32 (Figure 4.4) has the lowest R^2 value, i.e. the largest deviations from the linear trend line among the three wells. This can be attributed to the Wellington KGS #2-32 being drilled near the fault. The top 10 feet represented by yellow dots have an impedance range of 34,000 to 36,000 and a porosity ranging from 12 to 14. To the west of this well, the depositional environment is interpreted to have been slightly deeper setting when compared to the environment to the east, which sits atop a horst block; the elevated position to the east could also have led to erosion not seen in the western area.

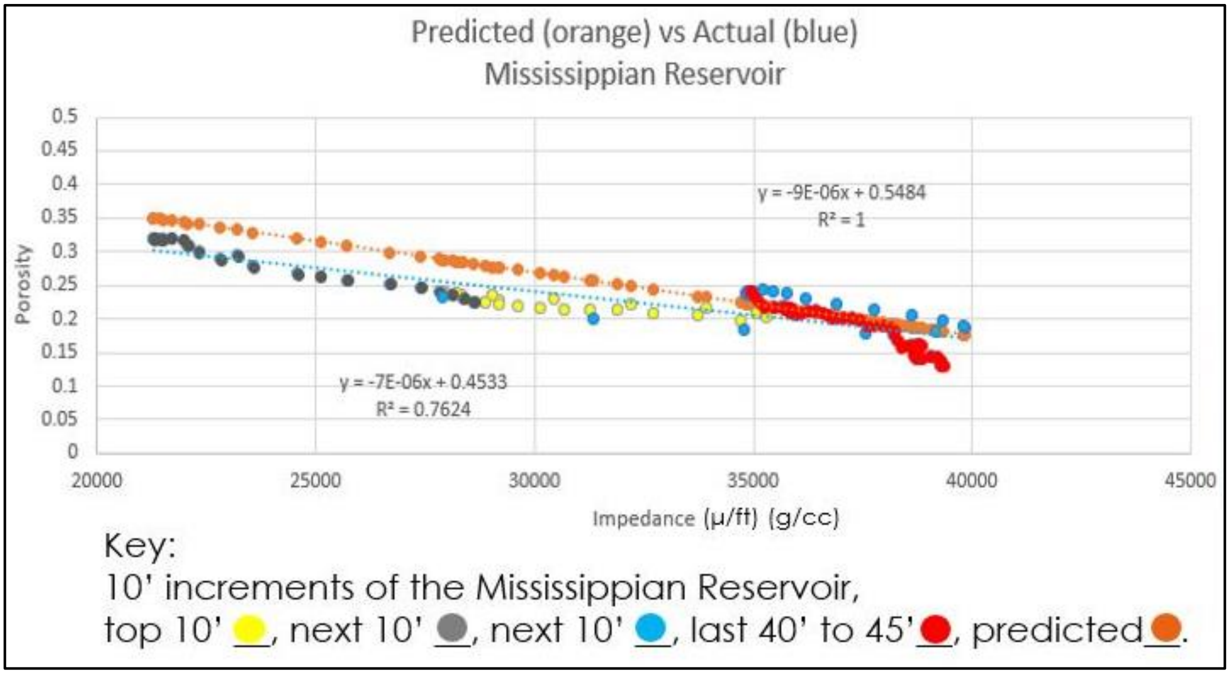

Figure 4.5. Calculated impedance using sonic log and density log plotted against neutron porosity in yellow, grey, blue and red from the Renn-Erickson #1. Average impedance vs porosity for three other wells in the study area showing a correlation of actual vs predicted.

The Renn-Erickson #1 (RE #1) (Figure 4.5) was used as a “blind” well to see how the linear averages of the Wellington KGS #1-28, Wellington KGS #1-32, and Wellington KGS #2-32 trends compares. The blue dots represent porosity-impedance of the reservoir at the Renn-Erickson #1 and the orange dots represent the average linear trends of the Wellington KGS #1-28, Wellington KGS #1-32, and Wellington KGS #2-32.

Comparing the Renn-Erickson #1 porosity-impedance with the predicted averages underestimates the prediction of porosity at impedance values under 35,000. Above an impedance of 35,000 the Renn-Erickson #1 show an over and under estimation of porosity.

Using the relationship shown in Figure 4.5, which shows that the predicted porosity/impedance in the Renn-Erickson #1 correlates with the actual impedance/porosity trends, therefore validating the method for the study wells. We have determined that porosity can be expressed as a linear function of impedance, (Equation 3) of alpha (*a* a coefficient), impedance (*x*) and the constant (*b*) (see Equation 1). The seismic trace is similar in form (Equation 3) in that the wavelet is a function of the extracted wavelet of the seismic data and reflection coefficient plus some noise, where the reflection coefficient can be scaled to predict porosity within the survey area using amplitude attributes.

$$\phi = ax + b$$

where ϕ *is porosity*, a is a coefficient, x is the impedance and b is a constant (see Equation 1)

Equation 3. A scalable linear equation in terms of porosity as a function of amplitude plus a constant.

Porosity prediction based on amplitude attribute

Geophysical well logs were used to provide petrophysical classification to the seismic attribute analysis. Seismic amplitude is related to porosity through the relationship with reflection coefficient, which is the product of density and velocity (acoustic impedance). Porosity affects the acoustic impedance by altering the density and velocity contrasts from each reflection.

Neutron porosity logs are sensitive to water, because water is so effective at slowing neutrons. The presence of water equates to having pores in which to hold it, this equates to porosity.

Figure 4.6 was constructed from wells that had modern neutron porosity logs and the amplitude attribute from Figure 4.8 in the Wellington Field. As shown in Figure 4.6, there is a correlation between seismic amplitude and porosity (determined via well logs) for most wells in the study area. Renn-Erickson #1 and Hamel #1 do not conform to this correlation, while the Meridith #2, Meridith #3, and the Meridith #4 wells exhibit a lower amplitude than might be expected (Figure 4.6). Reasons for these differences will be discussed in Chapter 5.

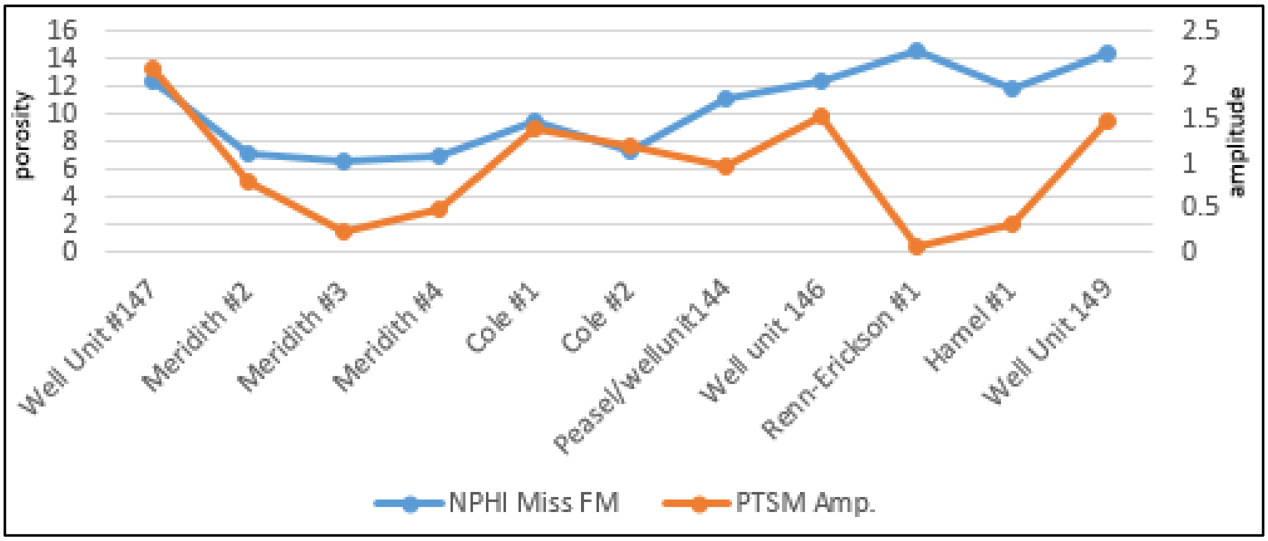

Figure 4.6. Showing amplitude horizon of the Mississippian and the average porosity of the Mississippian reservoir.

A porosity map was calculated using a composite amplitude attribute displaying higher porous zones (Figure 4.7). This was the first attribute calculated for this study for which shows there was a relationship between amplitude (Figure 4.8) and porosity.

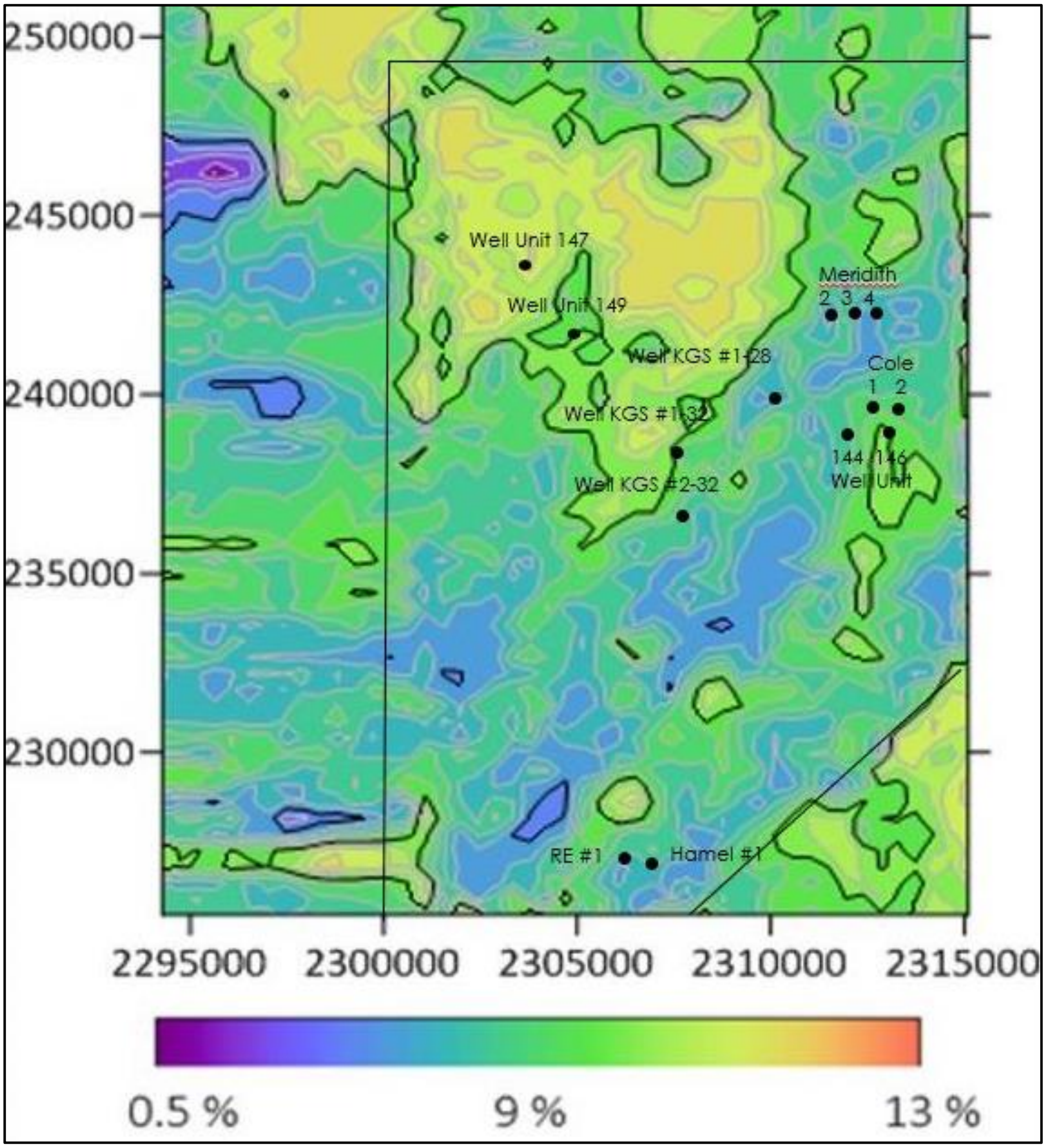

Figure 4.7. Predicted porosity map for the Mississippian reservoir facies based on composite amplitude horizon.

Extracted seismic attributes used for seismic facies

Amplitude is a principle component in seismic data for finding and exploitation hydrocarbons (Simm & Bacon, 2014). For this study, amplitude was used to capture petrophysical and lithological variances that relate to porosity measured from the well logs. The map shown in Figure 4.8 is the basis for picking seismic amplitude that are plotted with the respective neutron porosity of the reservoir as shown in Figure 4.6. In Figure 4.8 linear features are present and have a low amplitude (blue) area sub-parallel to the Nemaha uplift, having a trend of ~N030º.

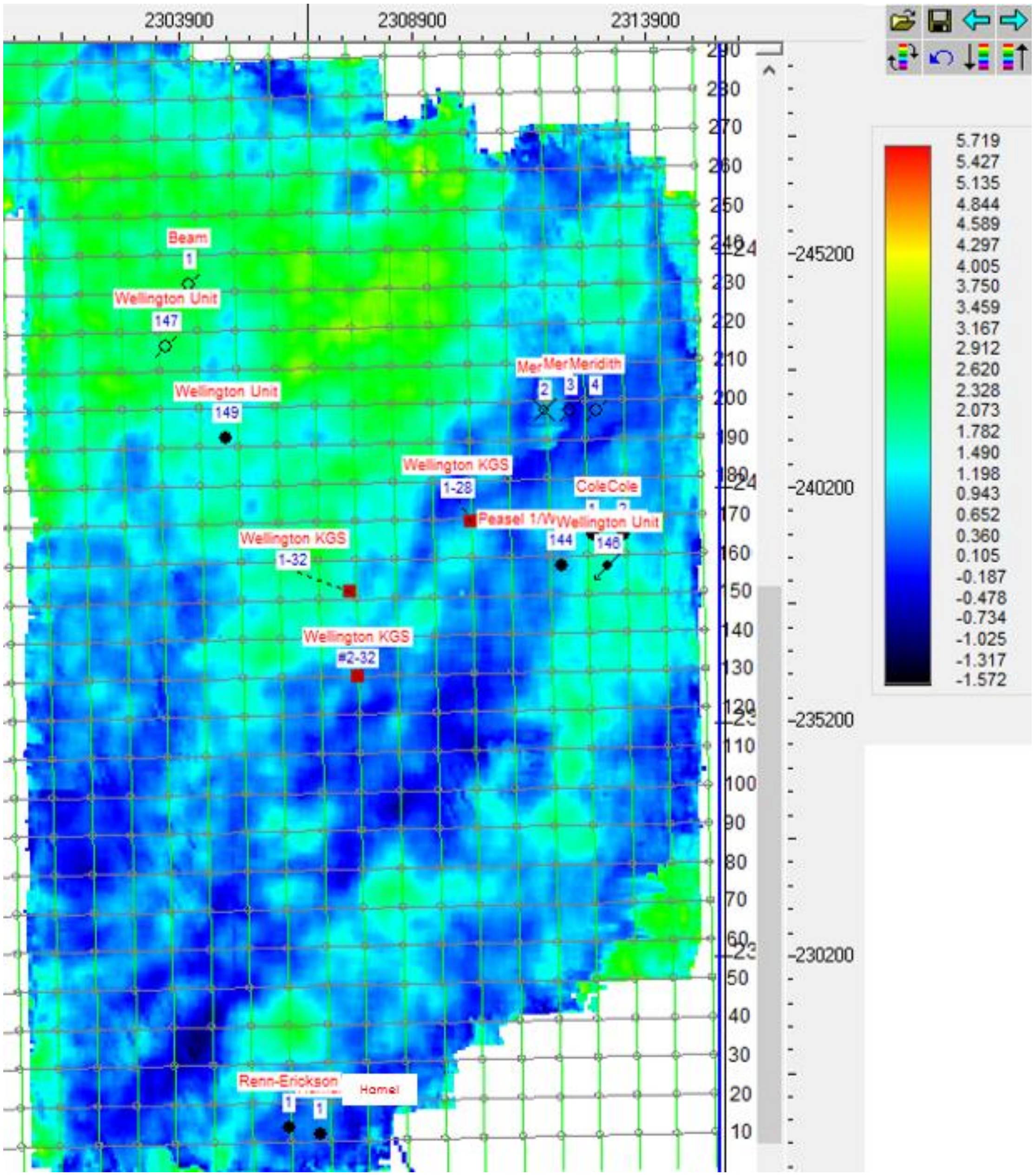

Figure 4.8 Seismic amplitude attribute rom Kingdom IHS attribute calculator that scans amplitudes and keeps the largest positive or negative amplitudes within a given horizon.

The Energy, Peakedness, and Bandwidth attributes (Figures 4.9-4.11, respectectivly) have anomalous features trending along the Nemaha Uplift, and the structural lower features have higher reservoir porosity to hold and contain hydrocarbons. Within the uplifted faulted blocks, all attributes provide insights on varying differences compared to the structurally lower areas.

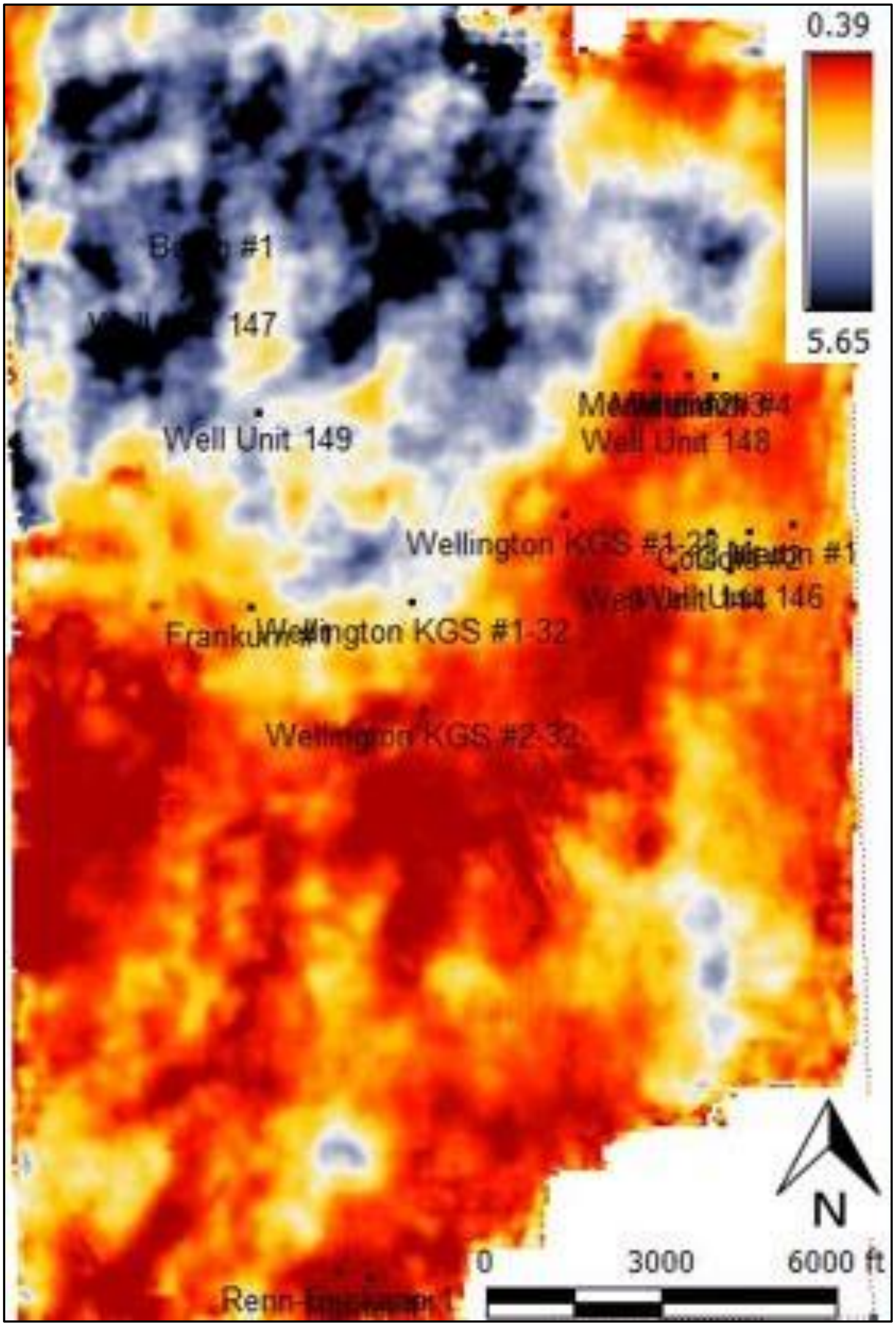

Figure 4.9. Energy attribute with a time window of -14ms above and 14ms below the Mississippian horizon. Note the linear trend that correlates with the N-NE Nemaha uplift.

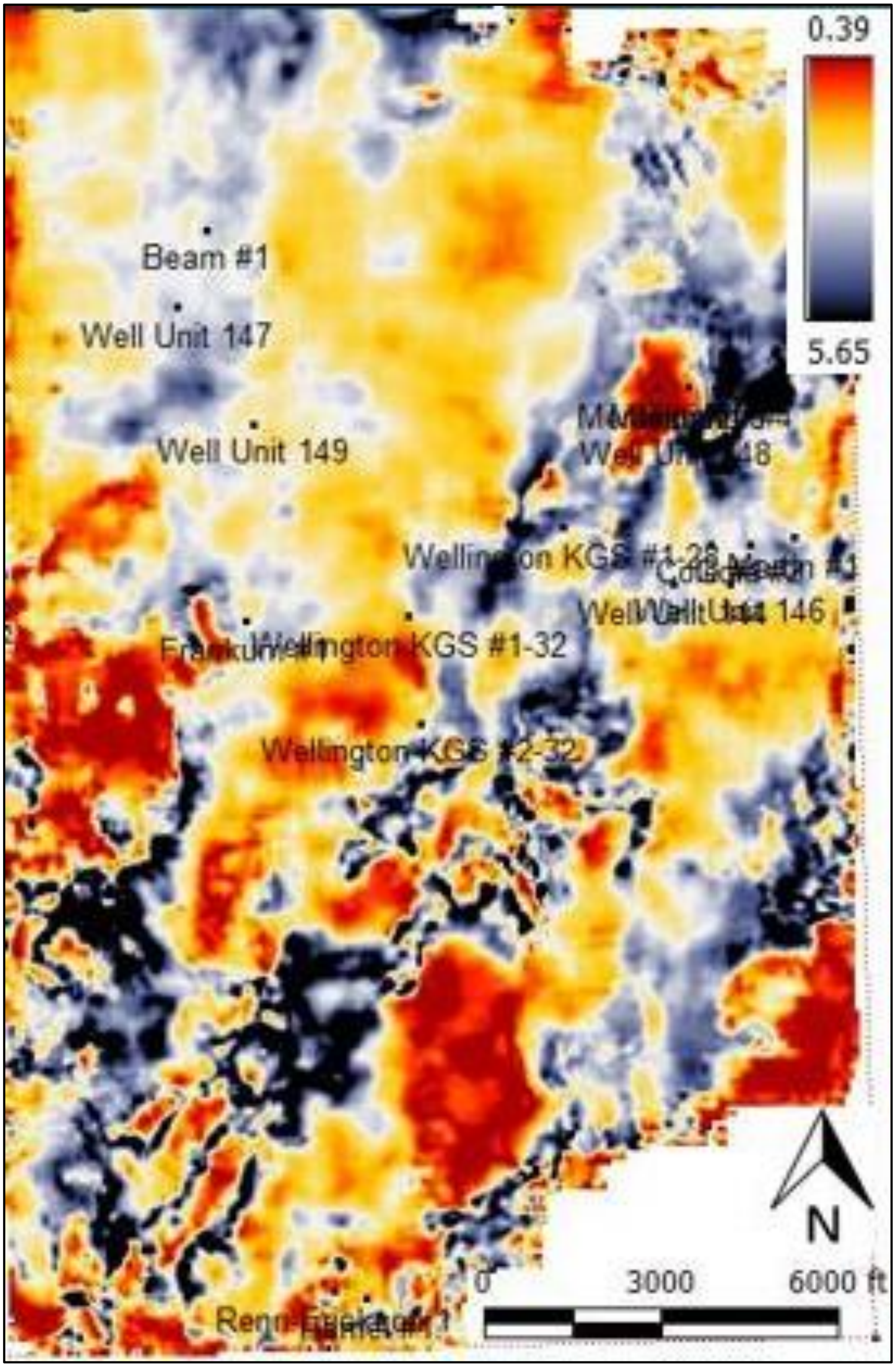

Figure 4.10. Bandwidth attribute map of the Mississippian horizon showing distinction between the areas of the survey.

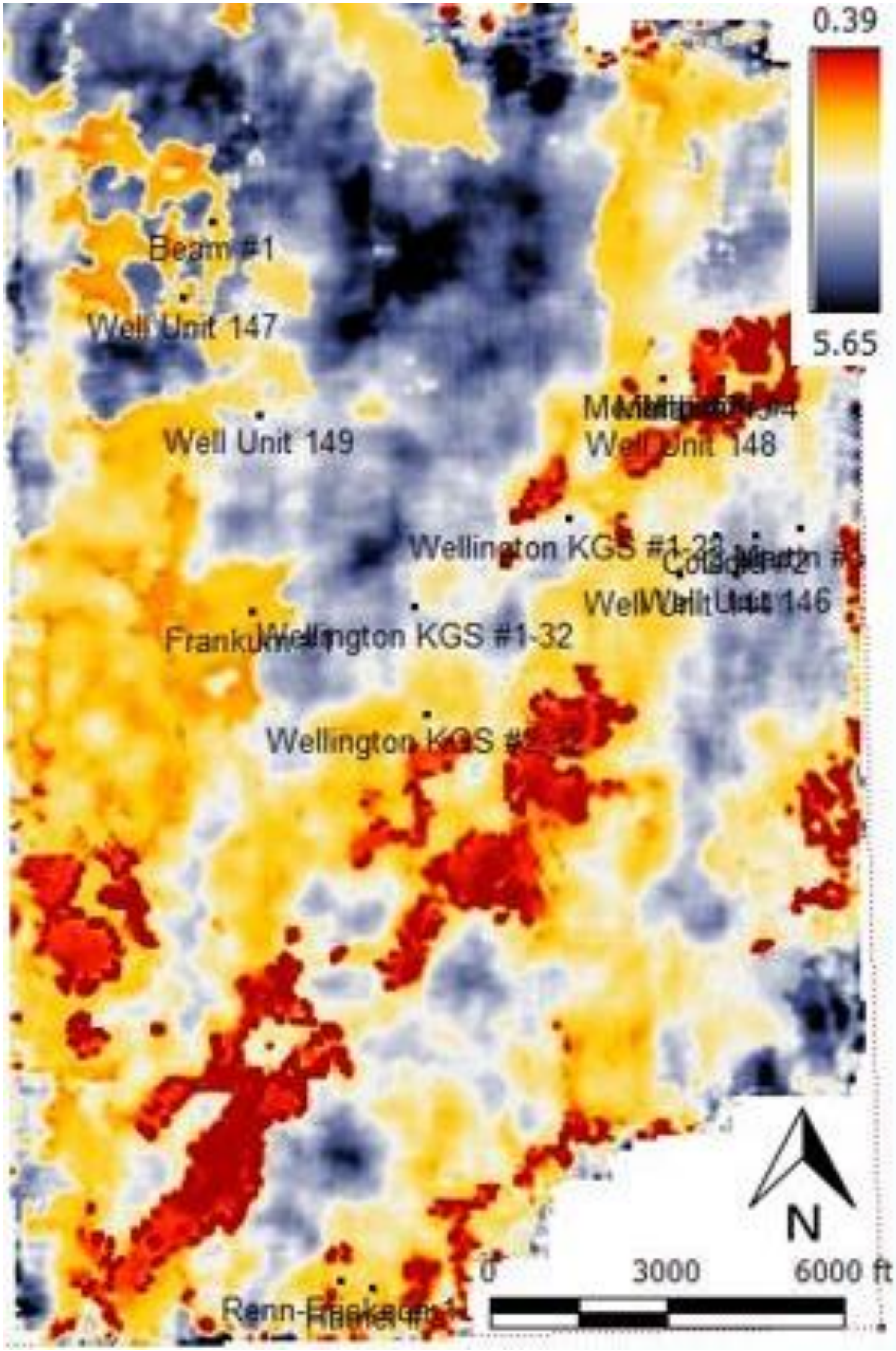

Figure 4.11. Peakedness attribute map of the Mississippian horizon showing a liner trend associated to the Nemaha Uplift .

The seismic facies prediction map was calculated using the following seismic attributes; peakedness, bandwidth, and energy (-12ms to 12ms) time window were used as the inputs for an unsupervised neural network with 3 classes, summarized in the facies prediction map shown in Figure 4.12. In this map, structural high areas can be interpreted as areas where the seismic facies are colored in red (low porosity) and structural low areas are displayed mainly in brown (high porosity) are projected to represent a different facies with a higher porosity. Features of interests from this map are associated with faults related to formation of the Nemaha Uplift. These features, e.g. faults, uplifts, etc., have altered the reservoir potential of the rocks formed due to reworking of sediments and erosion.

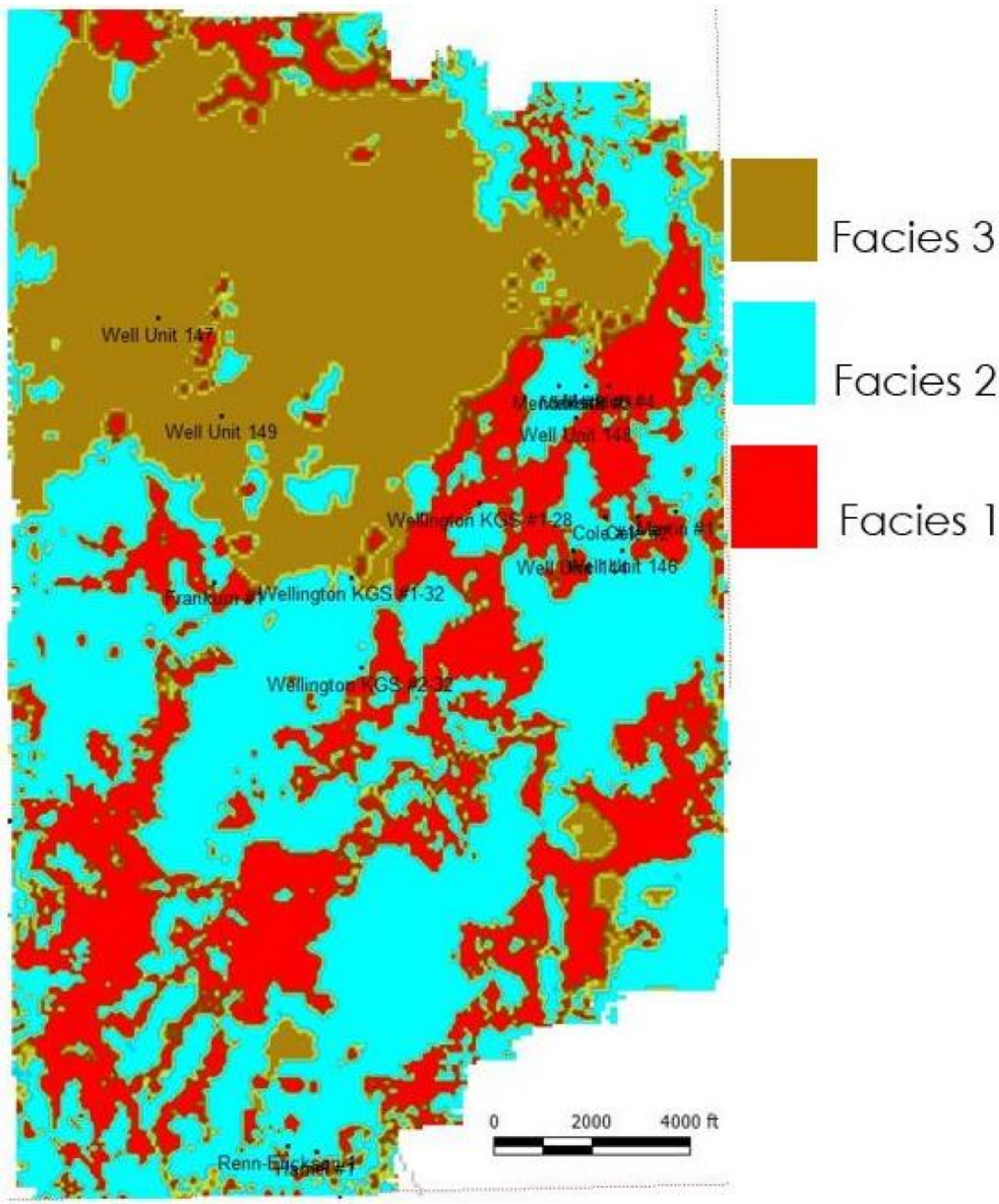

Figure 4.12. Seismic facies map of map of the Mississippian using Bandwidth, Peakedness, and Energy (-14ms to 14ms) attributes to train an unsupervised neural network. Facies 1 representing low porosity, Facies 2 representing median porosity class, and Facies 3 representing high porosity.

Chapter 5 - Discussion

Seismic Facies Characterization of the Mississippian

Boundaries of one, two, and three seismic facies are oriented in an N-NE / S-SW trend throughout the survey area (Figure 4.12) in a trend sub-parallel to the Nemaha Uplift, which indicates that the latter played a significant role for porosity in determining the seismic facies. However, Figure 4.6 suggests that not all wells conform to the correlation between (well-log) porosity and seismic impedance/amplitude. The conflicting wells are located in a portion of the survey where the Nemaha Uplift is smaller thus allowing for a regions belonging to a higher porosity seismic facies.

Figure 4.7 illustrates that amplitude can be scale by using neutron porosities logs to predict porosities from the Wellington Field. Porosities correlate with the actual porosities with exceptions from the Renn-Erickson #1 and Hamel #1 located in the southern area of the Wellington Field as shown in Figure 5.1.

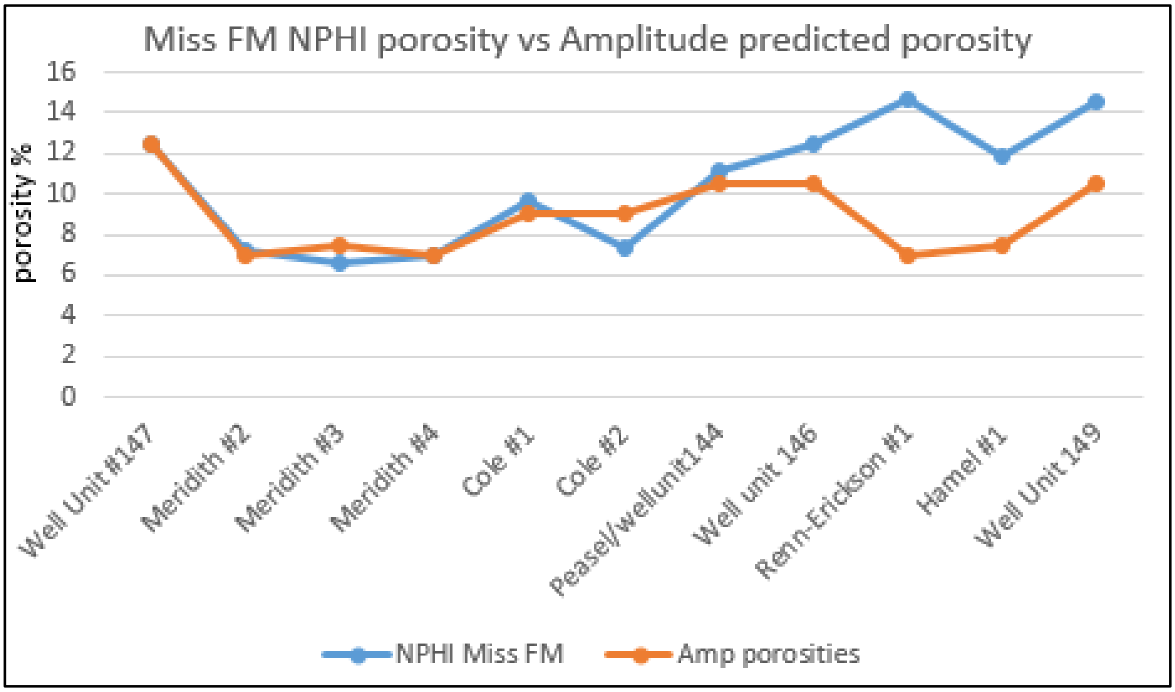

Figure 5.1. Showing neutron porosities of the Mississippian verses predicted porosity.

Results from the seismic facies (Figure 4.12) and time structural map (Figure 3.7) suggest a shallow marine environment (Suriamin and Pranter, 2018) where erosion has altered facies related to porosity and uplifts associated to change in depositional settings giving different porosity classes. The lack of high porosity reservoir on structural highs can be seen by Facies one. However, the structural lows are sites of deposition of eroded material. The eroded material, primarily limestone is a cause for secondary porosity by undergoing diagenesis. The abundance of dolomite in the structural low area was a mechanism for secondary porosity shown in by Facies 3.

The Renn-Erickson #1, Meridith #2, Meridith #3, and Meridith #4 did not correlate with Figure 4.6 and ultimately did not match with the porosity map. The Meridith wells are located on the outer boundaries of a circular object resembling a ooid shoal complex. Whereas the Renn-Erickson #1 landed in an area where porosity classes were sporadically distributed. A likely cause can be the result of small-scale faulting. Erosion was taking place in the structural highs, structural low areas received the small-scale debris flows that eroded from the structural highs during the Osagean Mississippian (Rogers, 2001). The Wellington KGS #2-32 landed on the boundary of Facies one and Facies two. This boundary correlates with a larger fault associated to the Nemaha Uplift, shown in Figure 3.4.

Figure 4.12 illustrates the ability of seismic attributes to predict seismic facies and porosity in carbonates, since the main factor in changing elastic properties in these rocks is porosity. Erosion was taking place in structural highs, whereas structural low areas dolomitized the carbonates. The prediction model was not able to identify small-scale debris flows, which are known to exist within the stratigraphy intersected by the Renn-Erickson #1, Wellington Unit 146, and Wellington KGS #2-32. Such debris flows could affect the porosity by increasing the amounts of limestone clasts which are responsible for secondary porosity. Comparted to the Facies one and two, porosity is reduced by the lack of secondary porosity; thus dolitmization has not happened which would increase secondary porosity on the structurally high areas.

On the northern half of the Wellington Field, where larger structural low areas are interpreted using the time structure map (Figure 3.7) the porosity prediction model was able to predict higher porosity (Facies three) accurately. The Wellington Unit 149 and Wellington Unit

147 are good examples of higher porosity classes that match with the well-log porosities. Referring to Figure 2.10, the highest porosity zones in the predicted porosity map can be interpreted as a dolomite with increasing amounts of muds and cherts from the structural high area. The structurally low areas, relative to the faulted horst blocks, are recipients of clastic debris flows that have been dolomitized and where the reservoir tends to be best (K., Crisler. Personal Communication, November 1, 2019) and porosity classes are the highest.

Neural networks are good interpolators, but not good in extrapolating. When training a neural network on a certain formation or interval, it is not recommended to apply it outside that formation or interval (from OpendTect, well-log prediction using supervised ANN).

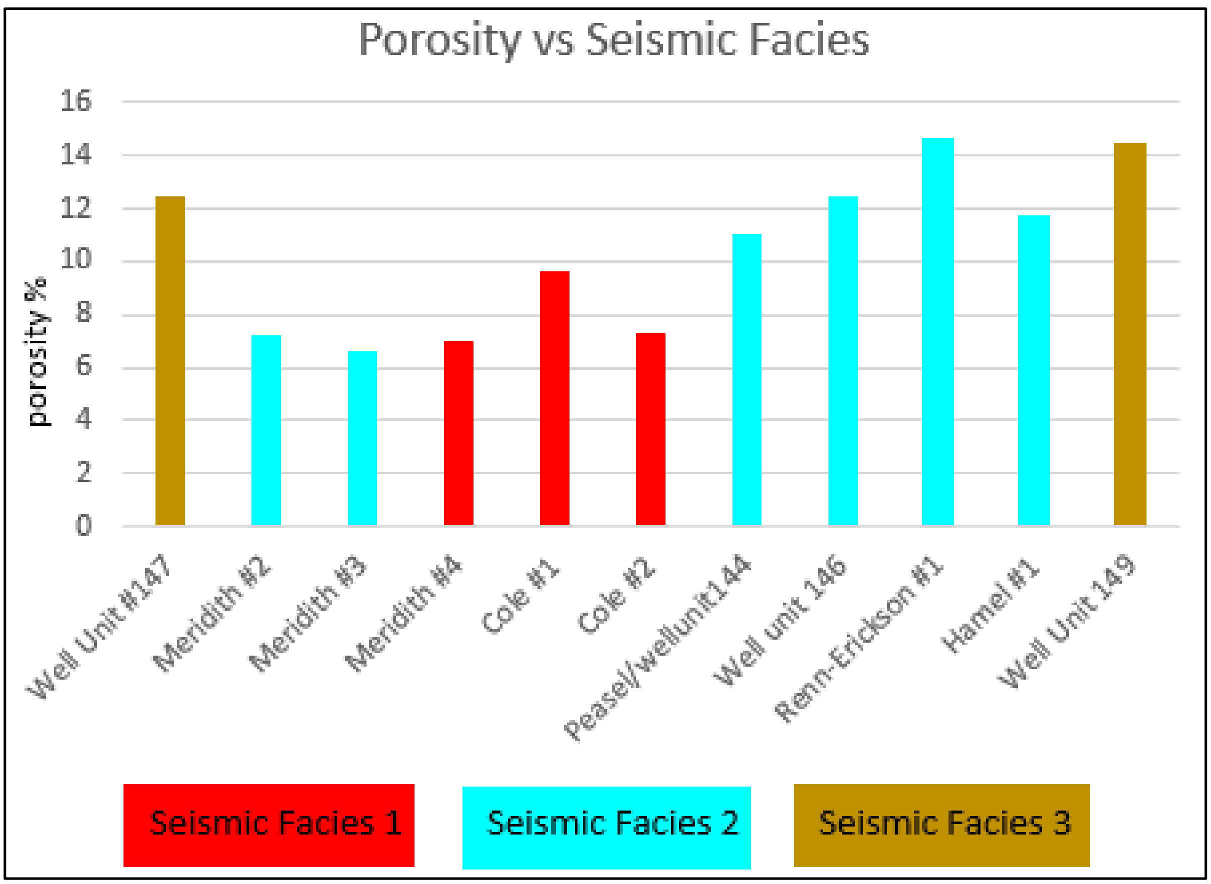

Figure 5.2. Mississippian porosities for each well through the study area and split into their respected classes based on seismic facies identified by the unsupervised neural network.

Figure 5.2 displays wells with their respective porosity from neutron well logs according to the seismic facies map. The unsupervised neural network had a large range in distinguishing lower porosity compared to the highest porosity classes. For example, Facies one had a porosity range from 7% to 9.6%, as opposed to less than 8% porosity when defined on the basis of well-logs. Thus, the porosity of Class One wells over-estimated from the model. Class two wells had the largest range picking the correct porosity. The unsupervised neural network was able to correlate a range of porosities for Facies Two of 6.6 to 14.7%, as opposed to 8% to 12% porosity range set by using well-logs. Facies three accurately in correlated porosities greater than 12%. Class one and two are closest to the faulted zones, which appear to affect the ability to predict porosities.

Figure 4.12 has a high variability in the correlating porosities from Facies one (red) to Facies two (blue), which indicate that the lower porosity facies are not registering as well with the seismic signal. This result correlates with there being smaller and fewer abundant pore spaces that do not change the elastic modulus compared to the higher porosity classes (Facies three). The vertical fractures associated to the faults have increased porosity at wells close to the fault zone which are independent from the depositional environment in low structural area are, making porosity Facies two difficult to predict. Another contributor to seismic reflection and porosity is chert.

Chert has been responsible for some of the best seismic markers, which contributes to secondary porosity associated to cool water temperatures that introduce silica precipitation. The light colored chert are often associated with late dolomite of hydrothermal (Chatellier, 2005). A more detailed description will follow in the subheading “CT scans”.

CT scans

Computed Tomography (CT) scans were conducted at the University of Texas at Austin CT (UTCT) on core samples from the Wellington KGS #1-32 and Wellington KSU #2-32 at selected intervals (top, middle, and bottom) of the Mississippian reservoir. From the scanned intervals, one image was selected from the top, middle, and bottom to provide a representation of the scanned interval. Resolution of the scans is 0.0376 mm voxels. Using the software provided by University of Texas at Austin Computer Tomography (3D Blob (Image from 3DBlob (https://www.ctlab.geo.utexas.edu/software/blob3d/), Version 2.0.2) the following images illustrate slices of the reservoir.

In Figure 5.3, scan 681 of 1661 from the Wellington KGS #1-32, represents the top part of the reservoir from 3672.3' to 3672.6' feet deep (1119.32 – 1119.41 meter). The perspective of the CT scan is from the z-axis. The different shades of grey reflect different densities, which in turn are related to differing lithologies. The lighter colored material readily reacted to HCl and has a hardness of 3 to 4, using Mohs hardness scale, indicating that this lithology is a limestone. The darker color is dolomite, which did not readily react to HCl and had a hardness greater than the limestone. The lightest color did not react to the HCl and had a hardness greater than a knife blade, indicating that this material is chert. The interface between chert and dolomite indicates hydrothermal events flushing hot fluids and precipitated in the dolomite as temperatures cooled (Chatellier, 2005).

The darkest areas (indicated by a green arrow) are pores. Located in the center of Figure 5.3 there is vuggy porosity, dominate throughout, displays a diameter of 1.1mm; pore space. Pore shapes range from circular to elliptical, reaching diameters of 5.0 mm; circular shapes predominate. The slit shape pores are primary fractures in the limestone; they have widths up to

0.3mm. Depending on the connectivity of intergranular pores, the fractured pores may increase porosity and permeability.

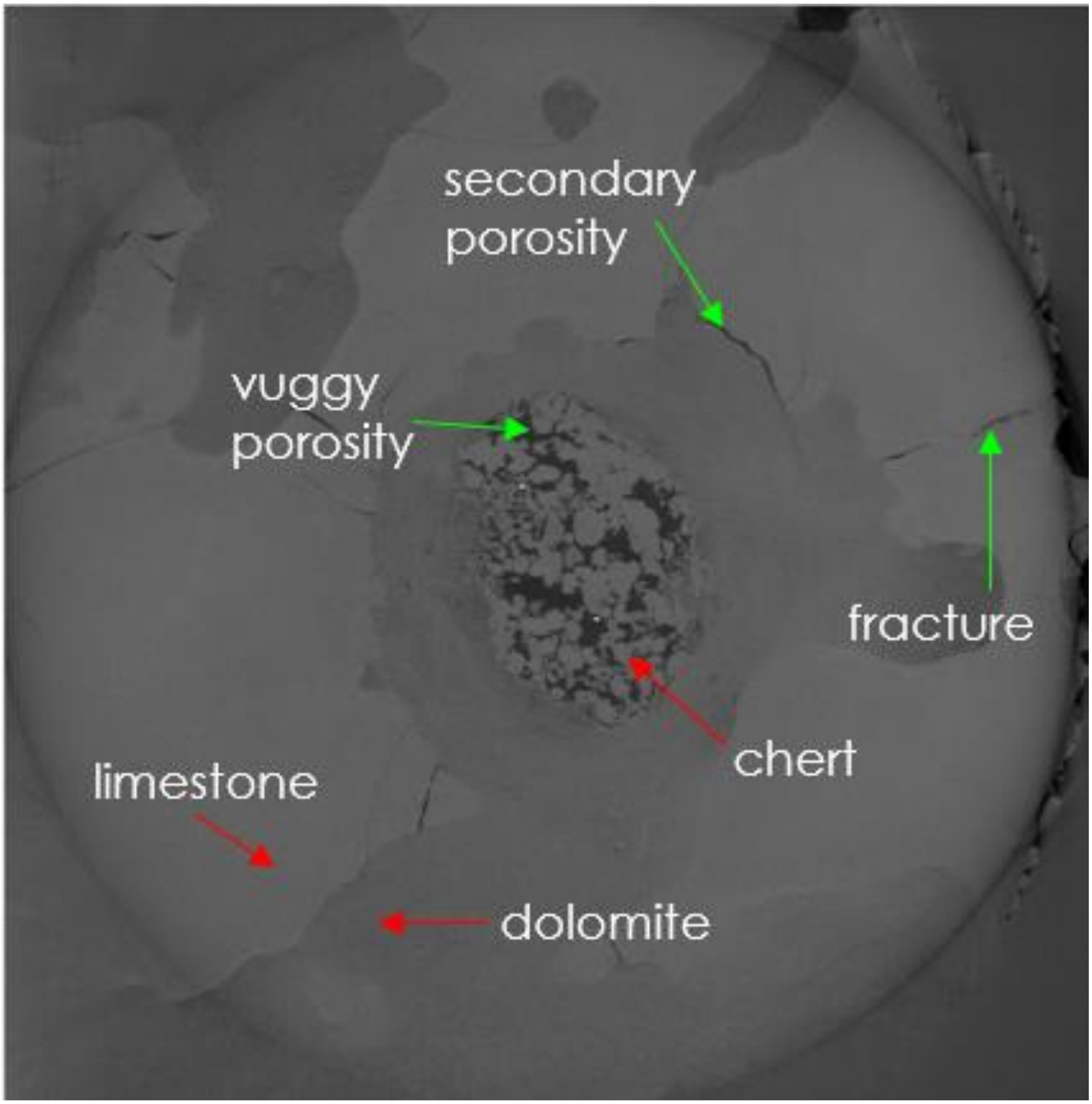

Figure 5.3. A 2D slice (681 of 1661) of a micro CT scan from 3672.3 to 3672.6 feet deep (1119.32 – 1119.41 meter) representing the top part of the Mississippian carbonate reservoir at the Wellington KGS #1-32 core. Vuggy pore spaces are centered and the fractures (width shape pores) are throughout the 2D slice.

Figure 5.4, scan 701 of 1661 from the Wellington KGS #1-32, represents the middle of the reservoir from 3683.6 to 3683.95 feet deep (1122.76 – 1122.87 meter). The perspective of the

CT scan is from the z-axis. Lighter colors portions are composed of limestone deposited first, the darker shade of grey represents dolomite, and the lightest shade of grey is chert, which formed last. The lighter colored mineral precipitated within the fracture is an unknown mineral, but likely calcite. The middle of the reservoir is primarily slit-shaped pores (fracture porosity) that have widths of 0.3 to 0.1 mm. Vuggy porosity is present throughout the scanned interval, but is not as prevalent as at the top reservoir. Pore shapes tend to be irregular with dimensions of 0.7 to 1.1mm.

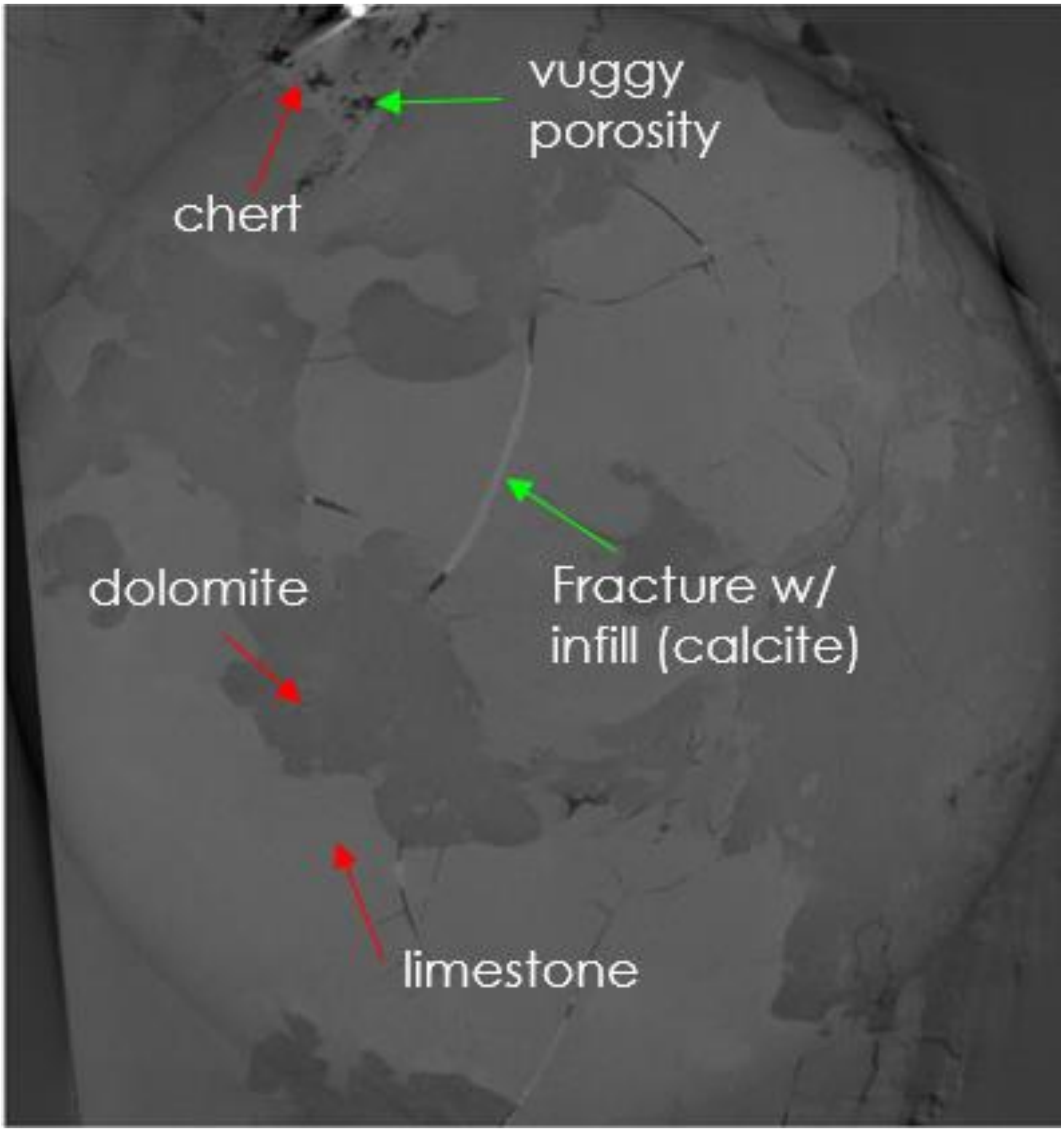

Figure 5.4. A 2D slice of a micro CT scan of 701 of 1661 from 3683.6 to 3683.95 feet deep (1122.76 – 1122.87 meter) representing the middle part of the Mississippian carbonate reservoir at the Wellington KGS #1-32 core. Vuggy pore spaces are less abundant and the fractures are more dominant (slit-shape shape pores) throughout the 2D slice.

Figure 5.5, scan 1116 of 1661 from the Wellington KGS #1-32, represents the bottom part of the reservoir from 3697.4 to 3697.7 feet deep (1126.97 – 1127.06 meter). The CT scan is viewed from the z-axis. This interval of the reservoir does not display vuggy porosity but it has fracture porosity located within the limestone indicated that faulting happened before diagenesis of dolomite and chert precipitation thus reducing porosity of the reservoir. Slit-shaped pores have a width of 0.4 to 0.1 mm.

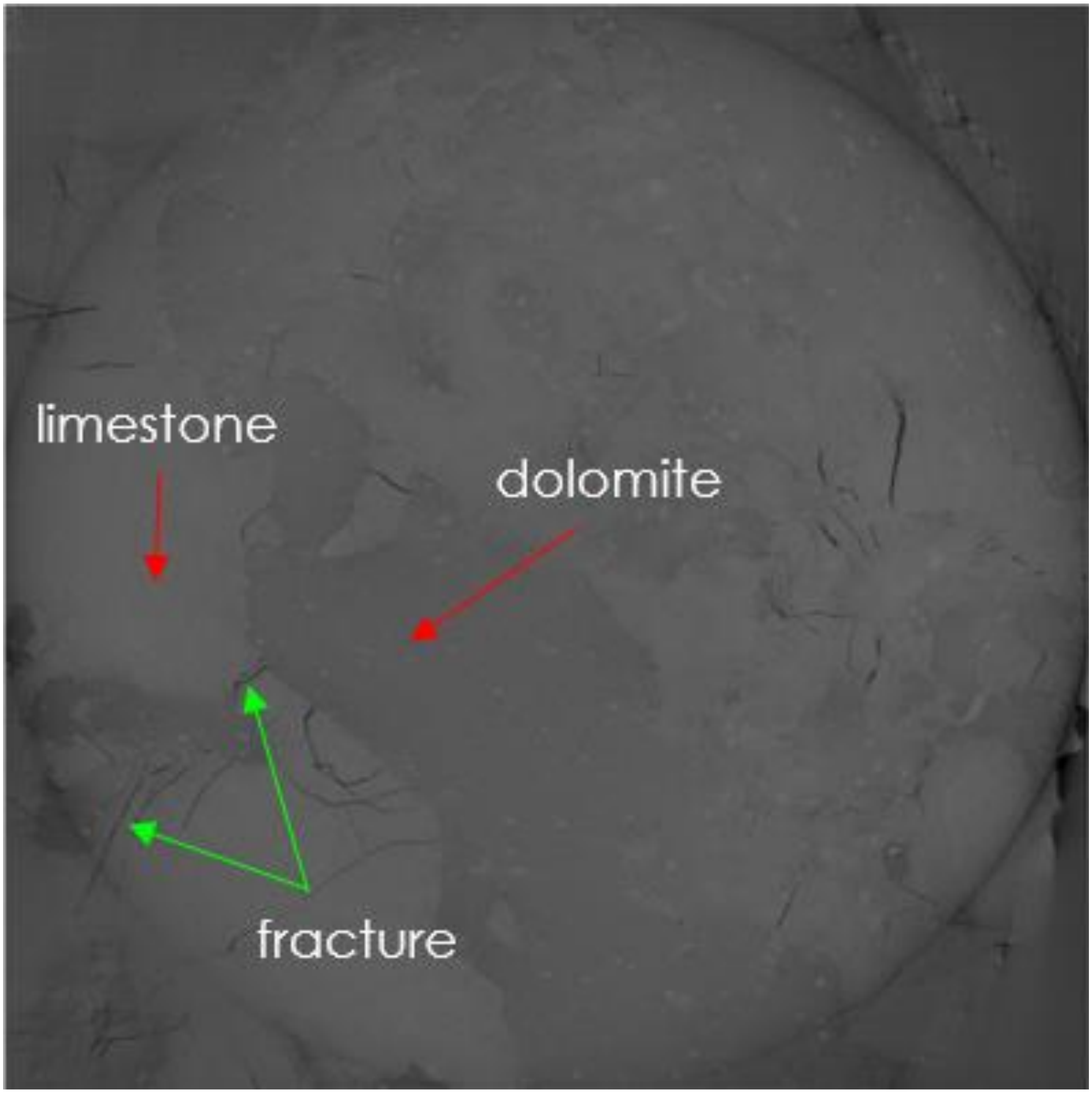

Figure 5.5. A 2D slice of a micro CT scan (1116 of 1661) from 3697.4 to 3697.7 feet deep (1126.97 – 1127.06 meter), representing the bottom part of the Mississippian carbonate reservoir at the Wellington KGS #1-32 core. Vuggy pore spaces are absent and fractures dominate (width shape pores) throughout the 2D slice.

Figure 5.6 is scan 1139 of 1661 from the Wellington KGS #2-32 representing the top part of the reservoir from 3673.3 to 3673.6 feet deep (1119.62 – 1119.71 meter). The CT scan is from the z-axis. The lighter color is the limestone, darker color is dolomite. Autoclastic brecciated dolomite and limestone clasts are present. Pores are slit-shaped, with a width of 0.2 to 0.07mm. The slit-shaped pores are on the boundary of the limestone and dolomite, suggesting secondary porosity.

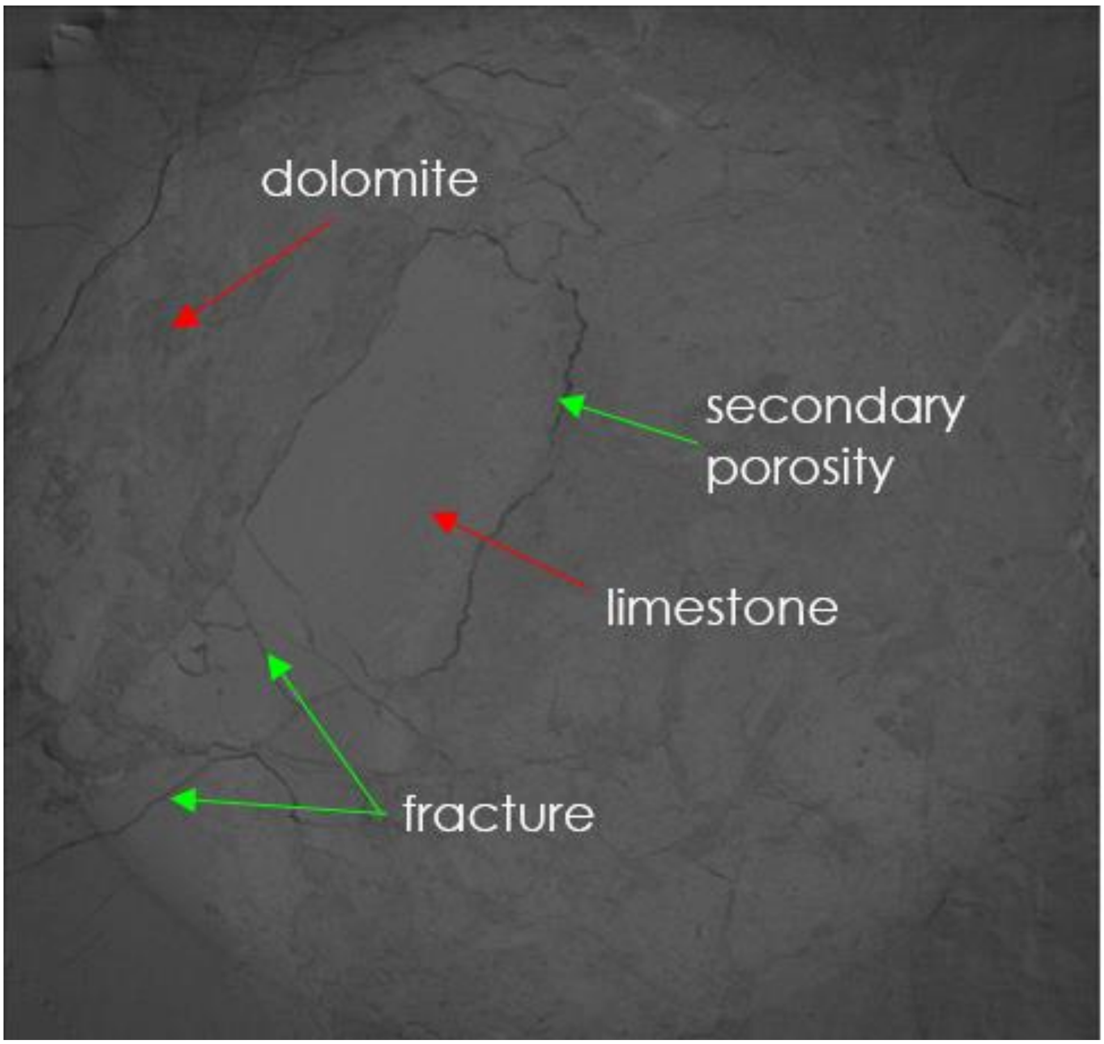

Figure 5.6. A 2D slice of a micro CT scan 1139 of 1661 from 3673.3 to 3673.6 feet deep (1119.62 – 1119.71 meter), representing the top part of the Mississippian carbonate reservoir at the Wellington KGS #2-32 core. Vuggy pore spaces are absent and fractures dominate (slit-shape pores) throughout the 2D slice. Image of slit-shaped pore surrounded by limestone clast.

Figure 5.7, scan 766 of 1661 from the Wellington KGS #2-32, represents the middle of the reservoir from 3704.3 to 3704.6 feet deep (1129.07 – 1129.16 meter). The scan is from the z-axis. This scan is primarily dolomite (darker color) with small fractures with a size of 0.08mm. The primary porosity is located within the limestone (lighter color), with slit-shaped porosity with a width of 0.2 mm. No vuggy porosity is present and chert is absent.

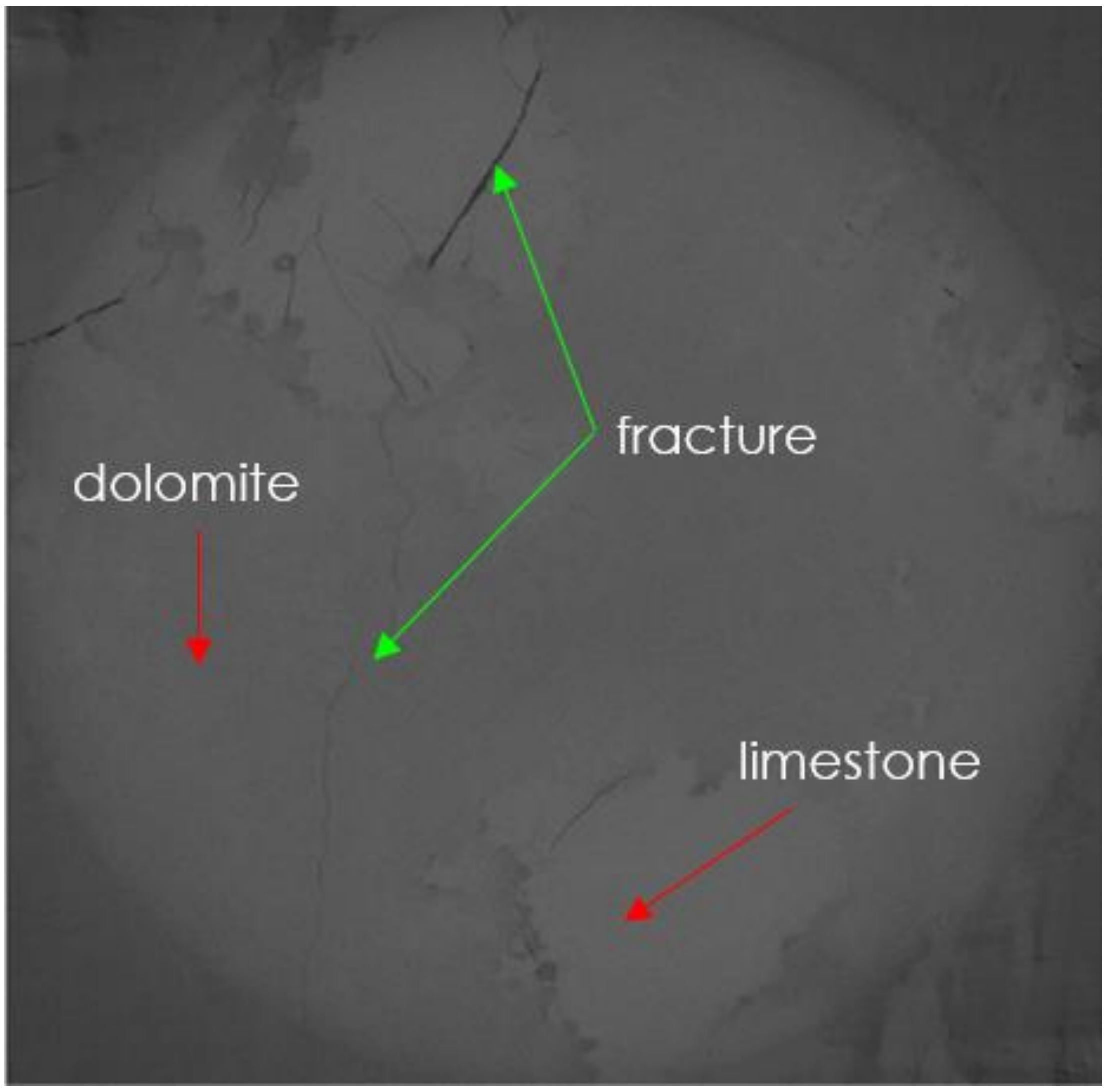

Figure 5.7. A 2D slice of a micro CT scan 766 of 1661 from 3704.3 to 3704.6 feet deep (**1129.07 – 1129.16 meter)**, **representing the middle part of the Mississippian carbonate reservoir at the Wellington KGS #2-32 core. Vuggy pore spaces are absent and fracture porosity dominates (**slit-**shape pores) throughout the 2D slice.**

Figure 5.8, scan 677 of 1661 from the Wellington KGS #2-32, representing the bottom of the reservoir from 3718.4 to 3718.7 feet deep (1133.37 – 1133.46 meter). The CT scans are from the z-axis. The image was selected due to the fracture porosity with precipitation of another mineral, likely to be chert. Slit-shaped pores have a width of 0.7 to 0.2mm. Vuggy porosity is present within large fractures where chert precipitated.

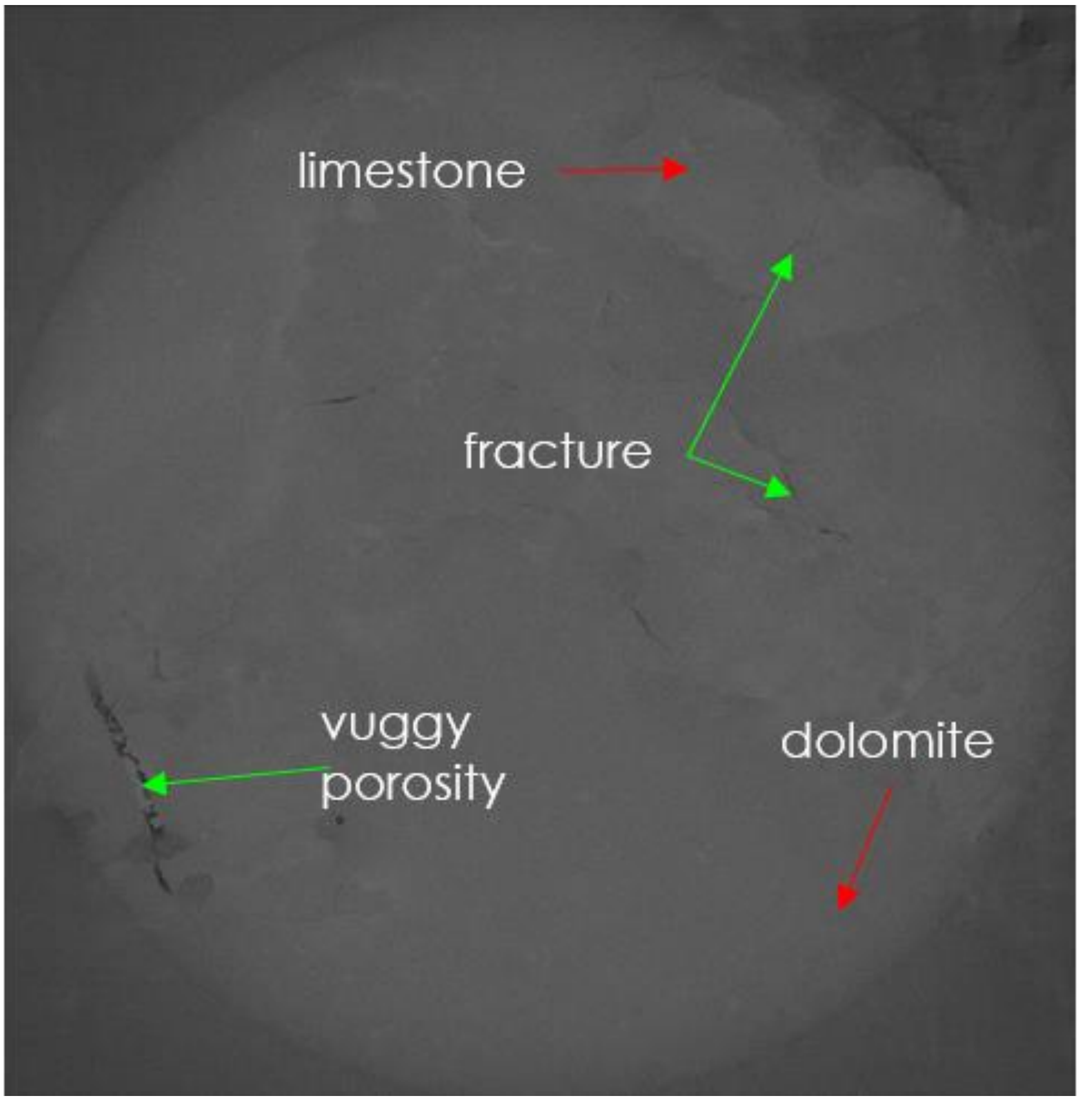

Figure 5.8. A 2D slice of a micro CT scan 677 of 1661 from 3718.4 to 3718.7 feet deep (1133.37 – 1133.46 meter), representing the bottom part of the Mississippian Carbonate reservoir at the Wellington KGS #2-32 core. Vuggy pore spaces are absent and the fractures dominate (width shape pores) throughout the 2D slice.

The CT scans indicate that the Wellington KGS #1-32 core has a greater range of pore structures from vuggy to slit-shape pores. The Wellington KGS #2-32 has less variation, and pores are primarily slit-shaped with few vuggy pores. The presence of light colored chert provides additional information on the depth of burial (light colored cherts indicated shallow burial depth) and cooled (Chatellier, 2005). A mechanism for the hot hydrothermal fluids to flow would be the faults associated to the Nemaha Uplift. The top part of the Wellington KGS #1-32 and the bottom part of the Wellington KGS #2-32 indicated precipitated and both are near a major fault.

Referring to Figure 4.3, we can see that the Wellington KGS #2-32 has the highest R^2 value and has the least variation in pore structures as shown in the CT scans. Unlike the Wellington KGS #1-32 has a lower R^2 value and pore structures range from large vugs to fractures.

Chapter 6 - Conclusions and Recommendation

Thinking in three dimensions is a critical ability for seismic interpreters (Brown, 2010). This study integrates several methods that can be utilized in the development of a field or even for exploration using a similar approach. As a seismic interpreter, integration of multiple forms of data can improve the resulting model.—Some of the data may be quantitative, like porosity and resistivity logs and amplitude, and some qualitative, like the CT scans and the interpretation of porosity and permeability inferred from resistivity well-logs.

Reservoir characterization has the challenge of integrating multiple data sets and types—such as 3D seismic data, geophysical well-logs, petrographic descriptions, computed tomography—to image and describe reservoir facies. Although there are several other methods to characterize the reservoir, predicting seismic reservoir facies allows for field-wide coverage to characterize the reservoir in terms of petrophysical variations. This study has illustrated that we can correlate reservoir facies in terms of porosity to offer operators further insights for well placement during enhanced oil recovery methods using geosequestration of carbon dioxide.

The Department of Energy and National Energy and Technology Laboratory emphasize the most critical factor for selecting candidates for CO_2-EOR is the growing consensus among experts that more detailed geophysical mapping of the remaining oil in a reservoir is needed especially in heterogeneous reservoirs. This study provides a detailed a porosity map in addition to a structure map that will aid tertiary recovery or building up-to-date models to simulate the CO_2 migration. Although many other criteria should be considered such as, pressure gradients, production history for each well, water wet reservoir vs. oil wet reservoir in the model, these efforts are not the aim but criterial that should be considered.

An optimal location to inject CO_2 would be where structure is low and has a facies (three) associated to high porosity. These two factors contribute to the enhanced recovery by putting the gas in a structural low area and allowing it to migrate/sweep upward into a structural high area to ensure the CO_2 can be dispersed throughout the formation and sweeping through the reservoir to a higher structure.

With the given number of wells drilled in the survey area placing future wells or repurposing abandoned wells can reduce the costs. Although there are several factors that should be investigated (well integrity, correct formation, and leakage) these are several aspects operators should consider if switching from secondary recovery to tertiary recovery.

Seismic facies map indicates where the more porous locations are which can have the higher percentage of fluids still in place. The miscible reaction that CO_2 has with a depleted reservoir can increase production and reduce the greenhouse gas CO_2.

Several factors should be considered when injecting the CO_2 in a depleted hydrocarbon reservoir. A fluid gradient, structural areas, and more importantly, porous zones. Since this reservoir has experienced secondary recovery methods (waterflood) the field potently has 50% to 70% of oil left in place but reported 40% oil left in place (Watney, 2015). If the oil left in place is in the lower porosity zones (Facies one and two) and considering the reaction that carbon-dioxide has with residual oil, an optimal place could reside in a lower porosity class located in a structural low area. The seismic facies porosity map can help producers drill new wells or repurpose old wells that land in optimal recovery locations.

The seismic faices map provides insights for drilling or repurposing old wells for enhanced oil recovery wells. By knowing where the highest porosity zones are provides insights for operators to model fluid flow.

The seismic waveform attributes of the Wellington Field on the Mississippian horizon have been analyzed with neutron, sonic, density, and nuclear magnetic resonance logs and CT scans at the top, middle, and bottom of the Mississippian reservoir to evaluate a predicted petrophysical classification map. Accuracy of the map has been verified with several wells in the study area using neutron porosity logs. Although the porosity map does not line up with all of the wells the possibilities range from faults increasing porosity, chert, and dolomite.

The Wellington KGS #2-32 resistivity logs indicate that there is an active water drive which requires porosity and permeability caused by the faults. The Renn-Erickson #1 is interpreted as an area that has experienced small scale faulting. Being that this area has experienced hydrothermal fluids (evidence by chert) this area could have secondary porosity if not vuggy chert. The Meridith #2, Meridith #3, and Meridith #4 wells all are on the outer bounds of a circular object. This object resembles a shoal complex.

The seismic reflection coefficient provides direct correlation to the petrophysical variations convolved within the seismic data that are extracted via amplitude bandwidth, peakedness, and energy attributes. Using the unsupervised neural network to classify these attributes for the Mississippian reservoir yielded a seismic facies map to correlate/predict porosity through the survey area with a degree of error. Figure 4.5 shows that neutron porosity and calculated impedance (density and velocity) from the well-logs are linearly correlated and that porosity can be expressed as a linear equation. Figure 4.6 illustrates that seismic amplitude can be correlated with porosity validating that the seismic attribute is a verifiable approach for correlating/predicting porosity using an unsupervised neural network.

The reservoir is complex in terms of lithofacies and porosity varies in both magnitude and architecture. Integrating the seismic facies map with petrophysical variations suggests that some aspects of porosity are associated with basement tectonics in the region. The Nemaha uplift has created subparallel structural features (e.g. faults) in the study area that contribute to variations in porosity; they can also be interpreted as areas for local sedimentary reworking processes that affect the ultimate petrophysical character of the formation rocks, which are then recorded differently on well-logs.

The Wellington KGS #1-32 contain vuggy porosity (see Figure 5.3) throughout the CT scans. Vuggy pore are not known to be connected to other vugs; instead, fractures likely provide the pathways between pores. The presence of light colored chert indicates that the reservoir had hydrothermal fluids by diagenetically changing the limestone to dolomite and ultimately precipitating to chert within the main hydrothermal pathways.

The Wellington KGS #2-32 should have landed in seismic Facies three but a contributor to producing incorrect facies can be attributed to the well being drilled on a fault. Porosity variations are mainly fracture pores, but a vuggy pores (see Figure 5.8) are indicated in the CT scans. This type of result is expected, given that the #2-32 land on the seismic porosity change of less than 8% and having greater than 12%. This well is structurally low and has a significant chance to disperse the carbon-dioxide throughout the reservoir.

Integrating multiple data sets with different magnitudes of resolution can be a concern, but the seismic data have the advantage of averaging well porosity. In contrast, the micro CT scans provide an image to see the details of pore architecture and how they vary not only within a well but also between wells. In this context, it is useful to contrast Wellington KGS #1-32 and the Wellington KGS #2-32, the latter of which is located near a fault. A caution should be placed on using CT scans, however, since they provide snap-shots of the reservoir and are not necessarily a direct correlation to the seismic data.

This study has demonstrated that a carbonate reservoir, the Mississippian carbonate reservoir in Sumner County, Kansas, United States, can be accurately described in terms of seismic facies that relate to petrophysical variations. Further investigation could be used in inversion but in a way, this is a quicker and less time-consuming for characterizing a carbonate reservoir.

The cherty dolomite contains secondary porosity contained within vuggy and pores between limestone and dolomite. This type of facies would be a hard reflector producing a high impedance value. Compared to the limestone with fracture that would registrar as a soft reflector.

In addition, a descriptive statistical analysis of the results could provide further insights by quantifying the results. The seal integrity should be carefully characterized using seismic characterization to ensure leakage does not permeate or flow via faults or faults caused by injecting carbon dioxide or wastewater. As complex tools become easily used to extract geological properties (porosity) the methods we utilize can become muddy by averages (seismic algorithms, linear trends, and neural networks) that require a geological understanding to differentiate the properties. A seismic interpreter will need the geological intuitiveness to understand results. A critical understanding of geological principles and physical laws and theories along with strong work ethic are critical to develop and advance the field of geophysics.

References

Andersen, E., & Boyd, J. (2004). Seismic waveform classification: techniques and benefits. *CSEG Recorder*, *29*(3).

Anees, M. (2013). Seismic attribute analysis for reservoir characterization. In *10th Biennial International Conference and Exposition*.

Asquith, G. B., & Gibson, C. R. (1982). Basic Relationships of Well Log Interpretation: Chapter I.

Baars, D.L. Basement Tectonic Configuration in Kansas, Kansas Geological Survey. 1995

Blakey, R**.**, 2010, Late Mississippian Paleogeography of North America: Colorado Plateau

Brown, A., 2010. Interpretation of Three-Dimensional Seismic Data.

Buggisch, W., M. M. Joachimski, G. Sevastopulo, and J. R. Morrow, 2008, Mississippian carbon 13 and Conodont apatite carbon 18 records – Their relations to the late Paleozoic Glaciation: Paleogeography, Paleoclimatology, Paleoecology

Chatellier, J. Y. (2005). Chert, a diagenetic and sedimentological indicator often misunderstood or forgotten. *Mississippian from Alberta and world analogues*, 1-10.

Coléou, T., Poupon, M., & Azbel, K. (2003). Unsupervised seismic facies classification: A review and comparison of techniques and implementation. *The Leading Edge*, *22*(10), 942-953.

Chopra, S., Marfurt, K. J., 2008. Seismic attributes for stratigraphic feature characterization. SEG Technical Program Expanded Abstracts

Doveton, J. (1999). Basics of Oil and Gas Log Analysis. Kansas Geological Survey. *The University of Kansas*.

Dyer, S., Ali, F., 1991. S.M. Mechanistic aspects and chemistry of immiscible carbon dioxide flooding. 86th American Institute of Chemical Engineers Symposium Series, pp. 44-51.

Franseen, E. K. (2006). Mississippian (Osagean) shallow-water, mid-latitude siliceous sponge spicule and heterozoan carbonate facies: an example from Kansas with implications for regional controls and distribution of potential reservoir facies.

Geldart, L. P., & Sheriff, R. E. (1999). *Exploration Seismology*. Cambridge University Press.

Henry, S., 2000. Pitfalls in synthetics. The Leading Edge. 19. 604.

Holubnyak, Y., Watney, W., Rush, J., Fazelalavi, M., Wreath, D., 2017. Pilot Scale CO2 EOR in Mississippian Carbonate Reservoir at Wellington Field in South-central Kansas

Infante-Paez, Lennon and Marfurt Kurt J. 2017. Seismic expression and geomorphology of igneous bodies: A Taranaki Basin, New Zealand, case study

Keast, R. T. (2018). *Modeling the Proterozoic basement's effective stress field, assessing fault reactivation potential related to increased fluid pressures in south central Kansas and north central Oklahoma, and improving seismic imaging of basement faulting within Wellington and Anson-Bates Fields, Sumner County, Kansas* (Doctoral dissertation).

Krehel, A. (2017). Investigation of time-lapse 4D seismic tuning and spectral responses to CO_2-EOR for enhanced characterization and monitoring of a thin carbonate reservoir (Doctoral dissertation, Kansas State University).

Laszlo, E. (2007). *Science and the Akashic field: An integral theory of everything*. Simon and Schuster.

Lee, G., Lee, K., & Kim, H. (2009). Tuning effects' impact on seismic. *AAPG Explorer, edited*.

Liu, G. (2012). Carbon dioxide geological storage: monitoring technologies review. *Greenhouse Gases-Capturing, Utilization and Reduction*, 299-338.

Marfurt, K. J., Kirlin, R. L., Farmer, S. L., & Bahorich, M. S. (1998). 3-D seismic attributes using a semblance-based coherency algorithm. *Geophysics*, *63*(4), 1150-1165.

Martin, K. G., Totten, M. W., & Raef, A. (2017). Characterization of a reservoir ooid shoal complex and Artificial Neural Networks application in lithofacies prediction: Mississippian St.

Louis formation, Lakin fields, western Kansas. *Journal of Petroleum Science and Engineering*, *150,* 1-12.

Mazzullo, S. J., Wilhite, B. W., & Woolsey, I. W. (2009). Petroleum reservoirs within a spiculite-dominated depositional sequence: Cowley Formation (Mississippian: Lower Carboniferous), south-central Kansas. *AAPG bulletin*, *93*(12), 1649-1689.

Mazzullo, S. J., Wilhite, B. W., & Boardman II, D. R. (2011). Lithostratigraphic architecture of the Mississippian reeds spring formation (middle Osagean) in southwest Missouri, northwest Arkansas, and northeast Oklahoma: Outcrop analog of subsurface petroleum reservoirs.

Mazzullo, S. J., Wilhite, B. W., & Morris, B. T. (2011). Mississippian oil reservoirs in the southern midcontinent: New exploration concepts for a mature reservoir objective: Search and discovery.

Mazzullo, S., Wilhite, B., 2011. A new understanding after all these years, Do you know the Mississippian?

Mazzullo, S., Wickstrom, H., 2011. It's not 'just the Miss…' Mississippian a Symphony, Not a Solo.

Mazzullo, S., 2011 Mississippian Oil Reservoirs in the Southern Midcontinent: New Exploration Concepts for a Mature Reservoir Objective.

Melzer, L. S. (2012). Carbon dioxide enhanced oil recovery (CO2 EOR): Factors involved in adding carbon capture, utilization and storage (CCUS) to enhanced oil recovery. *Center for Climate and Energy Solutions*.

Merriam, D. F. (1963). *The geologic history of Kansas*. University of Kansas publications.

NETL, N. (2010). Carbon dioxide enhanced oil recovery-untapped domestic energy supply and long term carbon storage solution. *The Energy Lab*.

Newell, K. D., Watney, W. L., Cheng, W. L., & Brownrigg, R. L. (1989). Stratigraphic and spatial distribution of oil and gas production in Kansas.

Nissen, S. E., K. J. Marfurt, and T. R. Car, 2004, Identifying subtle fracture trends in the Mississippian saline aquifer unit using new 3-D seismic attributes: KGS Open File Report.

Nobel, J., 2004. Seismic waveform classification: Techniques and Benefits, Boyd Petroresearch, Vol. 29 NO. 03

Newell, D., Watney, L., Cheng, S., Brownrigg, R., 1987. Stratigraphic and Spatial Distribution of Oil and Gas Production in Kansas. Kansas Geological Survey, Subsurface geology Series 9.

Ohl, D., & Raef, A. (2014). Rock formation characterization for carbon dioxide geosequestration: 3D seismic amplitude and coherency anomalies, and seismic petrophysical facies classification, Wellington and Anson-Bates Fields, Kansas, USA. *Journal of Applied Geophysics*, *103*, 221-231.geosequestration: 3D seismic amplitude and coherency anomalies, and seismic petrophysical facies classification, Wellington and Anson-Bates Fields, Kansas, USA. *Journal of Applied Geophysics*, *103*, 221-231.

Raef, A., Totten, M., Vohs, A., & Linares, A. (2017). 3D Seismic Reflection Amplitude and Instantaneous Frequency Attributes in Mapping Thin Hydrocarbon Reservoir Lithofacies: Morrison NE Field and Morrison Field, Clark County, KS. *Pure & Applied Geophysics*, *174*(12), 4379-4394.

Rogers, S. M. (2001). Deposition and diagenesis of Mississippian chat reservoirs, north-central Oklahoma. *AAPG bulletin*, *85*(1), 115-129.

Sayers, C., Chopra, S., 2009. Introduction to this special section: Seismic modeling. The Leading Edge.

Simm, R., Bacon, M., 2014. Seismic Amplitude An Interpreters Handbook.

Suriamin, F., Pranter, M., SEG, Interpretation 2018. Stratigraphic and lithofacies control on pore characterististics of Mississippian limestone and chert reservoirs of north-central Oklahoma

Stanulonis, S. F., & Tran, H. V. (1992). Method to determine porosity-thickness directly from 3-D seismic amplitude within the Lisburne Carbonate pool, Prudhoe Bay. *The Leading Edge*, *11*(1), 14-20.

Sprunt, Eve S., et al. "Method for determining lithological characteristics of a porous material." U.S. Patent No. 4,688,238. 18 Aug. 1987.

Steeghs, P., & Drijkoningen, G. (2001). Seismic sequence analysis and attribute extraction using quadratic time-frequency representations. *Geophysics*, *66*(6), 1947-1959.

Tittman, J. "Vertical Resolution of Well Logs: Recent Developments." *Oilfield Review* 3.3 (1991).

Verma, M. K. (2015). *Fundamentals of carbon dioxide-enhanced oil recovery (CO2-EOR): A supporting document of the assessment methodology for hydrocarbon recovery using CO2-EOR associated with carbon sequestration*. Washington, DC: US Department of the Interior, US Geological Survey.

Watney, L., 2015. A maturing Mississippian Lime Play in the Midcontinent – A Perspective on What We Know and Need to Know.

Watney, L., Rush, J., 2015. Modeling CO2 sequestration in Saline Aquifer and Depleted Oil Reservoir to Evaluate Regional CO2 sequestration Potential of Ozark Plateau Aquifer System, South Central Kansas.

West, B.P., May, S.R., Eastwood, J.E., Rossen, C., 2002. ExxonMobil Upstream Research Company. Interactive seismic facies classification using textural attributes and neural networks. Leading Edge 21(10), 1042-1049.

Widess, M. B. (1973). How thin is a thin bed?. *Geophysics*, *38*(6), 1176-1180.

Wethington, N. W., & Pranter, M. J. (2018). Stratigraphic architecture of the Mississippian limestone through integrated electrofacies classification, Hardtner field area, Kansas and Oklahoma. *Interpretation*, *6*(4), T1095-T1115.

Xu, S., & Payne, M. A. (2009). Modeling elastic properties in carbonate rocks. *The Leading Edge*, *28*(1), 66-74.

Zhao*, T., Verma, S., Qi, J., & Marfurt, K. J. (2015). Supervised and unsupervised learning: how machines can assist quantitative seismic interpretation. In *SEG Technical Program Expanded Abstracts 2015* (pp. 1734-1738). Society of Exploration Geophysicists.

Ziolkowski, A., Underhill, J.R., and Johnston, R.G.K., 1998. Wavelets, well ties, and the search for subtle stratigraphic traps. Geophysics. 63. 297-313.

Websites

dGB Earth Sciences, Opendtect. 2019. https://www.dgbes.com/

Department of Energy, National Energy Technology Labotory web page.

https://www.netl.doe.gov/sites/default/files/netl-file/CO2_EOR_Primer.pdf, 2010.

Geosystems, Inc., map, http://cpgeosystems.com/paleomaps.html.

Stratigraphy, Society for Sedimentary Geology http://www.sepmstrata.org/page.aspx?pageid=15

Kansas Geological Survey Resources: http://www.kgs.ku.edu/PRS/petroIndex.html

Kansas Geological Survey: https://maps.kgs.ku.edu/oilgas/index.html

https://www.sepm.org/